JAERI-M
84-089

DATA COMPILATION FOR RADIATION EFFECTS ON HYDROGEN RECYCLE IN FUSION REACTOR MATERIALS

May 1984

Kunio OZAWA, Kimichika FUKUSHIMA and Katsuyuki EBISAWA**

日本原子力研究所
Japan Atomic Energy Research Institute

JAERI-M レポートは，日本原子力研究所が不定期に公刊している研究報告書です。
入手の問合わせは，日本原子力研究所技術情報部情報資料課（〒319-11茨城県那珂郡東海村）あて，お申しこしください。なお，このほかに財団法人原子力弘済会資料センター（〒319-11 茨城県那珂郡東海村日本原子力研究所内）で複写による実費頒布をおこなっております。

JAERI-M reports are issued irregularly.
Inquiries about availability of the reports should be addressed to Information Section, Division of Technical Information, Japan Atomic Energy Research Institute, Tokai-mura, Naka-gun, Ibaraki-ken 319-11, Japan.

編集兼発行　日本原子力研究所
印　　刷　いばらき印刷㈱

JAERI-M 84-089

Data Compilation for Radiation Effects on Hydrogen Recycle in Fusion Reactor Materials

Kunio Ozawa, Kimichika Fukushima*
and Katsuyuki Ebisawa**

Department of Physics,
Tokai Research Establishment, JAERI

(Received April 19, 1984)

Irradiation tests of materials by hydrogen isotopes are under way, to investigate the hydrogen recycling process where exchange of fuel particles takes place between plasma and the wall of the nuclear fusion reactor. In the report, data on hydrogen irradiation are collected and reviewed from the view point of irradiation effects.

Data are classified into, (1) Re-emmission, (2) Retention, (Retained hydrogen isotopes, Depth profile in the materials and Thermal desorption spectroscopy), (3) Permeation and (4) Ion impact desorption. Research activities in each area are arranged according to the date of publication, research institutes, materials investigated, so that overview of present status can be made. Then, institute, author and reference are shown for each classification with tables. The list of literature is also attached.

Keywords: Re-emission, Retained Hydrogen Isotopes, Depth Profile, Thermal Desorption, Permeation, Ion Impact Desorption, Recycling, Plasma-Surface Interactions, Radiation Effects, Data Base.

---

* Research and Development Center, Kawasaki, Toshiba Corporation.
** Nuclear Energy Group, Mita, Tokyo, Toshiba Corporation.

This report was prepared as an account of work supported partly by a research contract of JAERI with Toshiba Corporation in fiscal year 1983.

JAERI－M 84－089

水素リサイクリング過程に対する照射効果データの収集

日本原子力研究所東海研究所物理部
小沢　国夫・福島　公親*・海老沢克之**

（1984年4月19日受理）

核融合炉のプラズマ・壁間で燃料粒子が交換される水素リサイクリング過程の研究として，第一壁候補材料に対する水素同位体の照射実験が行われている。本調査報告では，水素同位体の挙動に与える照射効果に関するデータを収集し下記の6項目の観点からまとめた。

実験データは，内容により(1)再放出，(2)保持（保持量，深さ分布，熱脱着分析），(3)透過，(4)イオン衝撃による脱着に分類した。最初に各分野の研究を発表年代，研究機関，研究材料で整理し研究活動の現状が概観できるようにまとめた。次に，それぞれの分類別に各実験研究の研究機関，著者，出典を示し実験データの図表を添付した。

また，調査した文献を各分類ごとにリストアップした。

＊ 株式会社東芝総合研究所
＊＊ 株式会社東芝原子力事業本部

Contents

1. Introduction 1
2. Overview of Hydrogen Irradiation Experiments 2
3. Experimental Data on Hydrogen Irradiation 8
3.1 Re-emission 8
3.2 Retention 33
3.2.1 Retained Amount 33
3.2.2 Depth Profile in the Materials 71
3.2.3 Thermal Desorption Spectroscopy 108
3.3 Permeation 122
3.4 Ion Impact Desorption 132
4. Closing Remarks 139

目　　次

1. はじめに 1
2. 水素照射実験の概観 2
3. 水素照射の実験データ 8
3.1 再放出 8
3.2 保　持 33
3.2.1 保持量 33
3.2.2 材料中分布 71
3.2.3 熱脱着スペクトル 108
3.3 透　過 122
3.4 イオン衝撃による脱着 132
4. おわりに 139

1. Introduction

Due to diffusion and charge exchange phenomena, hydrogen isotopes leak out of plasma of the nuclear fusion reactor and bombard the first wall, limitter and divertor. A part of hydrogen isotopes bombarding materials are reflected back to plasma on the surface. The rest of hydrogen isotopes may be captured by lattice defects caused by irradiation, or re-emitted back to plasma by diffusion, or penetrate into cooling water.

Plasma-wall interaction, where fuel particles are bouncing back and forth between plasma and the wall, affects directly the balance of the density and the composition of plasma. It also affects their energy balance. Hydrogen isotopes retained in the materials could cause hydrogen embrittlement. Tritium, one of the hydrogen isotopes, retained in the materials would cause troubles to maintenance and repair operation. If they penetrate into cooling water, it would be the cause of component contamination.

Behavior of these hydrogen isotopes is now being gradually clarified that are implanted in the materials. The report summarizes the survey on the hydrogen bombardment experiments that are focused on the irradiation effects by hydrogen isotopes such as formation of lattice defects which trap hydrogen isotopes, radiation-induced emission of hydrogen isotopes, etc.

In Chapter 2, survey of research activities is stated and in Chapter 3, experimental data are exhibited.

2. Overview of Hydrogen Irradiation Experiments

In this chapter, hydrogen irradiation experiments are classified into 6 areas, namely, (1) re-emission, (2) retention, (3) depth profile in the materials, (4) thermal desorption spectroscopy, (5) permeation and (6) ion impact desorption. Then, they are summarized in Table 2.1 through Table 2.6 in order. In the Tables, experiments of each item are arranged according to the date of publication and the research institute. Materials studied are designated by different symbols.

Researches on re-emission, retention and depth profile exceed in numbers and not so many of those on permeation and ion impact desorption are reported. Among research institutes, Sandia National Laboratory (Livermore, Albuquerque) and Max-Plank-Institute für Plasmaphysik (Garching) are making most of the researches and stainless steel and graphite are investigated most among materials concerned.

Index Number Description

Index number is given in the form of AB-mn, where AB and mn show the classification for experiments and materials, respectively.

AB

- RE : Re-emission
- RT : Retention
- DP : Depth profile in materials
- TD : Thermal desorption spectroscopy
- PM : Permeation
- ID : Ion impact desorption

mn

- 0n : Stainless steel
- 1n : Ni, Mo, Fe
- 2n : W, Cu
- 3n : Zr, Ti, V
- 4n : Other alloys
- 5n : C (Graphite)
- 6n : Si
- 7n : Other low-z materials

Table 2.1 Experiments on Re-Emission

	SNL(L)	MPI	CL	OU	GIT	ORNL	JSI
1969			Ni				
1974	V,Mo,SS						
1976	SS						
1978		SS	SS			SS	
1980	△	□	C SS C				□
1981	SS	◎		Ni,Mo			
1982	SS		C		SS		

SNL(L) : Sandia National Laboratories (Livermore)
MPI : Max-Plank-Institute (Garching)
CL : Culham Laboratory
OU : Osaka University
GIT : Georgia Institute of Technology
ORNL : Oak Ridge National Laboratory
JSI : J. Stefan Institute

SS : Stainless Steel
C : Carbon (Graphite)
△ : Ti/Cu, TiB_2/C
□ : SS, Inconell 600, Hastelloy B, PE 16
◎ : Si, TiO_2, TiC, Spinel
Alumina, Aluminatitania

Table 2.2 Experiments on Retention

	SNL(L)	SNL(A)	MPI	CL	UA	KfA	AWE
1966							SS
1976	Mo		C Zr,Ti		Mo		
1977					Mo		
1978		C	SS SS SS C		Zr		
1980	SS, △ SS	□	Mo ◎ Mo	C	Ni	C	
1981	▲ ■		SS				
1982		C	C ●				

SNL(L) : Sandia National Laboratories (Livermore)
SNL(A) : Sandia National Laboratories (Albuquerque)
MPI : Max-Plank-Institute (Garching)
CL : Culham Laboratory
UA : University of Aarhus
KfA : Kernforshungsanlage Jülich GmbH
AWE : Atomic Weapon Establishment (UK)

SS : Stainless Steel
C : Carbon (Graphite)
△ : Ti/Cu, Ti/C, TiB_2/C
□ : B, C, Si, TiB_2, B_4C, VB_2
◎ : BeO
▲ : B/C
■ : C, TiC
● : TiO_2, Spinel, Alumina Alumina-titania

Table 2.3 Experiments on Depth Profile

	SNL(L)	SNL(A)	MPI	CL	UA	USSR	ORNL	Others
1976		Mo	C,Si					Si,W ①,②
1977								Ni ③
1978		C	SS SS C		Zr		Si	Si ④,⑤ Si ②
1979	Si	△						
1980	SS □	Si	SS Mo Si ◎		Ni	Ni,Mo		Si ⑥ Si ⑤,⑦
1981	C SS ▲	Si	SS					C ⑤
1982	SS	SS Ni	SS		Ni			C,SS ⑧

SNL(L) : Livermore
SNL(A) : Albuquerque
MPI : Garching
CL : Culham Laboratory
UA : University of Aarhus

△ : B_4C, TiB_2
□ : Ti/Cu, TiB_2/C
◎ : BeO
▲ : B/C

① : Wright Nuclear Structure Laboratory, Yale University
② : IBM ③ : Ruhr Universität
④ : Bell Laboratories ⑤ : RCA Laboratories
⑥ : Gesellschaft für Stralen-und Unweltforshung mbH
⑦ : Plasma Physics Laboratory, Princeton University
⑧ : Research Institute of Physics, Stockholm

Table 2.4 Experiment on Thermal Desorption Spectroscopy

	SNL(L)	ANL(A)	MPI	CL	UA	ORNL	US
1974				Mo	Mo		
1978	SS	C	C				SS
1980	SS △ Fe □		SS		Ni		
1982		SS				SS	

SNL(L) : Sandia National Laboratories (Livermore)
SNL(A) : Sandia National Laboratories (Albuquerque)
MPI : Max-Plank-Institute (Garching)
UA : University of Aarhus
ORNL : Oak Ridge National Laboratory
US : University of Salford

SS : Stainless Steel
C : Carbon (Graphite)
△ : Ti/Cu, TiC/C, TiB_2/C
□ : B/C

Table 2.5 Experiment on Permeation

	SNL(L)	SNL(A)	MPI	KfA	USSR	OU	EGGI
1974	SS	SS					
1978				SS			
1980			SS		Ni,Mo		
1981						Ni,Mo	

SNL(L) : Sandia National Laboratory (Livermore)
SNL(A) : Sandia National Laboratory (Albuquerque)
MPI : Max-Plank-Institute (Garching)
KfA : Kernforshungsanlage Jülich GmbH
OU : Osaka University
EGGI : EG&G Idaho
ANL : Argonne

Table 2.6 Experiments on Ion Impact Desorption

	SNL(L)	MPI	CL	IPP
1974			Mo	
1978		SS		
1980				Ti,Mo
1981	SS			

SNL(L) : Sandia National Laboratories (Livermore)
MPI : Max-Plank-Institute (Garching)
CL : Culham Laboratory
IPP : Institute of Plasma Physics
(Nagoya University)

3. Experimental Data on Hydrogen Irradiation

Experimental data surveyed are summarized in order of re-emission, retention, permeation and ion impact desorption in the end of the chapter. Data on retention are further devided into amount of retention, depth profile in the materials and thermal desorption. Reference number of literature, author, research institutes and source are also attached.

3.1 Re-emission

Reference number RE-01 through 09 are concerned with re-emission by stainless steel. RE-11 through 14 are concerned with Ni and Mo, RE-31 with V, RE-41, with alloys, RE-51 through 53, with graphite and RE-71 and 72, with Ti and low mass number materials, respectively.

When hydrogen irradiation is tried to stainless steel, Ni and Mo that are not reactive with hydrogen, re-emission is not observed under a certain level of irradiation, as shown in RE-04, 14 and 41. In case of V and Ti that react with hydrogen, the amount of re-emission is relatively small at lower temperature, as shown in RE-31 and 71. When the temperature is raised, re-emission from materials increases as shown in RE-06, 07, 11, 13 and 72. Energy dependency of re-emission is shown in RE-03, 04, 12, 51 and 53 where the time to saturation is shorter for lower energy.

RE-41 shows the effects of oxide on the surface to the amount of re-emission. Re-emission takes place of accumulated hydrogen when the oxide on the surface is sputtered, and the amount soon decreases and reaches to saturation. As shown in RE-08 and 11, time to reach to saturation is shorter as the flux is higher. In RE-02 and 51, hydrogen irradiation effect on re-emission of D are reported.

RE-01

Title	Helium and Hydrogen Re-Emission during Implantation of Molybdenum, Vanadium and Stainless Steel
Reference	J. Nucl. Mat., 53 (1974) 127
Authors	W. Bauer, G.J. Thomas
Institution	Sandia Laboratories, Livermore, USA

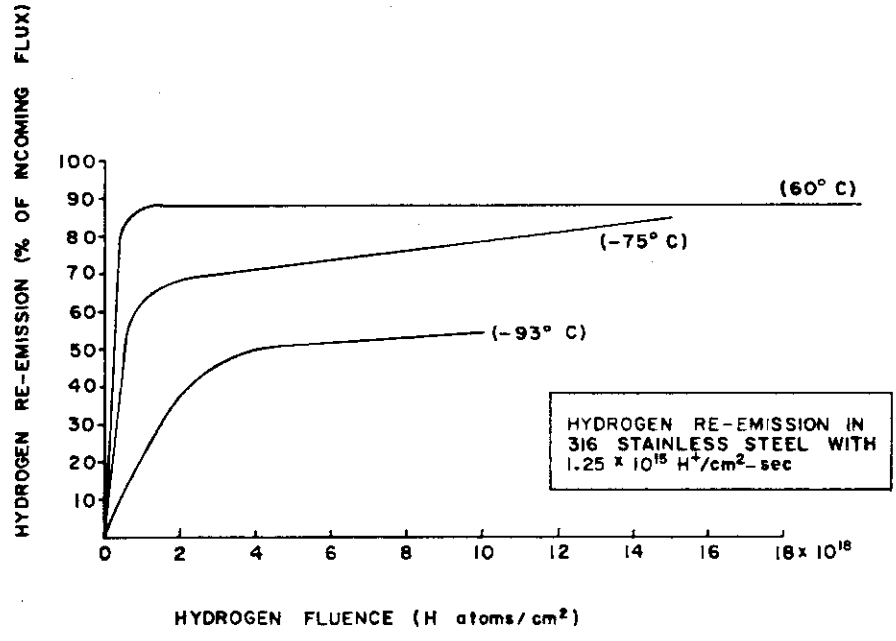

Fig. 4. Hydrogen re-emission during 150 keV H implantation as a function of fluence in 316 stainless steel at three different implantation temperatures.

RE-02

Title	Ion-Induce Release of Deuterium Trapping in Stainless Steel
Reference	J. Nucl. Mat., 76 & 77 (1978) 298
Authors	C.M. Braganza, S.K. Erents, E.S. Hotston, G.M. McCracken
Institution	UKAEA, Culham Laboratory, UK

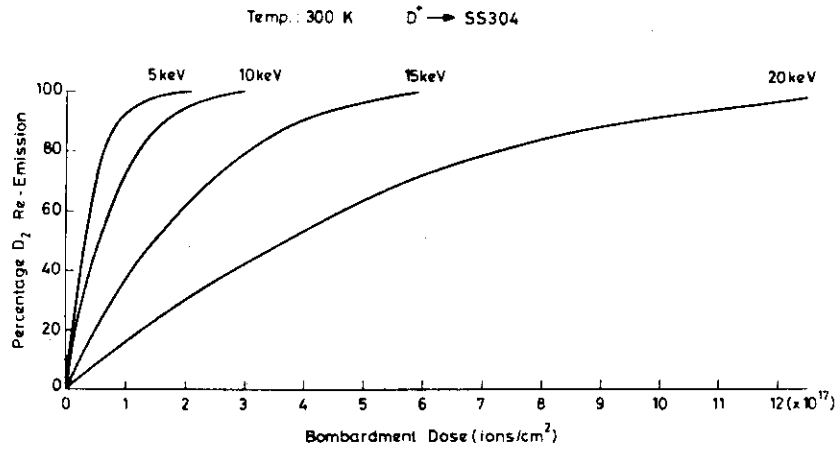

Fig. 1. Release of D_2 from 304 stainless steel target during bombardment by deuterons of various energies. Target temperature 300 K.

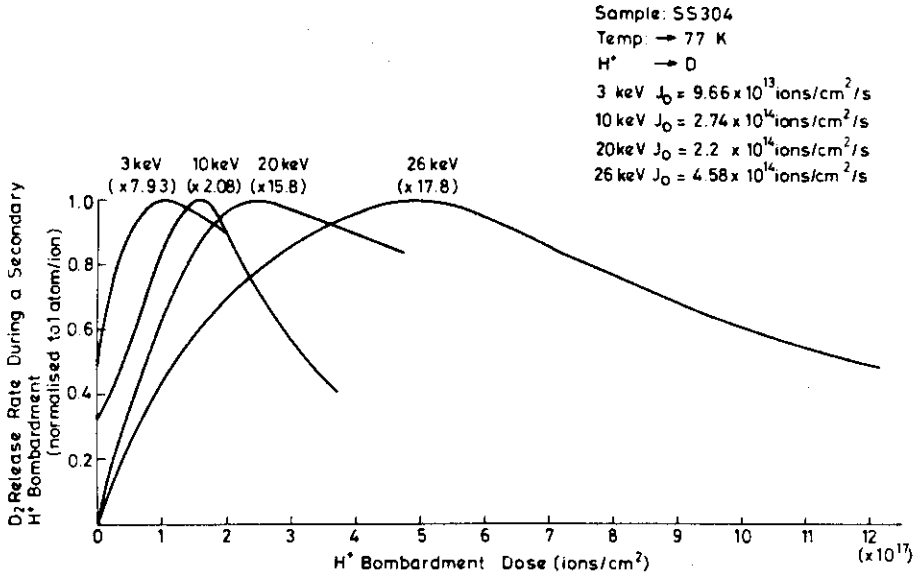

Fig. 5. Release of D_2 from 304 stainless steel during bombardment by protons after prior implantation with deuterons. Target temperature 77 K. The yields have been normalized to 1 atom/ion athe maximum yield.

RE-03

Title	Trapping and Replacement of 1-14 keV Hydrogen and Deuterium in 316 Stainless Steel
Reference	J. Nucl. Mat., 76 & 77 (1978) 305
Authors	R.S. Blewer, R.Behrisch, B.M.U. Scherzer, R.Schulz
Institution	Max-Plank-Institut für Plasmaphysik, Garching, F.R.G.

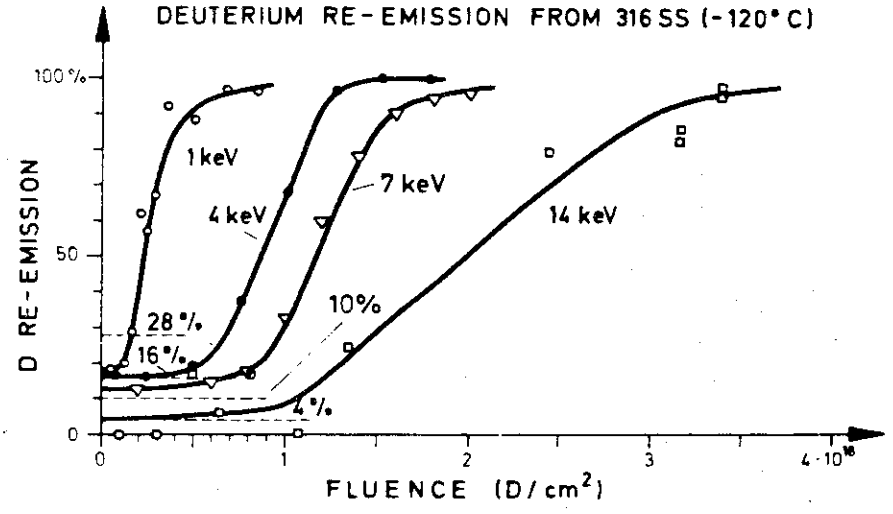

Fig. 3. Re-emission of deuterium as a function of fluence. Reflection coefficient values calculated by Oen and Robinson [13] are shown for each energy by dashed lines.

RE-04

Title	Retention and Re-Emission of 0.125-1 keV Deuterium in Stainless Steel
Reference	J. Appl. Phys., 51 (1980) 1176
Authors	E.W. Thomas
Institution	Culham Laboratory, UK

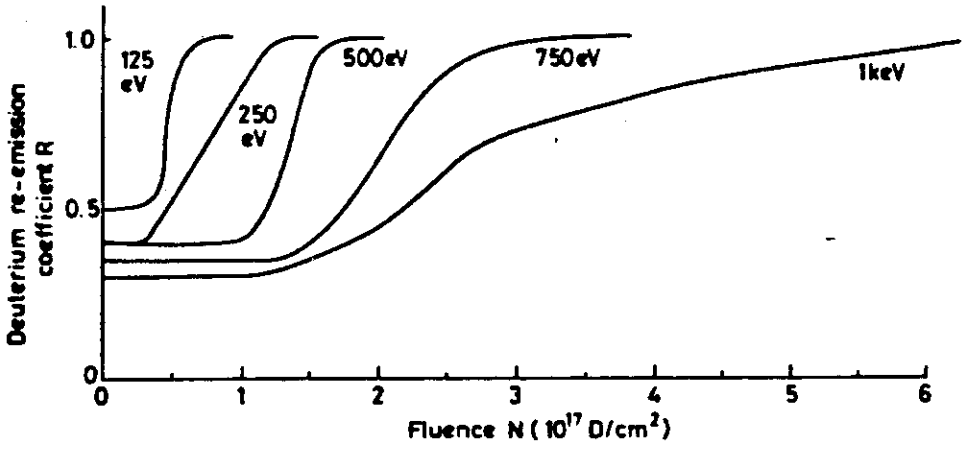

FIG. 3. Re-emission of deuterium from stainless steel bombarded by D^+ ions of various energies; the target temperature is 90 °K.

RE-05

Title	Studies of Hydrogen Recycle from the Wall in Tokamaks Using a Plasma-Wall Interaction Simulator
Reference	J. Nucl. Mat., 76 & 77 (1978) 267
Authors	R.E. Clausing, L.C. Emerson, L. Heatherly
Institution	Oak Ridge National Laboratory, USA

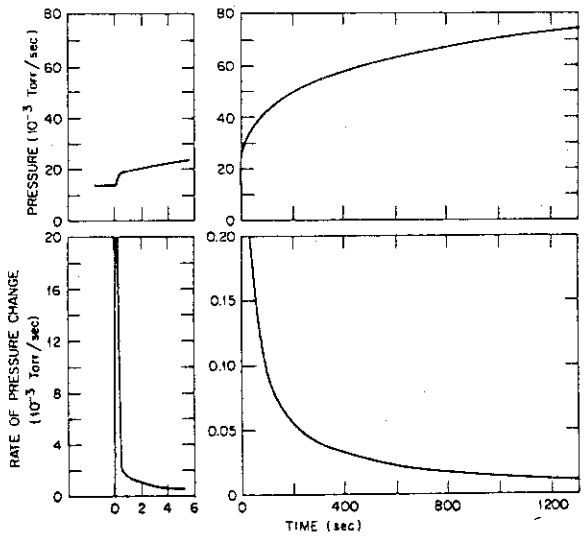

Fig. 4. The re-emission of hydrogen from the stainless steel wall after the discharge is turned off reveals that there is a very rapid recycling mechanism and a slower one. The figure shows the increase in chamber pressure and the rate of increase in chamber pressure for short and long time processes.

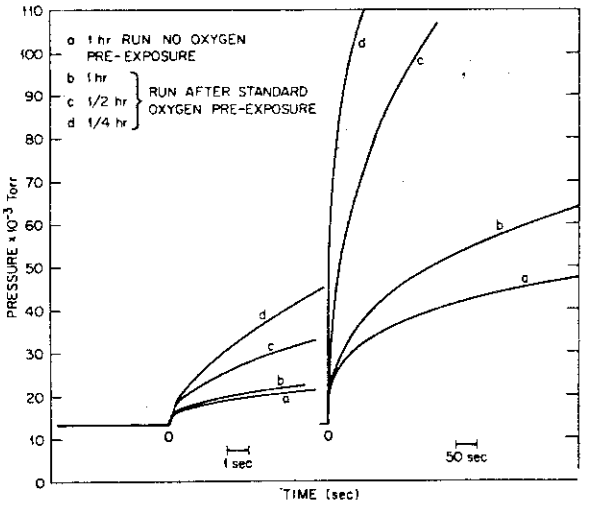

Fig. 5. Shows the effect of wall conditioning on hydrogen recycling. The pre-conditioning is as follows (a) several hours exposure to the plasma during previous runs. (b, c, d) Exposed to 1 atm oxygen for $\frac{1}{2}$ h and then exposed to bombardment with 100 eV hydrogen ions at 6×10^{15} ions/cm^2 · s for the time indicated. Oxygen is removed during the plasma exposure so that the $\frac{1}{4}$ h, $\frac{1}{2}$ h and 1 h exposure have decreasing amounts of oxygen.

RE-06

Title	Hydrogen Recycling in Properties in Stainless Steel
Reference	J. Nucl. Mat., 103 & 104 (1981) 453
Authors	K.L. Wilson
Institution	Sandia National Laboratories, Livermore, USA

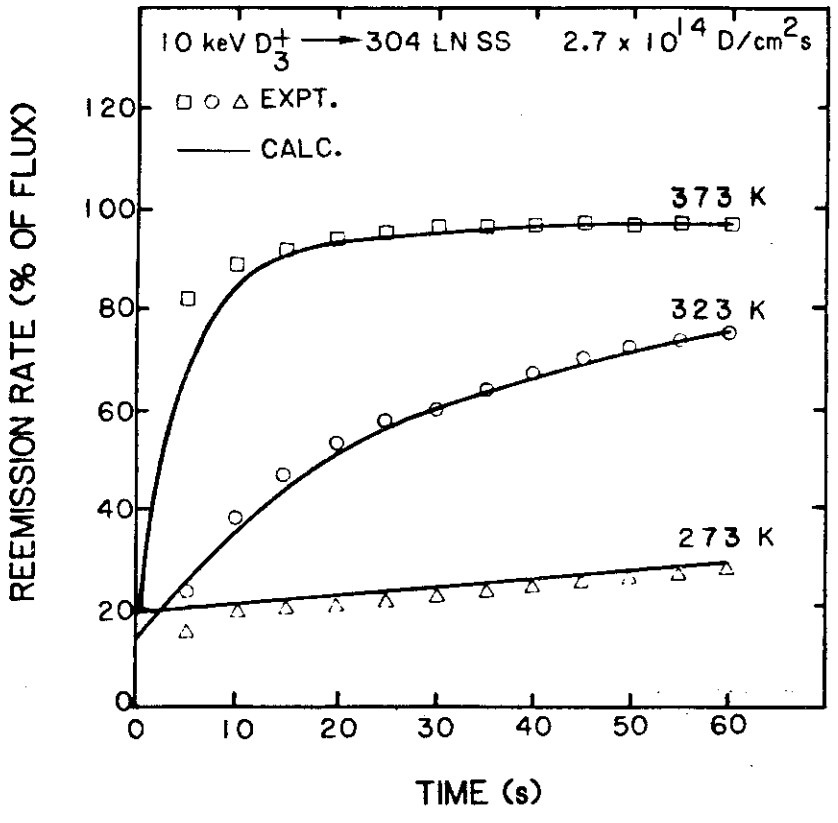

Figure 12. Experimental data and calculations of reemission for 10 keV D_3^+ implantation of 304 LN stainless steel at various temperatures. Calculation parameters include trap concentration: 0.07 atom fraction; trap binding energy: 0.1 eV; diffusivity: 0.1 exp (-0.6/kT) cm^2/s; k_r: $(4.5 \times 10^{-15}/\sqrt{T})$ exp(-0.52/kT) cm^4/s; reflection: 0.15 [97].

RE-07

Title	Deuterium Re-Emission from 304 LN Stainless Steel
Reference	J. Nucl. Mat., 111 & 112 (1982) 622
Authors	K.L. Wilson, M.I. Baskes
Institution	Sandia National Laboratories, Livermore, USA

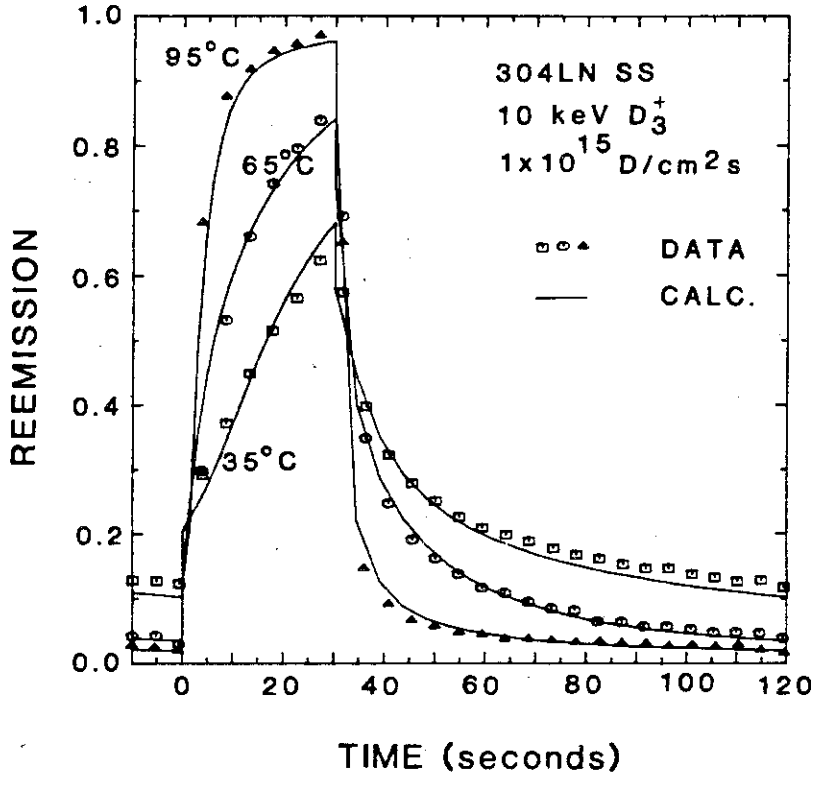

Fig. 2. Measured and calculated steady-state re-emission for electropolished 304LN stainless steel implanted cyclicly at 35, 65, or 95°C. Implantations were conducted from 0–30 s. A re-emission of unity corresponds to a release rate of 1×10^{15} D cm^{-2} s^{-1}.

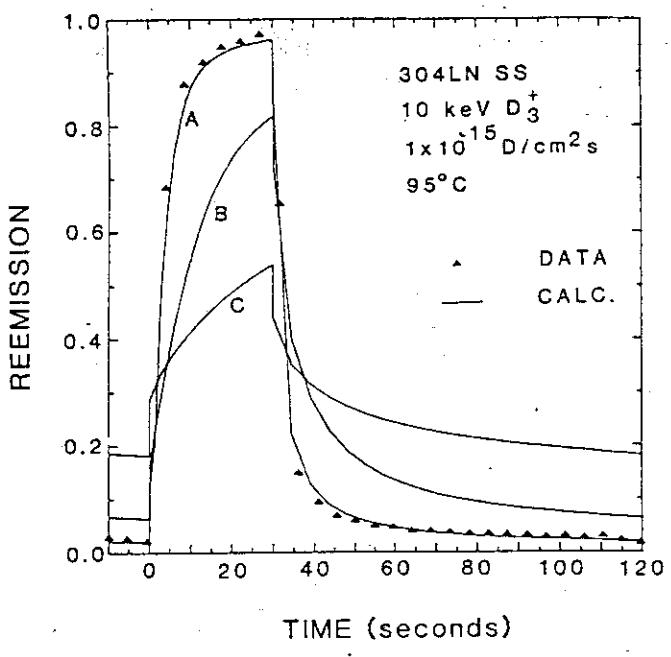

Fig. 3. The effect of the recombination rate constant (K_r) on the calculated re-emission for the 95°C data (▲) of fig. 2. Curve A: $K_r = 2 \times 10^{-23}$ cm^4 s^{-1} (the present calculation); curve B: $K_r = 3 \times 10^{-26}$ cm^4 s^{-1} [4]; curve C: $K_r = 6 \times 10^{-28}$ cm^4 s^{-1} [21].

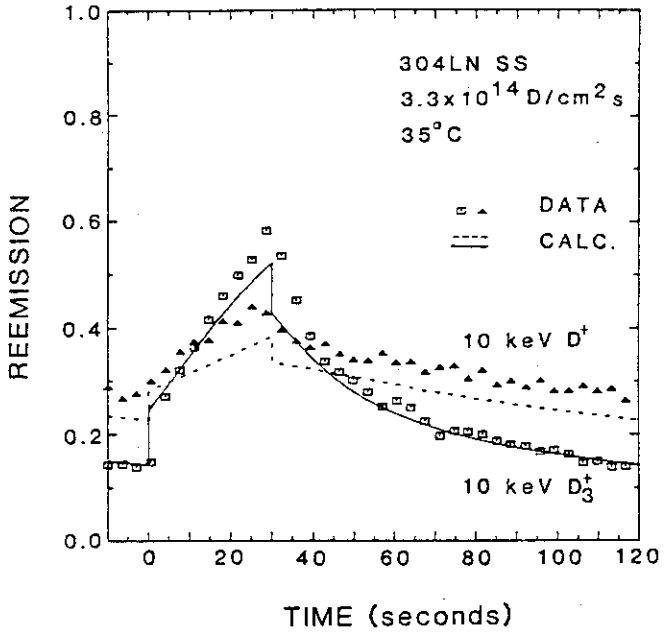

Fig. 4. Measured and calculated steady-state re-emission for electropolished 304LN stainless steel implanted by 10 keV D_3^+ or D^+ with a flux of 3.3×10^{14} D cm^{-2} s^{-1} at 35°C from 0 to 30 s. A re-emission of unity corresponds to a release rate of 3.3×10^{14} D cm^{-2} s^{-1}.

RE-08

Title	Re-Emission of Implanted Deuterium from the Back Side of a Stainless Steel Membrane
Reference	J. Nucl. Mat., 111 & 112 (1982) 642
Authors	R. Young, E.W. Thomas, B. Emmoth
Institution	School of Physics, Georgia Institute of Technology, USA

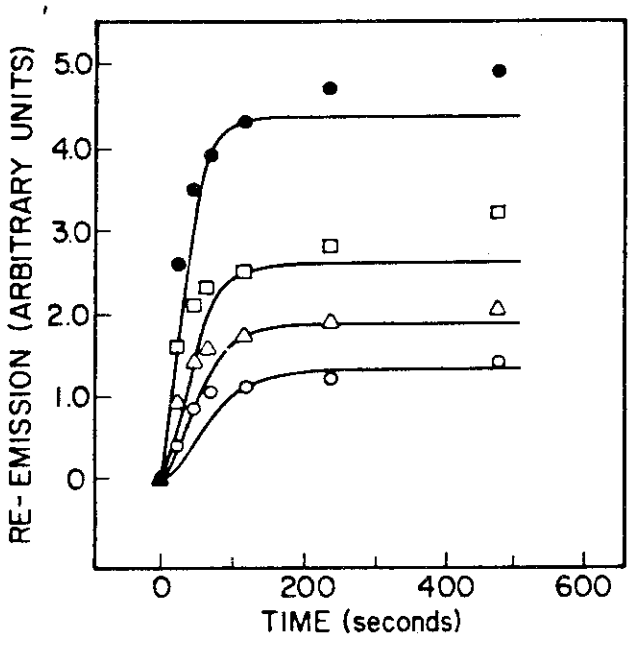

Fig. 1. Re-emission for 10 keV D^+ incident on a stainless steel target at 100°C for different target fluxes. The open circles, triangles, squares, and solid circles correspond to fluxes of 4.0, 7.0, 9.9, and 15.9×10^{13} (D^+ cm^{-2} s^{-1}), respectively. Solid lines are predictions of eq. (3).

RE-09

Title	Low-Energy Proton Implantation of Stainless Steel
Reference	Nucl. Tech., 29 (1976) 322
Authors	K.L. Wilson, G.J. Thomas, W. Bauer
Institution	Sandia National Laboratories, Livermore, USA

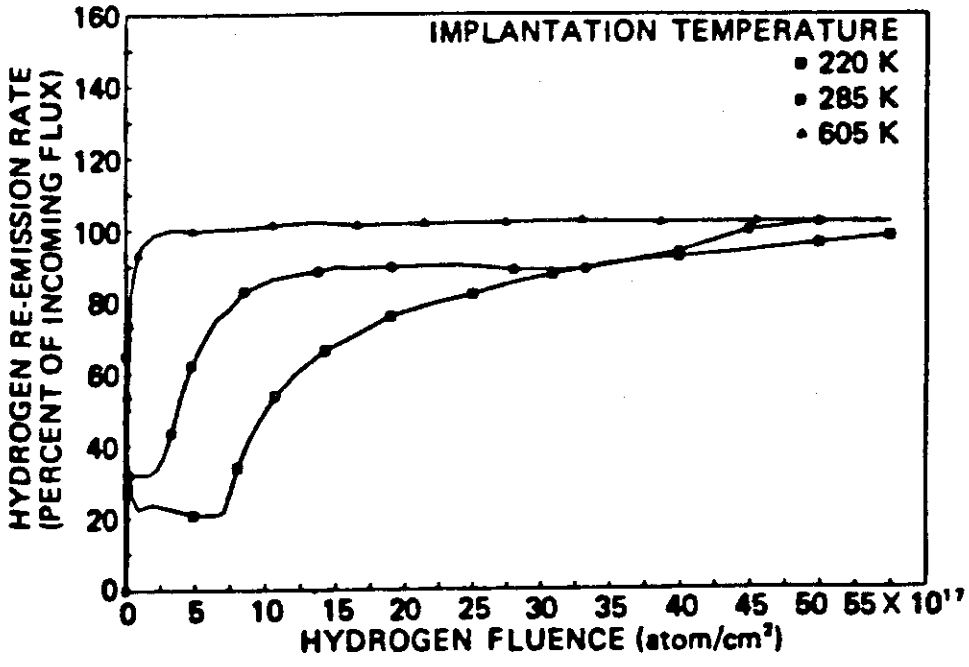

Fig. 1. Hydrogen re-emission rate from as-received Type 316 stainless steel during 20-keV H^+ implantation as a function of fluence at three implantation temperatures.

RE-11

Title	Trapping and Re-Emission of Fast Deuterium Ions from Nickel
Reference	J. Phys. D, 2 (1969) 1397
Authors	K. Erents, G.M. McCracken
Institution	Culham Laboratory, UK

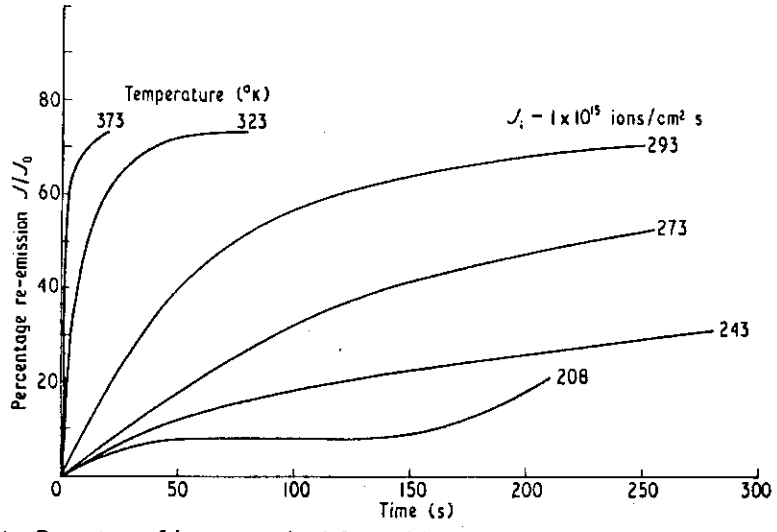

Figure 4. Percentage of beam re-emitted from nickel as a function of bombardment time, at different target temperatures.

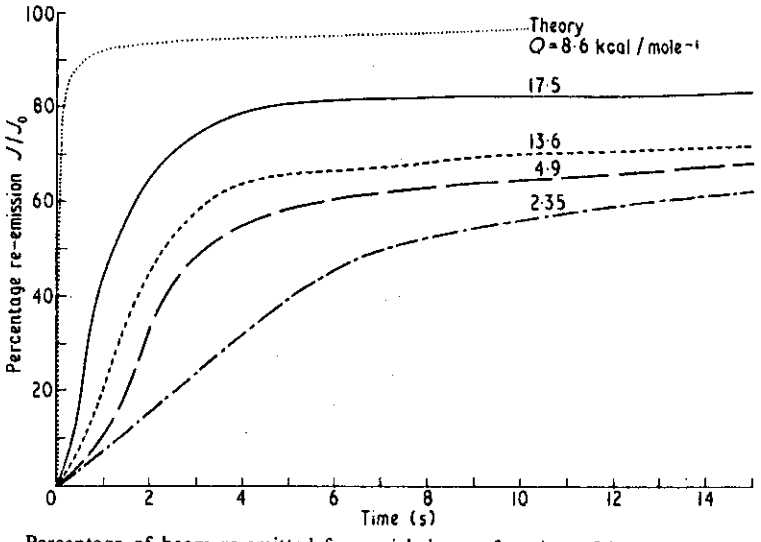

Figure 5. Percentage of beam re-emitted from nickel as a function of bombardment time, for different D^+ dose rates (in 10^{14} ions/cm² s) at 373 °K.

RE-12

Title	Trapping and Re-Emission of Deuterium from Molybdenum following Bombardment at 77K
Reference	Vacuum, 24, (1974) 445
Authors	S.K. Erents
Institution	Culham Laboratory, UK

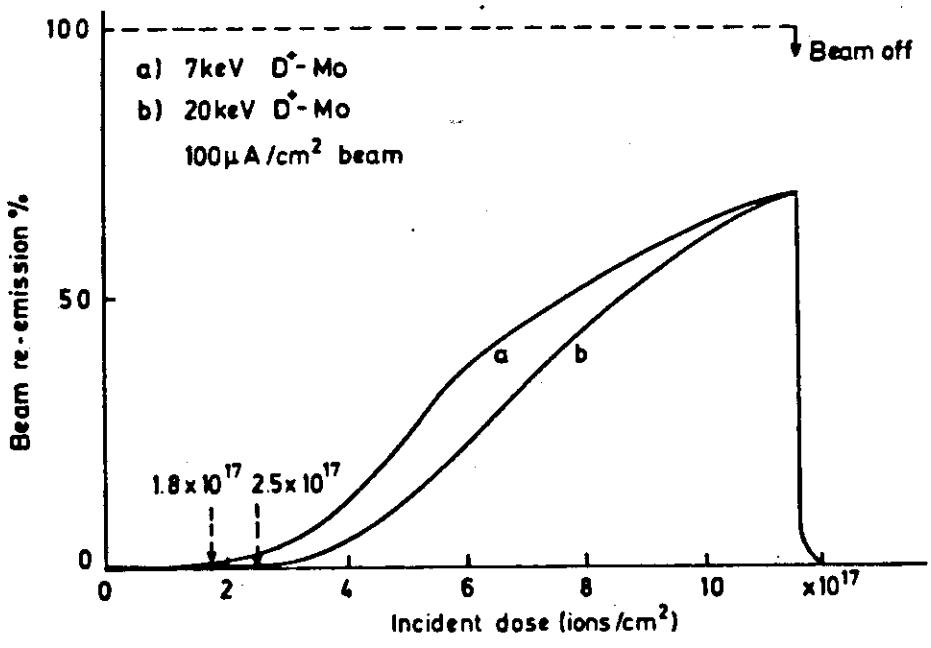

Figure 2. Trapping of D^+ in Mo at 77 K.

RE-13

Title	Permeation and Reemission of Deuterium Implanted in Fast Wall Materials
Reference	J. Nucl. Mat., 103 & 104 (1981) 483
Authors	T. Tanabe, N. Saito, Y. Etoh, S. Imoto
Institution	Department of Nuclear Engineering, Osaka University, Japan

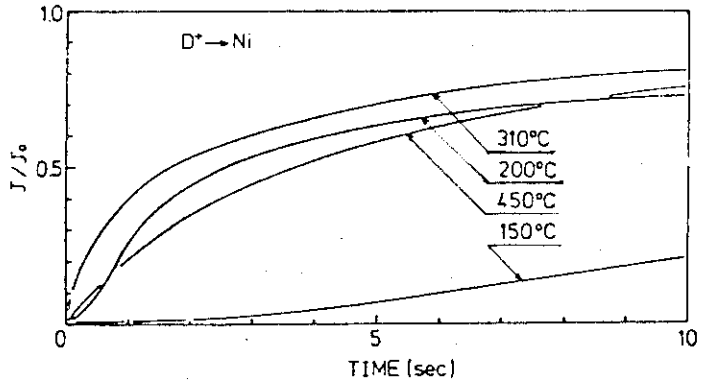

Fig.4 Reemission rate of deuterium from Ni during 20 keV D^+ implantation

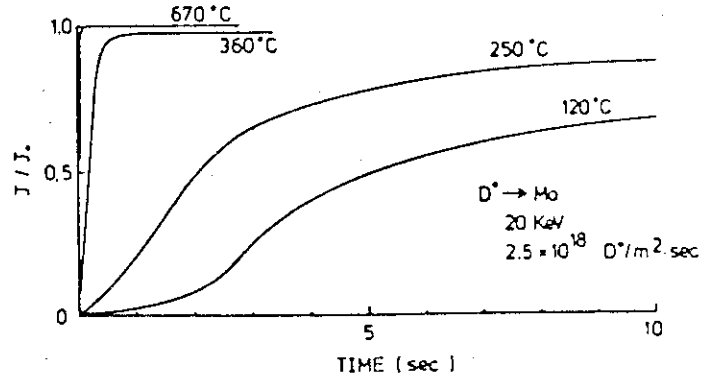

Fig.6 Reemission rate of deuterium from Mo during 20 keV D^+ implantation

RE-14

Title	Helium and Hydrogen Re-Emission during Implantation of Molybdenum, Vanadium and Stainless Steel
Reference	J. Nucl. Mat., 53 (1974) 127
Authors	W. Bauer, G.J. Thomas
Institution	Sandia Laboratories, Livermore, USA

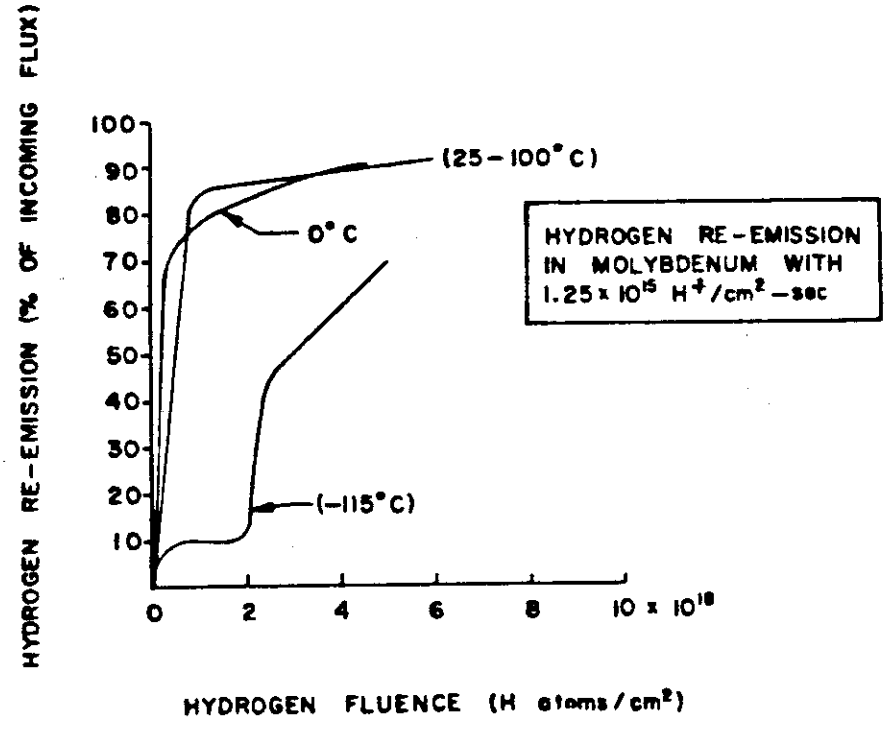

Fig. 5. Hydrogen re-emission during 150 keV H implantation as a function of fluence in molybdenum at three different implantation temperatures.

RE-31

Title	Helium and Hydrogen Re-Emission during Implantation of Molybdenum, Vanadium and Stainless Steel
Reference	J. Nucl. Mat., 53 (1974) 127
Authors	W. Bauer, G.J. Thomas
Institution	Sandia Laboratories, Livermore, USA

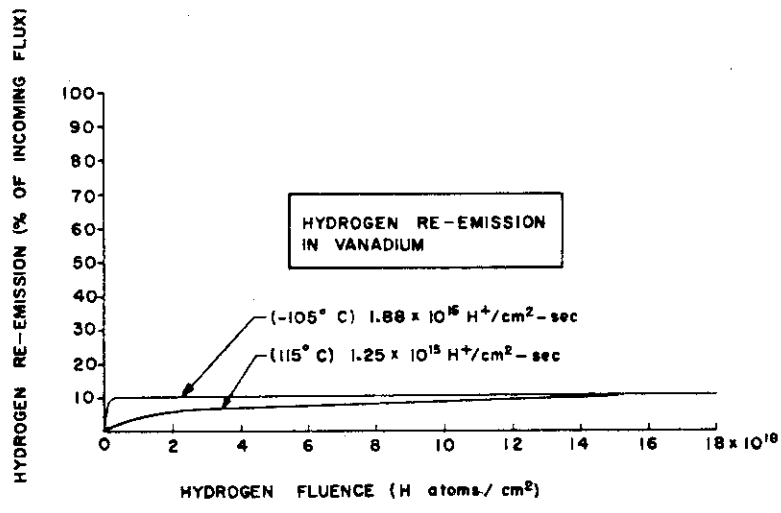

Fig. 6. Hydrogen re-emission during 150 keV H implantation as a function of fluence in vanadium at two different implantation temperatures.

RE-41

Title	Blistering and Deuterium Trapping Induced by D^+ Ion Bombardment in Metal Alloys
Reference	J. Nucl. Mat., 93 & 94 (1980) 739
Authors	B. Navinsek, M. Peternel, Zabkar(a) S.K. Brentz(b)
Institution	(a) J. Stefan Institute, University of Ljubljana, Yugoslavia (b) Culham Laboratory, UKAEA, UK

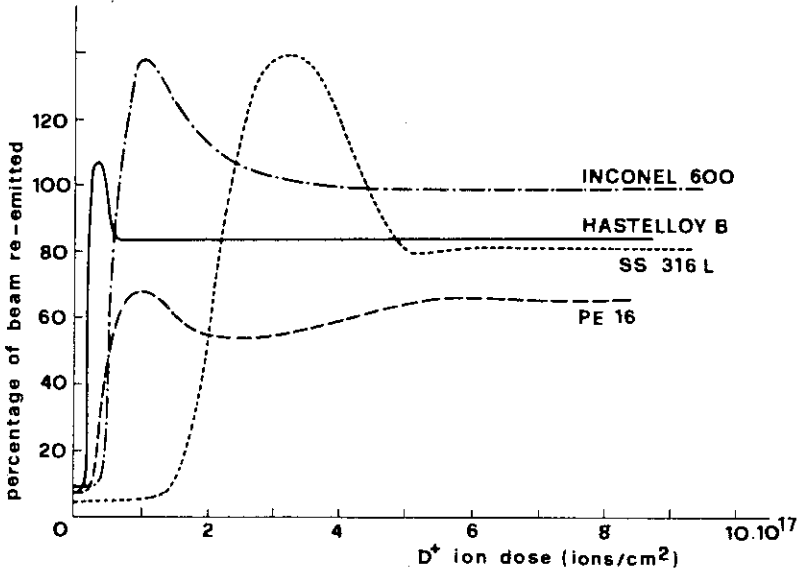

Fig. 1. Re-emission of D_2 during 36 keV D^+ bombardment of various stainless steels and nickel-based alloys at 300 K.

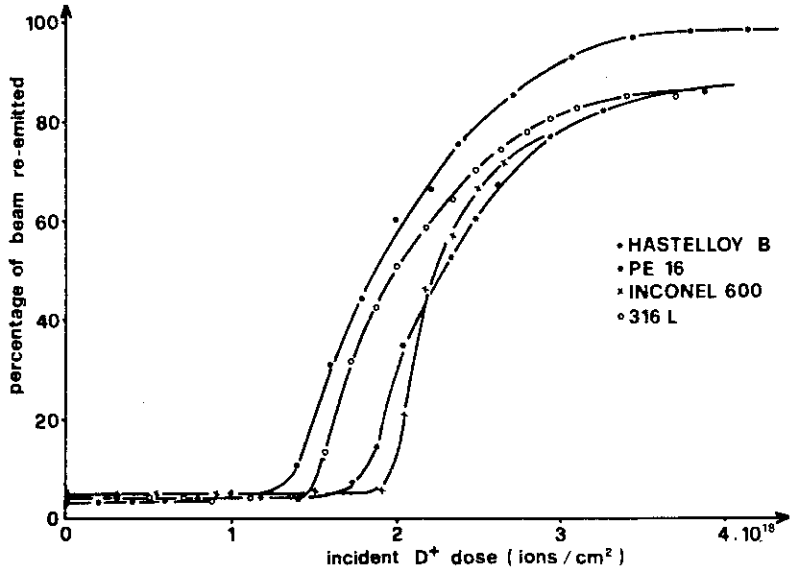

Fig. 2. Re-emission of D_2 during 33 keV D^+ bombardment of various stainless steels and nickel-based alloys at 77 K.

RE-51

Title	Low Energy Proton Induced Re-Emission of Deuterium from Carbon
Reference	Nucl. Instr. Methods, 170 (1980) 455
Authors	S.K. Erents
Institution	Culham Laboratory, UK

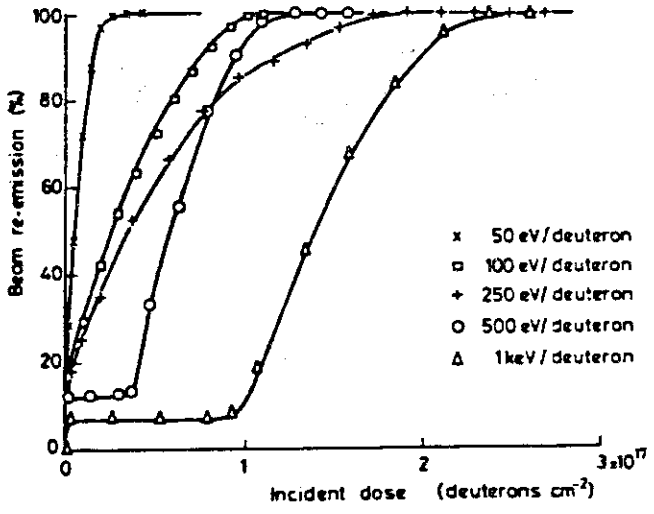

Fig. 1. Deuterium ion trapping in carbon.

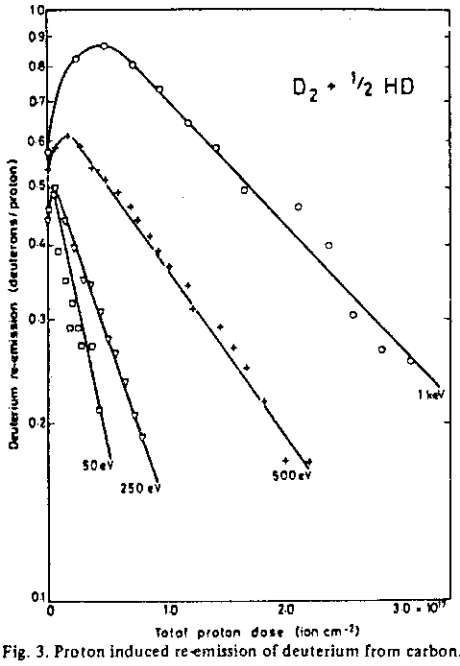

Fig. 3. Proton induced re-emission of deuterium from carbon.

RE-52

Title	Experimental Measurement of Hydrogen Isotope Exchange in Carbon Surfaces under Ion Bombardment
Reference	J. Nucl. Mat., 93 & 94 (1980) 575
Authors	M.C. Underwood, S.K. Erents, E.S. Hotston
Institution	Culham Laboratory, UK

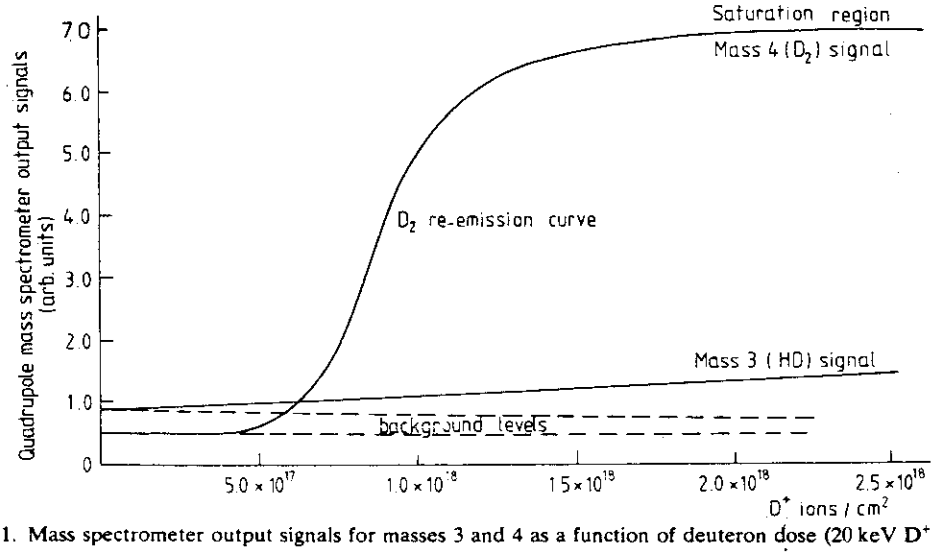

Fig. 1. Mass spectrometer output signals for masses 3 and 4 as a function of deuteron dose (20 keV D^+ ions).

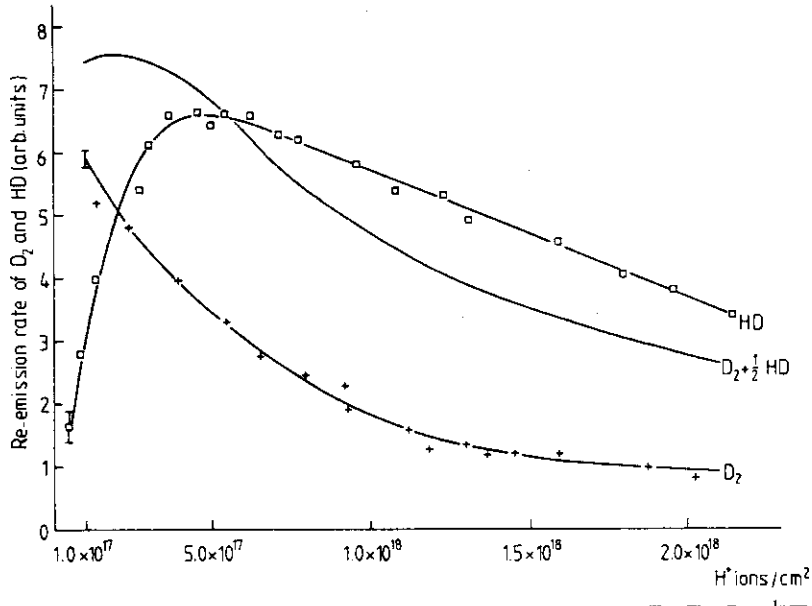

Fig. 2. Background corrected mass spectrometer output signals for the release of D_2 and HD. The $D_2 + \frac{1}{2}$HD curve is also shown (20 keV D^+ and H^+ ions).

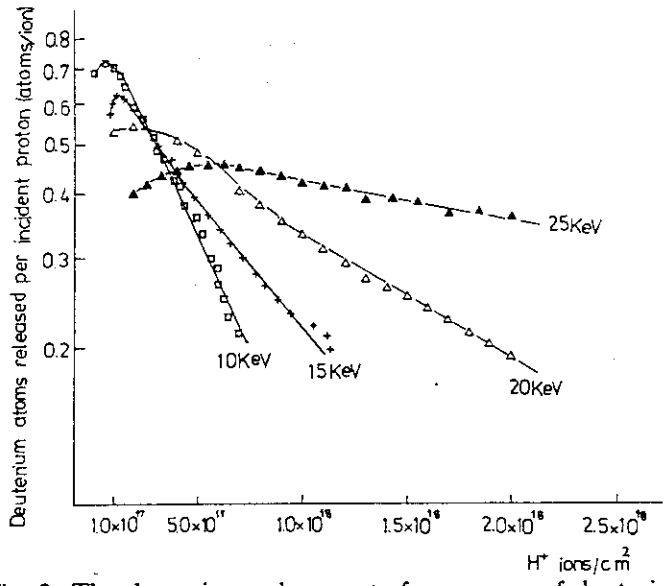

Fig. 3. The deuterium release rate for a range of deuterium implantation energies using protons at energies corresponding to the deuteron energy, as a function of proton dose.

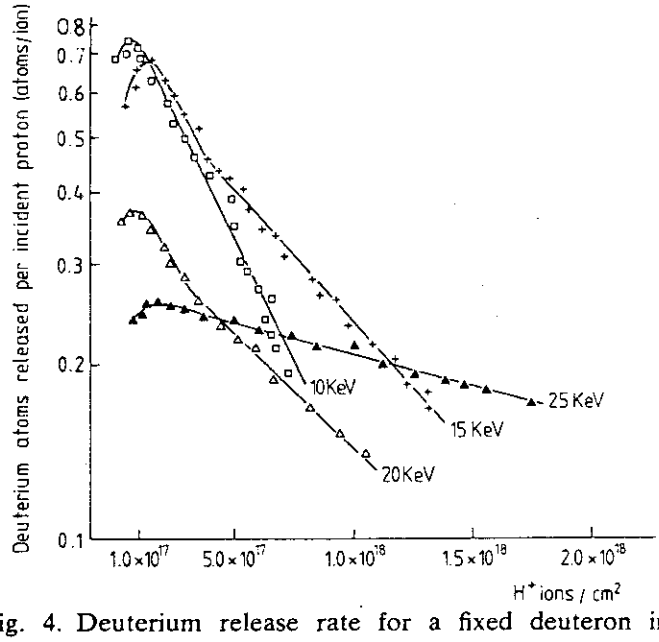

Fig. 4. Deuterium release rate for a fixed deuteron implantation energy of 10 keV and a range of proton energies, as a function of proton dose.

RE-53

Title	The Effect of Radiation Damage on Deuteron Re-Emission and Trapping in Carbon
Reference	J. Nucl. Mat., 111 & 112 (1982) 606
Authors	K. Sone, G.M. McCracken
Institution	UKAEA Culham Laboratory, UK

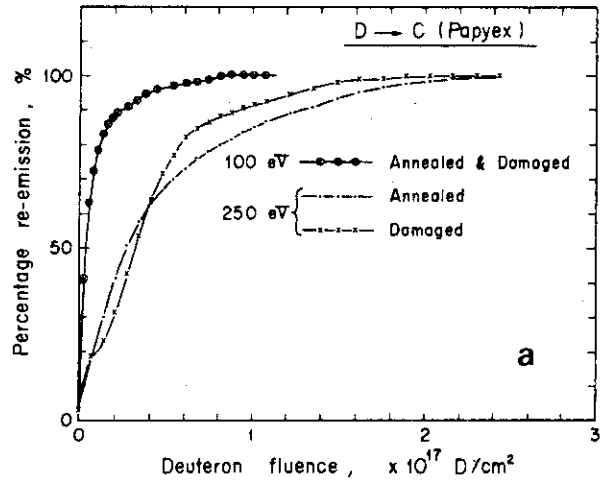

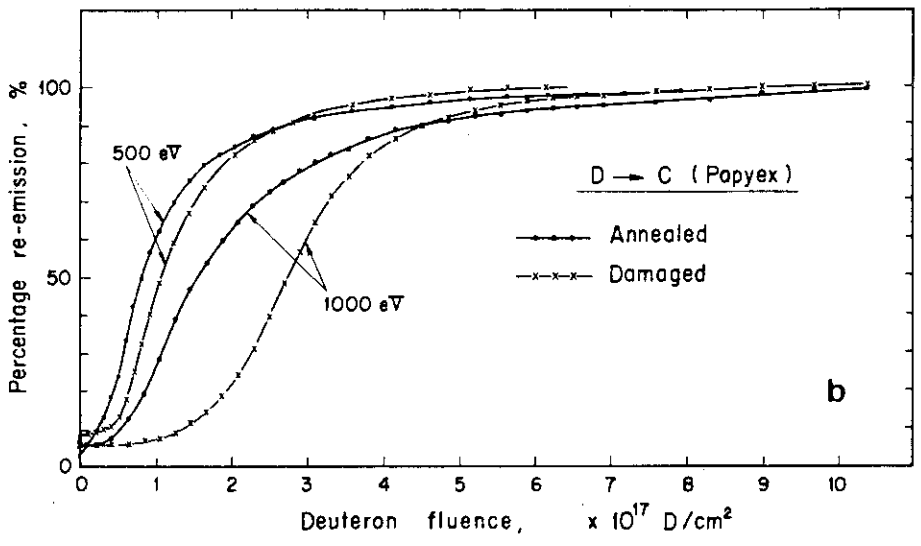

Fig. 1. Typical experimental data of deuterium re-emission from annealed and damaged carbon samples during bombardment with deuterons at room temperature as a function of deuteron fluence for different energies: (a) 100 eV and 250 eV, (b) 500 eV and 1000 eV. In the case of 100 eV the two re-emission curves are not resolved within experimental accuracy.

RE-71

Title	Deuterium Trapping and Release in Titanium-Based Coatings for TFTR
Reference	J. Nucl. Mat., 93 & 94 (1980) 569
Authors	K.L. Wilson, A.E. Pontau
Institution	Sandia National Laboratories, Livermore, USA

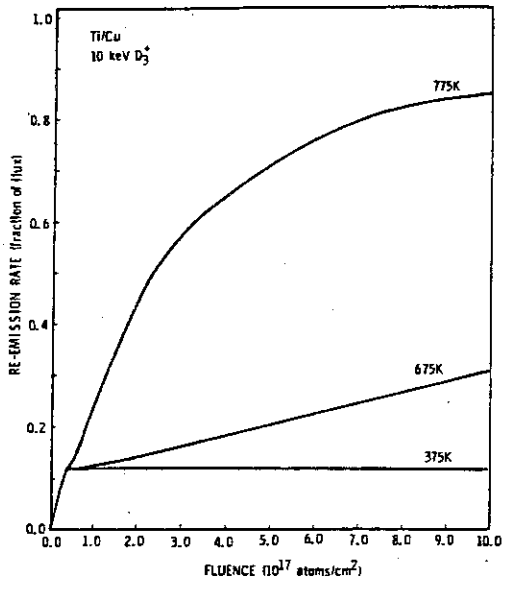

Fig. 1. The re-emission rates as a function of fluence for Ti/Cu claddings implanted at three temperatures.

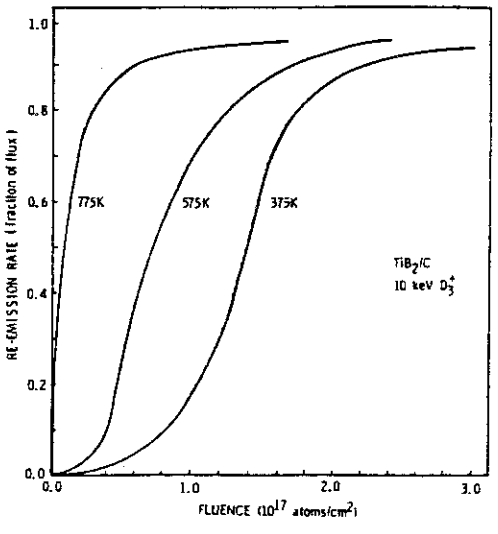

Fig. 4. The re-emission rates as a function of fluence for TiB_2/C implanted at three temperatures.

RE-72

Title	Deuterium Trapping in Low-Z Coatings
Reference	J. Nucl. Mat., 111 & 112 (1982) 590
Authors	S.K. Erents
Institution	Culham Laboratory, UK

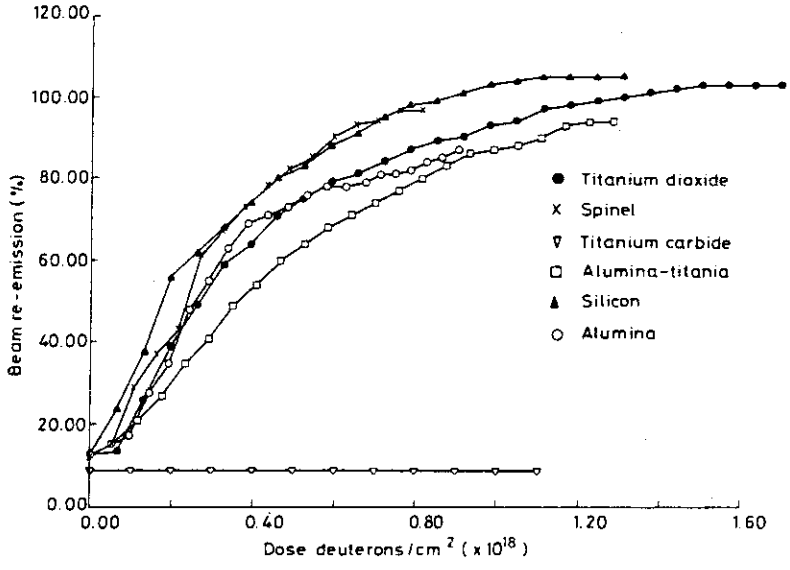

Fig. 1. Beam re-emission as a function of deuteron dose for 2 keV D_2^+ bombardments at 300 K.

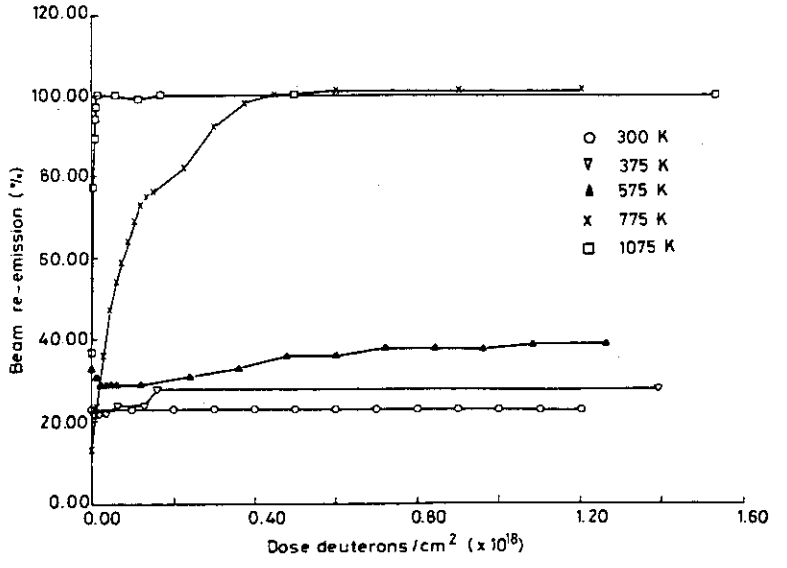

Fig. 6. Beam re-emission from titanium carbide as a function of implant temperature. 500 eV D_2^+ bombardements.

References

RE-01 W. Bauer and G.J. Thomas : Helium and Hydrogen Re-Emission during Implantation of Molybdenum, Vanadium and Stainless Steel, J. Nucl. Mat., 53 (1974) 127.

RE-02 C.M. Braganza and S.K. Erents, E.S. Hotston and G.M. McCracken : Ion-Induce Release of Deuterium Trapping in Stainless Steel, J. Nucl. Mat., 77 & 78 (1978) 298.

RE-03 R.S. Blewer, R. Behrisch, B.M.U. Scherzer and R. Schulz : Trapping and Replacement of 1-14 keV Hydrogen and Deuterium in 316 Stainless Steel, J. Nucl. Mat., 76 & 77 (1978) 305.

RE-04 E.W. Thomas : Retention and Re-Emission of 0.125 - 1 keV Deuterium in Stainless Steel, J. Appl. Phys., 51 (1980) 1176.

RE-05 R.E. Clausing, L.C. Emerson and L. Heatherly : Studies of Hydrogen Recycle from the Wall in Tokamaks Using a Plasma-Wall Interaction Simulator, J. Nucl. Mat., 76 & 77 (1978) 267.

RE-06 K.L. Wilson : Hydrogen Recycling in Properties in Stainless Steel, J. Nucl. Mat., 103 & 104 (1981) 453.

RE-07 K.L. Wilson and M.I. Baskes : Deuterium Re-Emission from 304LN Stainless Steel, J. Nucl. Mat., 111 & 112 (1982) 622.

RE-08 R. Young, E.W. Thomas and B. Emooth : Re-Emission of Implanted Deuterium from the Back Side of a Stainless Steel Membrance, J. Nucl. Mat., 111 & 112 (1982) 642.

RE-09 K.L. Wilson, G.J. Thomas and W. Bauer : Low Energy Proton Implantation of Stainless Steel, Nucl. Tech., 29 (1976) 322.

RE-11 K. Erents and G.M. McCracken : Trapping and Re-Emission of Fast Deuterium Ions from Nickel, J. Phys. D, 2 (1969) 1397.

RE-12 S.K. Erents : Trapping and Re-Emission of Deuterium from Molybdenum following Bombardment at 77K, Vacuum, 24, 445.

RE-13 T. Tanabe, N. Saito, Y. Etoh and S. Imoto : Permeation and Re-Emission of Deuterium Implanted in Fast Wall Materials, J. Nucl. Mat., 103 & 104 (1981) 483.

RE-14 See RE-01.

RE-31 See RE-01.

RE-41 B. Navinšek, M. Peternel, Žabkar and S.K. Brontz : Blistering and Deuterium Trapping Induced by D^+ Ion Bombardment in Metal Alloys, J. Nucl. Mat., 93 & 94 (1980) 739.

RE-51 S.K. Erents : Low Energy Proton Induced Re-Emission of Deuterium

from Carbon, Nucl. Instr. Methods, 170 (1980) 455.

RE-52 M.C. Underwood, S.K. Erents and E.S. Hotston : Experimental Measurement of Hydrogen Isotope Exchange in Carbon Surfaces under Ion Bombardment, J. Nucl. Mat., 93 & 94 (1980) 575.

RE-53 K. Sone and G.M. McCracken : The Effect of Radiation Damage on Deuteron Re-Emission and Trapping in Carbon, J. Nucl. Mat., 111 & 112 (1982) 606.

RE-71 K.L. Wilson and A.E. Pontau : Deuterium Trapping and Release in Titanium-Based Coatings for TFTR, J. Nucl. Mat., 93 & 94 (1980) 569.

RE-72 S.K. Erents : Deuterium Trapping in Low-Z Coatings, J. Nucl. Mat., 111 & 112 (1982) 590.

3.2 Retention

3.2.1 Amount of Retention

RT-01 through 06 are concerned with the amount of retention in stainless steel, RT-11 through RT-17, in Ni, Mo and Fe, RT-31 and 32, in Ti and Zr, RT-51 through 57, in graphite and RT-71 through 76, in low mass number materials, respectively.

Hydrogen retention reaches to suturation at a certain level of fluence. RT-04, 11 and 13 refer to the experiments where preliminary bombardment by He increases the retained amount of hydrogen isotopes. As the amount of He pre-irradiation increases, then that of hydrogen isotopes retention increases, too. It is, however, true that retained hydrogen isotopes decreases as the time passes for He preirradiation lower than 10^{17} He^{+}/cm^{2} and as He pre-irradiation increases, amount of retention also increases. For the amount of He pre-irradiation more than 10^{17} He^{+}/cm^{2}, the amount of retention decreases as the amount of pre-irradiation increases and it stays same after saturation, according to RT-04.

Temperature dependency of hydrogen isotopes retention is shown in RT-02, 32, 51, 52, 72 through 75. For lower temperature, the amount of retention increases. Energy dependency of retention is shown in RT-51, 55 and 76. For higher energy, retention increases. RT-03, 14, 57 and 71 show the experimental results in which retained hydrogen isotopes are released by bombardment of other hydrogen isotopes and He. RT-03, 14 and 71 show energy dependency of release and RT-57 shows temperature dependency.

RT-01 shows flux dependency of retention where higher flux gives rise to larger retention but it eventually agrees with the case for lower flux. In RT-71 and 72, comparison with retention by lower mass number materials is shown. Lower mass number materials such as graphite show higher retention compared with stainless steel.

RT-01

Title	Depth Profiling of Deuterium Implanted into Stainless Steel at Room Temperature
Reference	Nucl. Instr. Methods, 149 (1978) 59
Authors	J. Altstetter, R. Behrisch, J.Bøttiger, P. Pohl, B.M.U. Scherzer
Institution	Max-Plank-Institut für Plasmaphysik, Garching, F.R.G.

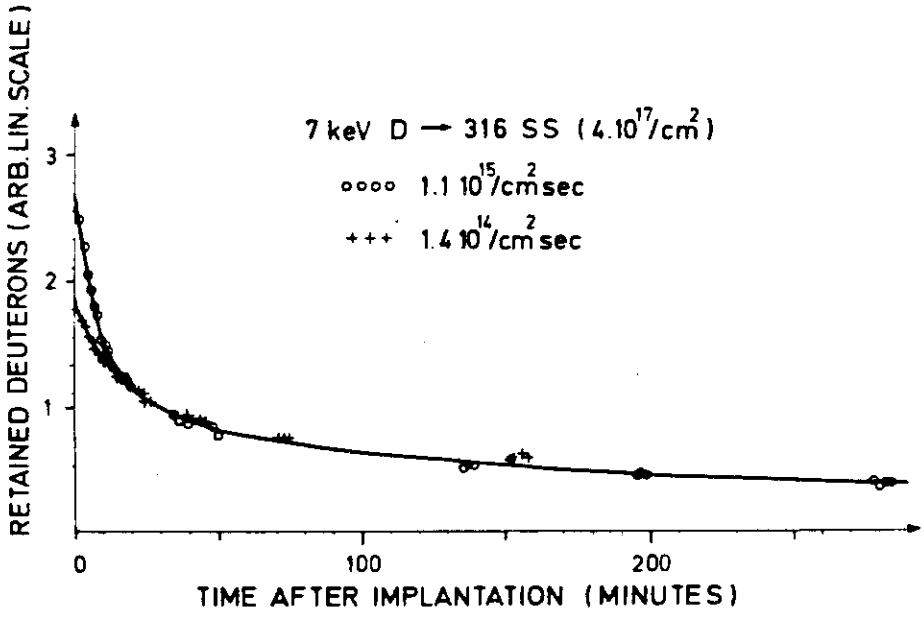

Fig. 1. Deuterium retained in 316 stainless steel in a surface layer of ~400 nm as a function of time after implantation for two different implantation rates. The ^{3}He energy was equal to 0.79 MeV.

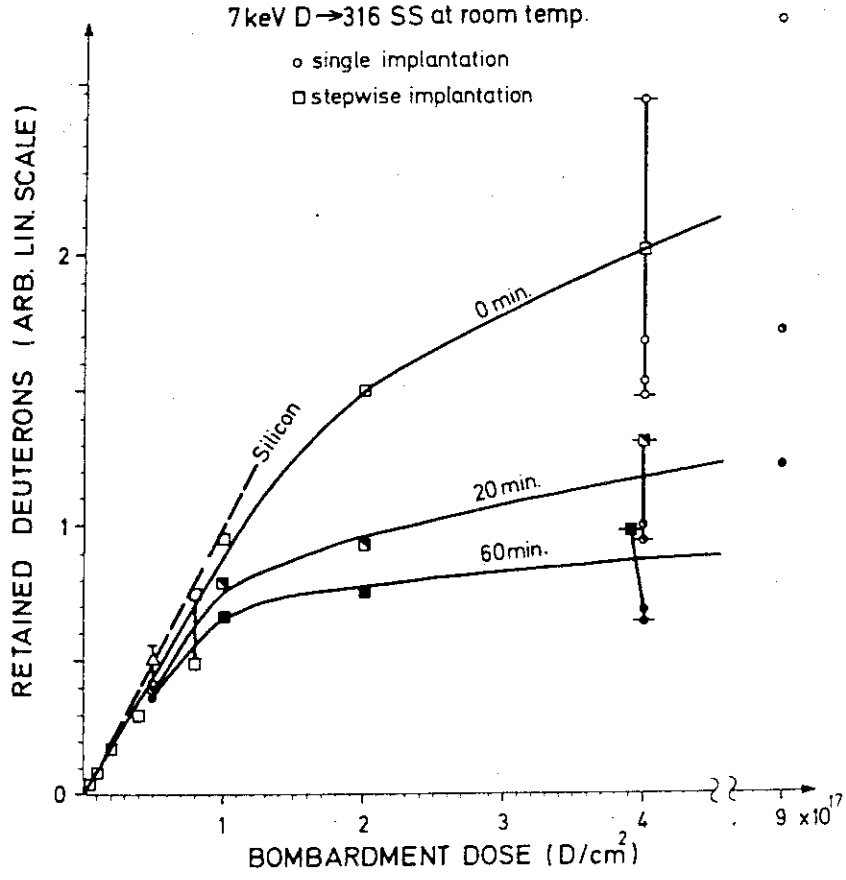

Fig. 2. Deuterons retained in 316 stainless steel as a function of bombardment dose.

RT-02

Title	Trapping of Deuteron Implanted into Stainless Steel at Low Temperature
Reference	J. Vac. Sci. Tech. 15 (1978) 706
Authors	C.J. Altstetter, R. Behrisch, B.M.U. Scherzer
Institution	Max-Plank-Institut für Plasmaphysik, Garching, F.R.G.

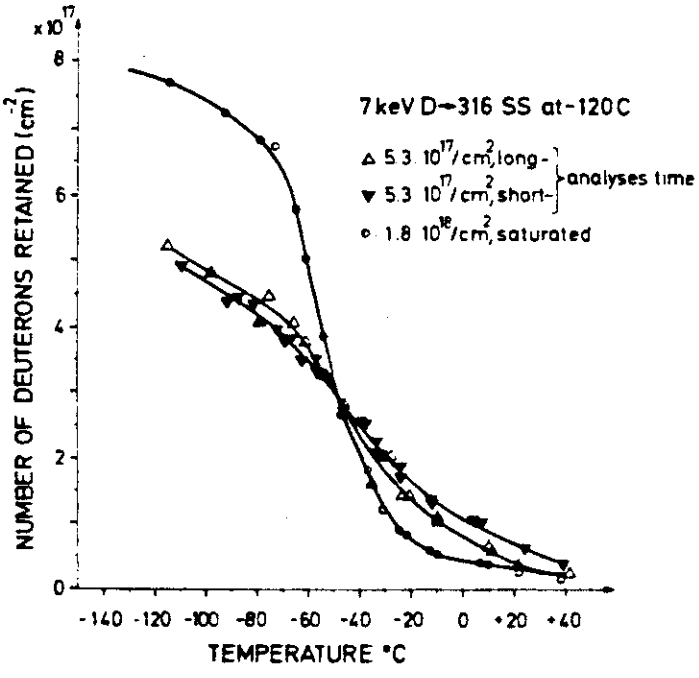

FIG. 4. Loss of deuterium during heating after implantation of 316 stainless steel at 7 keV at −120° C.

RT-03

Title	Trapping and Replacement of 1-14 keV Hydrogen and Deuterium in 316 Stainless Steel
Reference	J. Nucl. Mat., 76 & 77 (1978) 305
Authors	R.S. Blewer, R. Behrish, B.M.U. Scherzer, R. Schule
Institution	Max-Plank-Institut für Plasma, F.R.G.

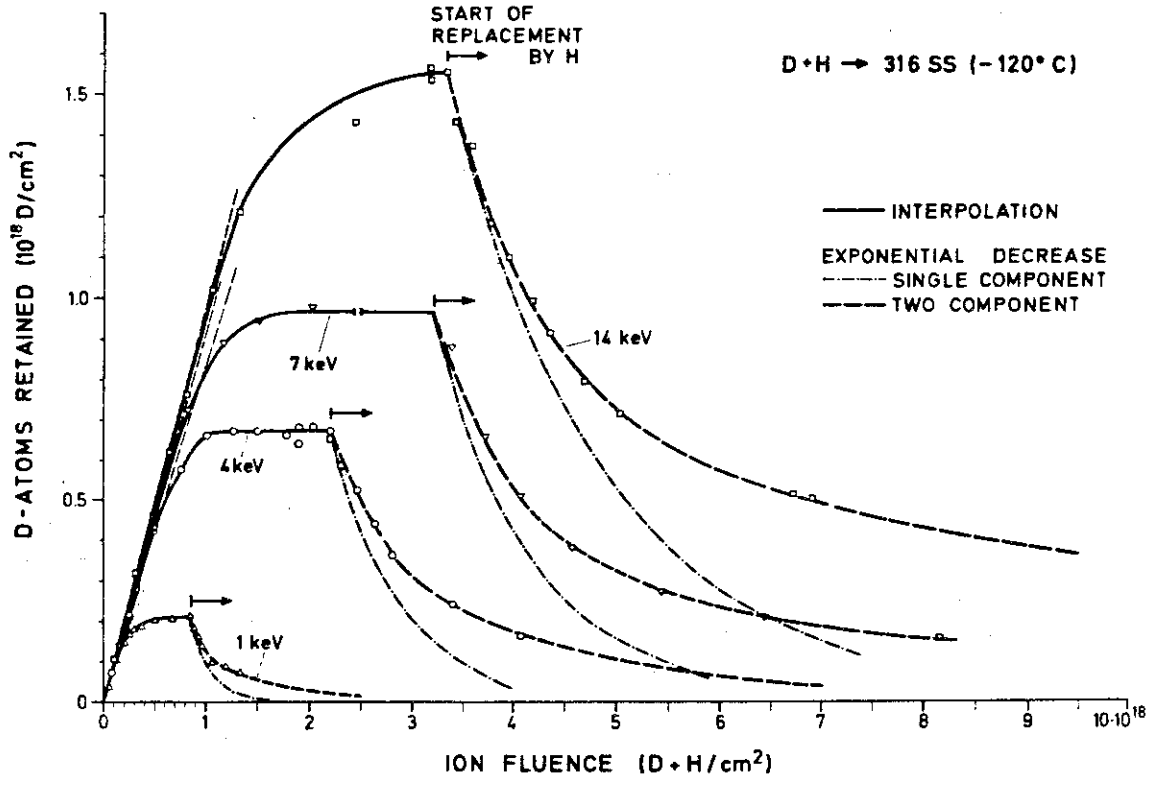

Fig. 2. Trapping and replacement behavior of deuterium implanted stainless steel at 150 K as a function of fluence. The thin dashed lines in the linear portion of the trapping curves represent 100% trapping after kinematic reflection is taken into account. The break in the 7 keV curve at saturation corresponds to an additional fluence of 2×10^{18} D/cm^2.

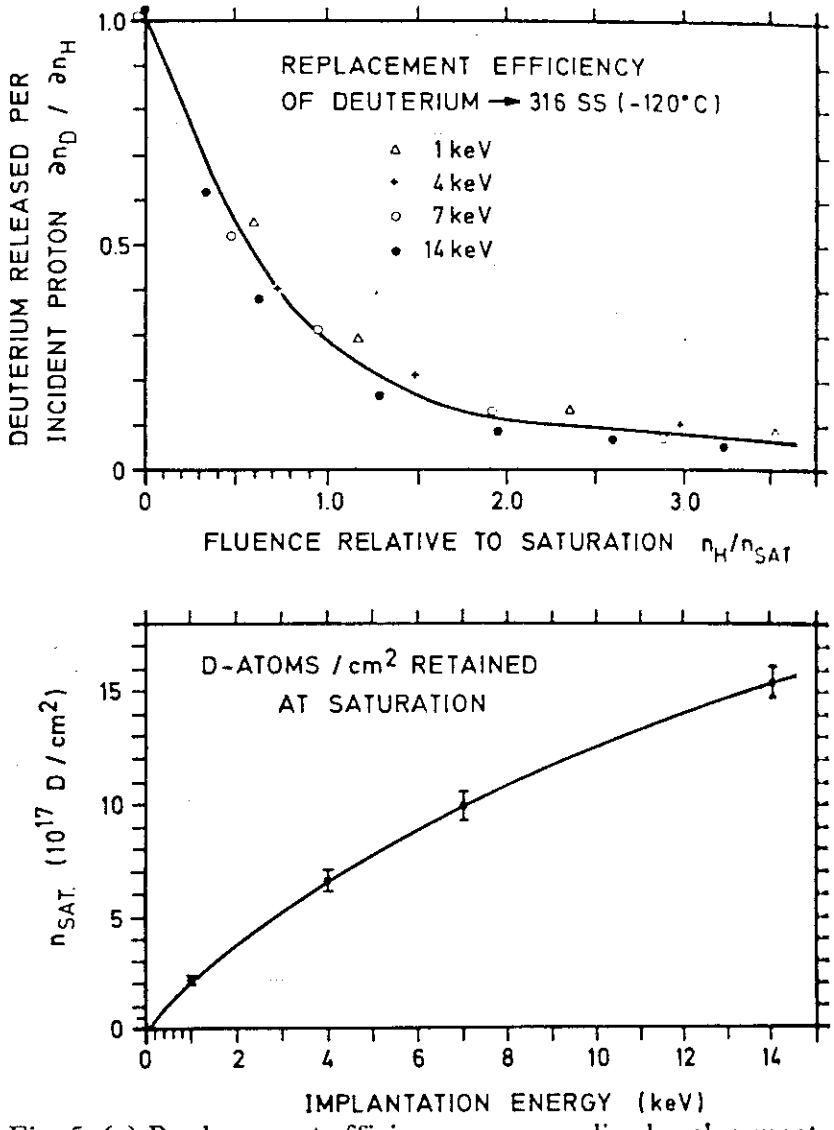

Fig. 5. (a) Replacement efficiency vs. normalized replacement fluence. (b) Trapped deuterium at saturation n_{sat} in units of areal density, vs. implant energy.

RT-04

Title	Trapping of Deuterium in Helium-Damaged Steel: He^+ Fluence Dependence
Reference	J. Nucl. Mat., 103 & 104 (1981) 493
Authors	K.L. Wilson, A.E. Pontau, L.G. Haggmark, M.I. Baskes(a) J. Bohdansky, J.Roth(b)
Institution	(a) Sandia National Laboratories, Livermore, USA (b) Max-Plank-Institut für Plasmaphysik, Garching, F.R.G.

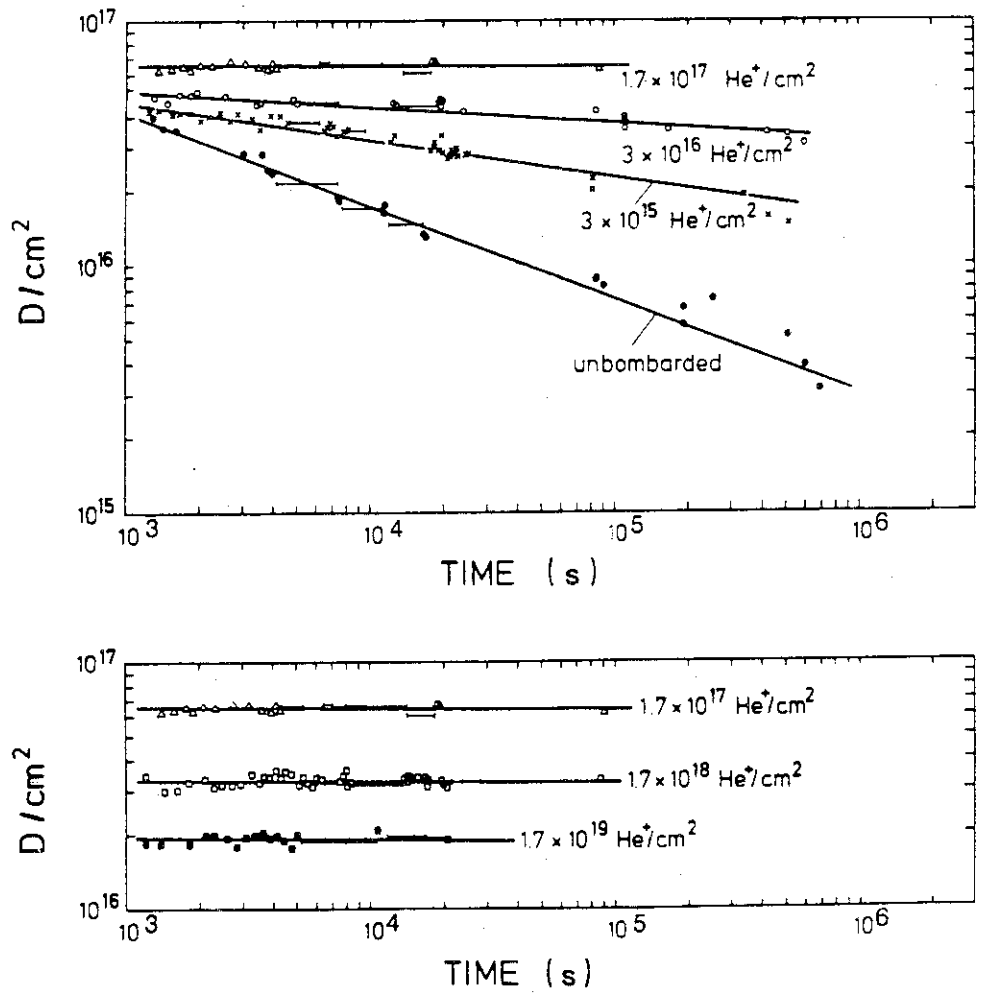

Figure 1. Near-surface deuterium retention (0.5 μm depth) as a function of time for 12R72HV stainless steel samples predamaged with 8 keV He^+ to various fluences followed by a standard implant of 6 keV D_3^+ to 5 x 10^{18} D/cm² fluence at room temperature.

RT-05

Title	Combined Depth Profiling and Thermal Desorption of Implanted Deuterium in 304 LN Stainless Steel
Reference	J. Nucl. Mat., 93 & 94 (1980) 594
Authors	K.L. Wilson, A.E. Pontau, L.G. Haggmark, M.I. Baskes
Institution	Sandia National Laboratories, Livermore, USA

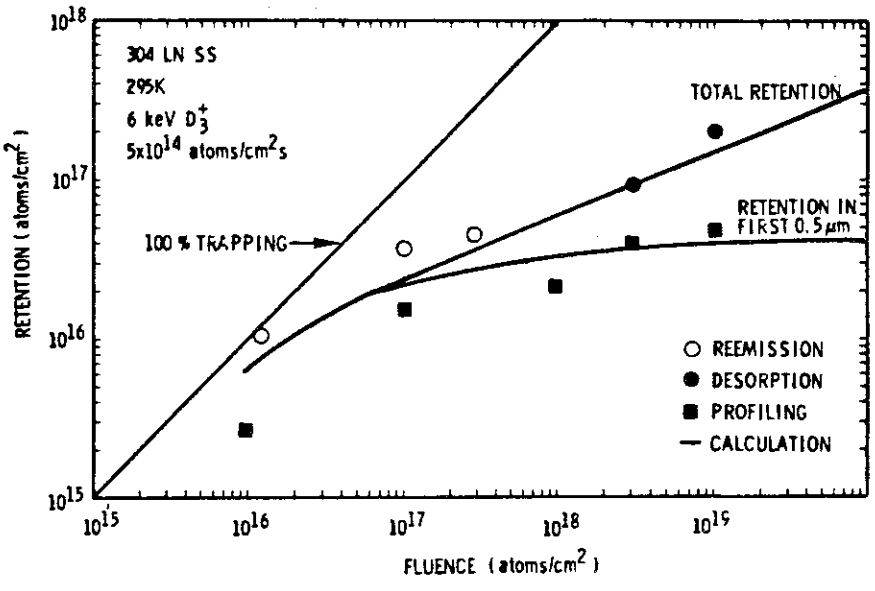

Fig. 3. Retention of deuterium in 304LN stainless steel as a function of fluence. Total retention in the sample was determined from gas re-emission or thermal desorption, while retention in the first 0.5 μm depth was obtained from $D(^3H, \alpha)H$ nuclear reaction profiling. Desorption and profiling samples were quenched after implantation at ≃0.25 K/s. Also shown are DIFFUSE calculations for the two cases.

RT-06

Title	Burial of 60 keV Deuterium Ions in Stainless Steel and Titanium
Reference	Nature, 212 (1966) 1346
Authors	N.J. Freeman, I.D. Latimer, N.R. Daly
Institution	Atomic Weapons Establishment, UK

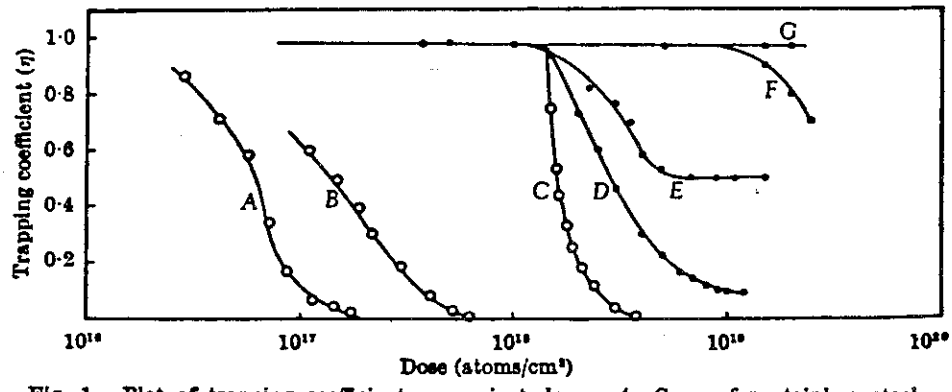

Fig. 1. Plot of trapping coefficient, η, against dose. *A*, Curve for stainless steel, temperature (T) = 390° K; *B*, curve for stainless steel, T = 300° K; *C*, curve for stainless steel, T = 173° K; *D*, curve for titanium, T = 180° K; *E*, curve for titanium, T = 630° K; *F*, curve for titanium, T = 330° K; *G*, curve for titanium, T = 400° K.

RT-11

Title	Hydrogen Trapping in Ion-Implanted Nickel
Reference	J. Nucl. Mat., 93 & 94 (1980) 617
Authors	F. Besenbacher, J. Bøttiger, T. Laursen, W. Möller
Institution	Institute of Physics, University of Aarhus, Denmark

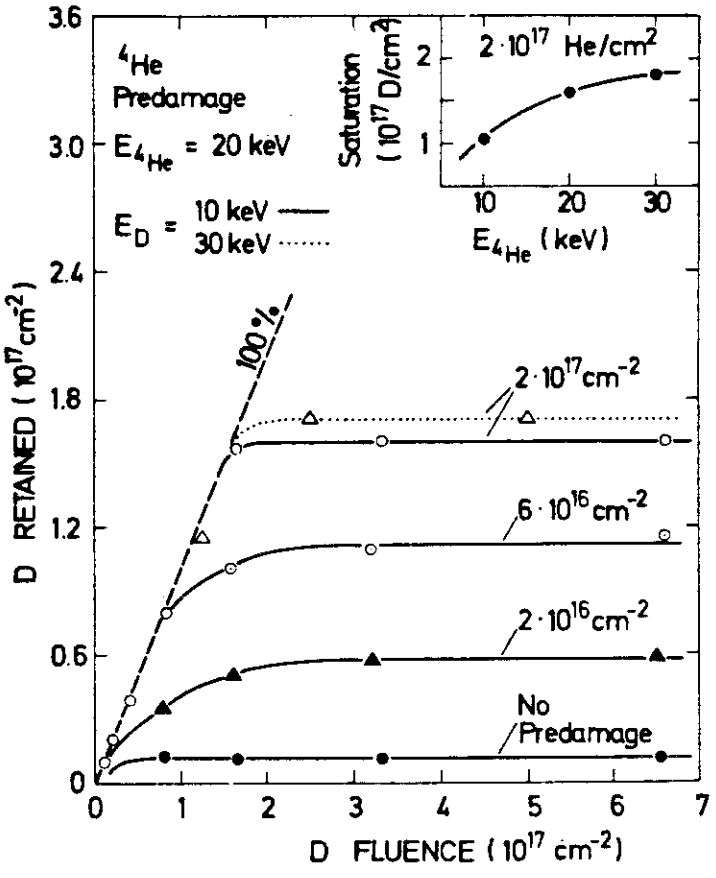

Fig. 2. The total amount of D retained in the near-surface region as a function of D fluence for different He-implantation doses. All measurements performed at room temperature. Insert shows D-saturation levels as a function of He^+ energy.

RT-12

Title	D and ^{3}He Trapping and Mutual Replacement in Molybdenum
Reference	Nucl. Instr. Methods, 168 (1980) 295
Authors	R. Schulz, R. Behrisch, B.M.U. Scherzer
Institution	Max-Plank-Institut für Plasmaphysik, Garching, F.R.G.

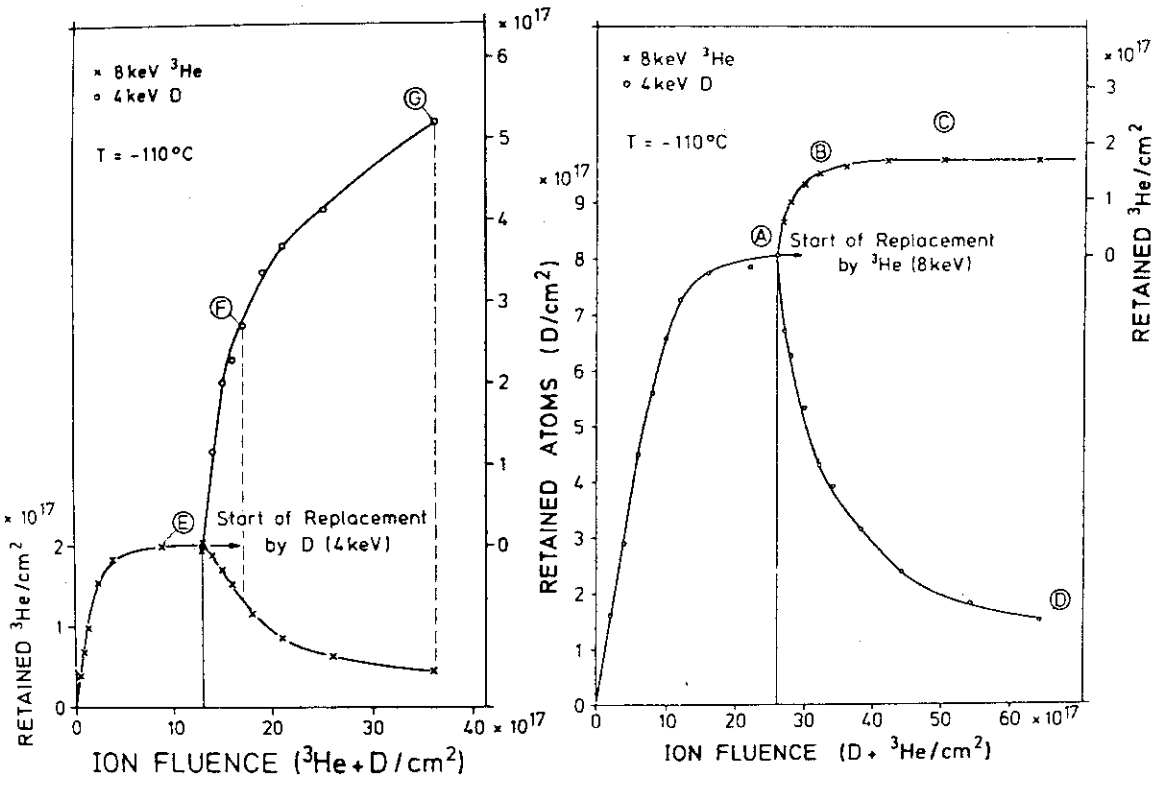

Fig. 1. (a) Areal density of retained ^{3}He and D in polycrystalline Mo as a function of fluence for implantation with 8 keV ^{3}He ions and subsequent replacement by 4 keV D ions. (b) Areal densities for a first implantation with D ions and subsequent replacement by ^{3}He ions. The letters A to G mark the fluences were the depth profiles of fig. 2 were taken.

RT-13

Title	Enhanced Hydrogen Trapping due to He Ion Damage
Reference	J. Nucl. Mat., 63 (1976) 110
Authors	S.T. Picraux(a) J. Bøttiger, N. Rud(b)
Institution	(a) Sandia Laboratories, Albuquerque, USA (b) University of Aarhus, Denmark

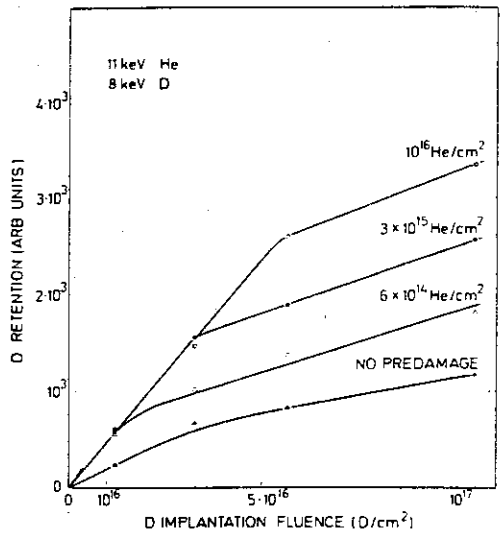

Fig. 2. Total near-surface D retention in single-crystal Mo versus 8 keV D injection fluence as a function of 11 keV ^{4}He predamage fluence.

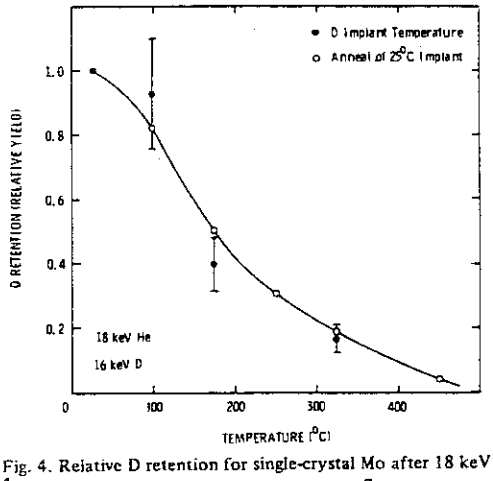

Fig. 4. Relative D retention for single-crystal Mo after 18 keV ^{4}He bombardment at room temperature to a fluence 3×10^{15}/cm^2 followed by 16 keV D injection to a fluence of 1.9×10^{16}/cm^2 at various temperatures (filled circles). Also shown is the D retention versus anneal temperature for a sample with the same He predamage and 25°C D injection to $\approx 8 \times 10^{16}$/cm^2 (open circles).

RT-14

Title	Trapping and Mutual Release of D and ^{3}He in Molybdenum
Reference	J. Nucl. Mat., 93 & 94 (1980) 608
Authors	R. Schulz, R. Behrisch, B.M.U. Scherzer
Institution	Max-Plank-Institut für Plasmaphysik, Garching, F.R.G.

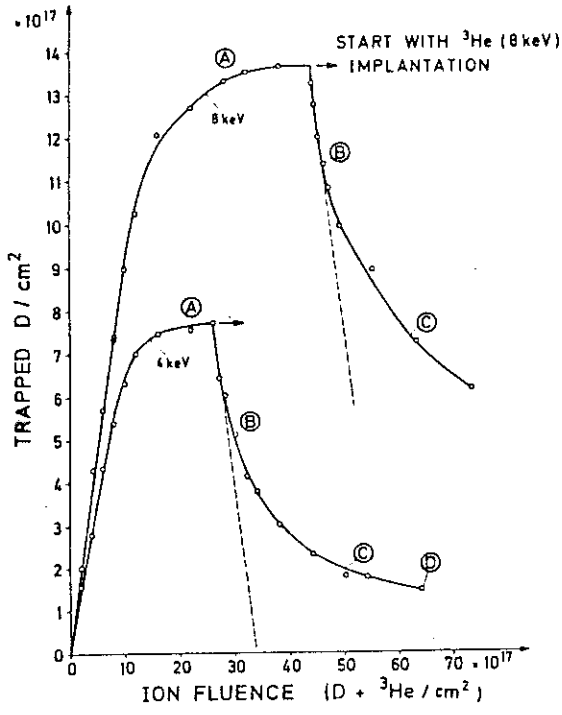

Fig. 1. Areal densities of retained D at 4 and 8 keV in polycrystalline Mo at $T = 160$ K as a function of implantation fluence and subsequent detrapping by 8 keV ^{3}He ions. The letters A, B, etc. mark the fluence where the depth profiles (figs. 8 and 9) were taken. The initial decrease of the first implant during the second bombardment is marked by the dashed lines.

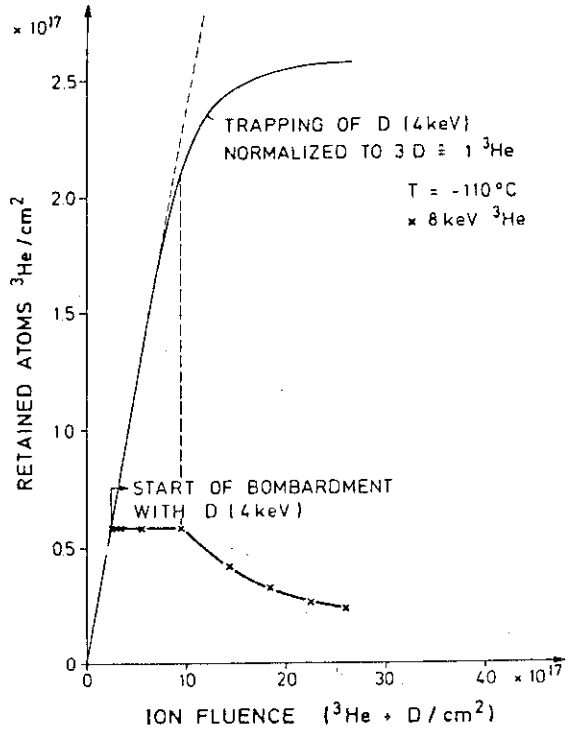

Fig. 3. Areal densities of 8 keV ^{3}He (unsaturated) as a function of postbombarded 4 keV D ion fluence.

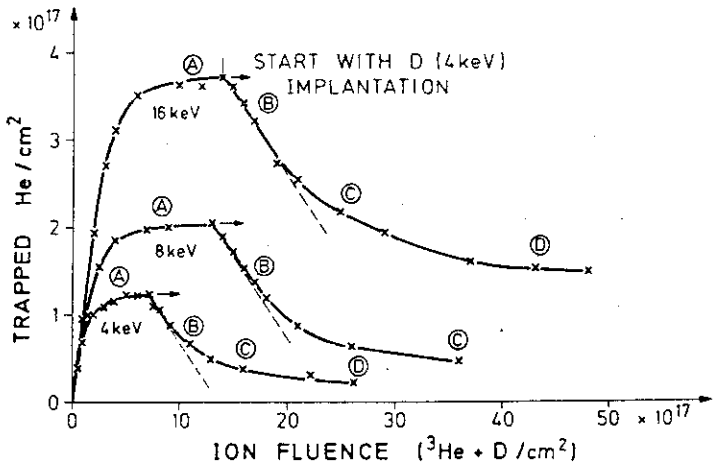

Fig. 2. Areal densities of retained ^{3}He at 4, 8, and 16 keV as a function of implantation fluence and subsequent detrapping by 4 keV D ions.

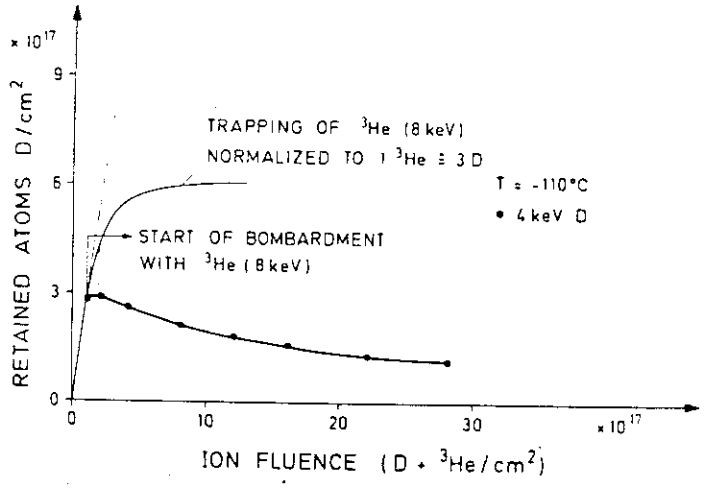

Fig. 4. Areal density of 4 keV D (unsaturated) as a function of postbombarded 8 keV ^{3}He ion fluence.

RT-15

Title	Profile Studies of Hydrogen Trapping in Metals due to Ion Damage
Reference	Appl. Phys. Lett., 28 (1976) 179
Authors	S.T. Picraux, J. Bøttiger, N. Rud
Institution	University of Aarhus, Denmark

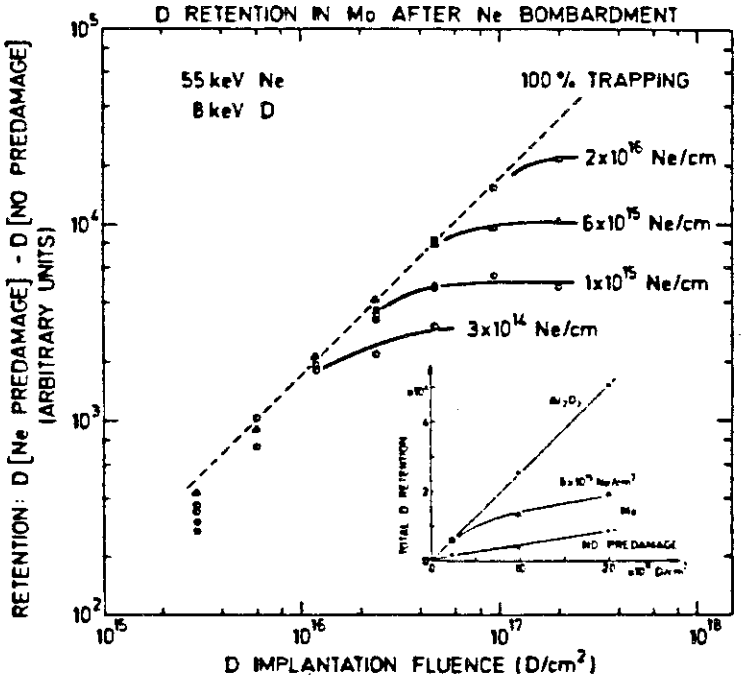

FIG. 2. Total D retained in the near surface region of Mo predamaged with 55-keV Ne less the amount retained without predamage plotted as a function of 8-keV D implantation fluence for the Ne predamage fluences indicated. The inset shows selected raw data. The dashed line corresponds to 100% of the D which comes to rest in the Mo being trapped and is determined by D implants in Al_2O_3 together with correction for D reflection. The filled circles correspond to a 1×10^{15} Ne/cm^2 implanted sample which was annealed to 300 °C for 10 min prior to D bombardment.

RT-16

Title	Trapping of Hydrogen Isotopes in Molybdenum and Niobium Predamaged by Ion Implantation
Reference	J. Appl. Phys., 48 (1979) 920
Authors	J. Bøttiger, S.T. Picraux, N. Rud, T. Laursen
Institution	University of Aarhus, Denmark

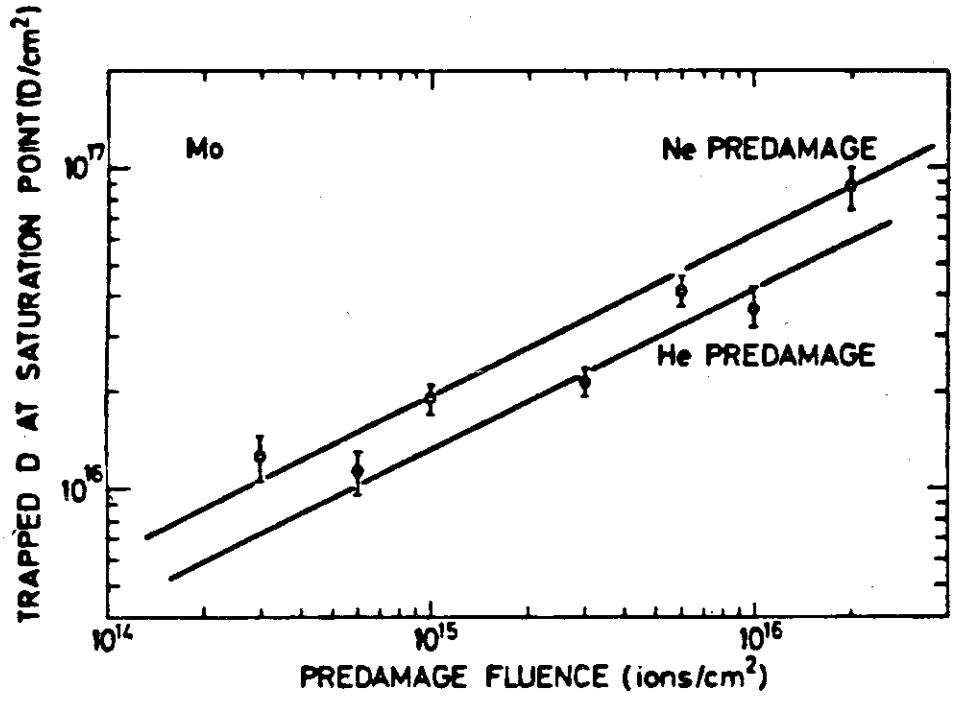

FIG. 4. The amount of D retained at the incident D fluence where saturation occurs shown as a function of predamage fluence for Ne and He. Solid lines correspond to square-root dependence.

RT-17

Title	Deep Deuterium Traps in Y-Implanted Fe
Reference	Appl. Phys. Lett., 37 (1980) 168
Authors	S.M. Myers, S.T. Picraux(a) R.E. Stoltz(b)
Institution	(a) Sandia National Laboratories, Albuquerque, USA (b) Sandia National Laboratories, Livermore, USA

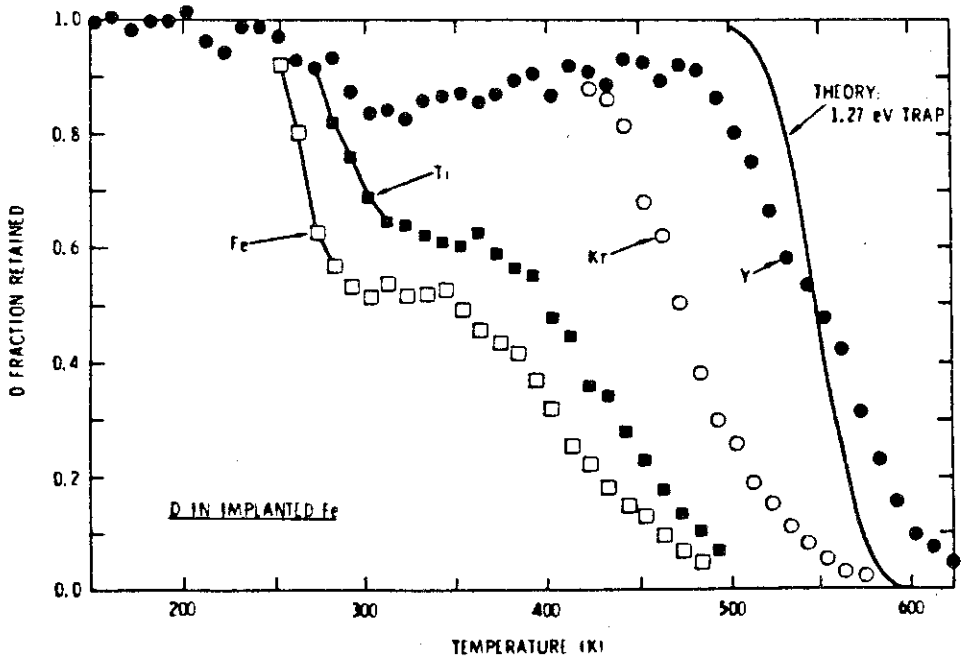

FIG. 1. Deuterium release during linear ramping of temperature for Fe implanted with Y, Kr, Ti, or Fe ions.

RT-31

Title	Trapping Coefficients of Energetic Hydrogen (0.3-0.8 keV) in Ti at High Doses
Reference	J. Nucl. Mat., 63 (1976) 115
Authors	J. Bohdansky, J. Roth, M.K. Sinha, W. Ottenberger
Institution	Max-Plank-Institut für Plasmaphysik, Garching, F.R.G.

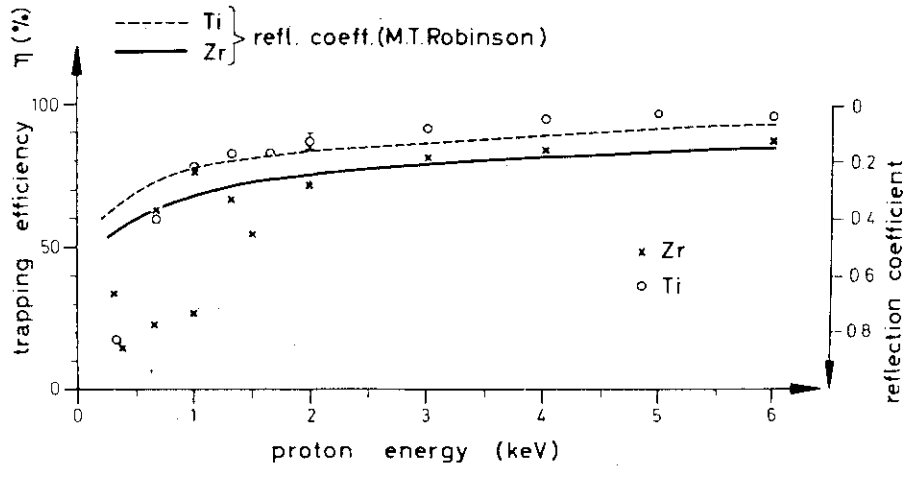

Fig. 1. Experimental values of hydrogen trapping in Zr and Ti compared with calculated reflexion coefficients [8].

RT-32

Title	Temperature-Dependent Depth Profiles of Deuterons Implanted into Zirconium
Reference	J. Nucl. Mat., 76 & 77 (1978) 287
Authors	W. Möller, P. Borgesen, J. Bøttiger
Institution	Institute of Physics, University of Aahus, Denmark

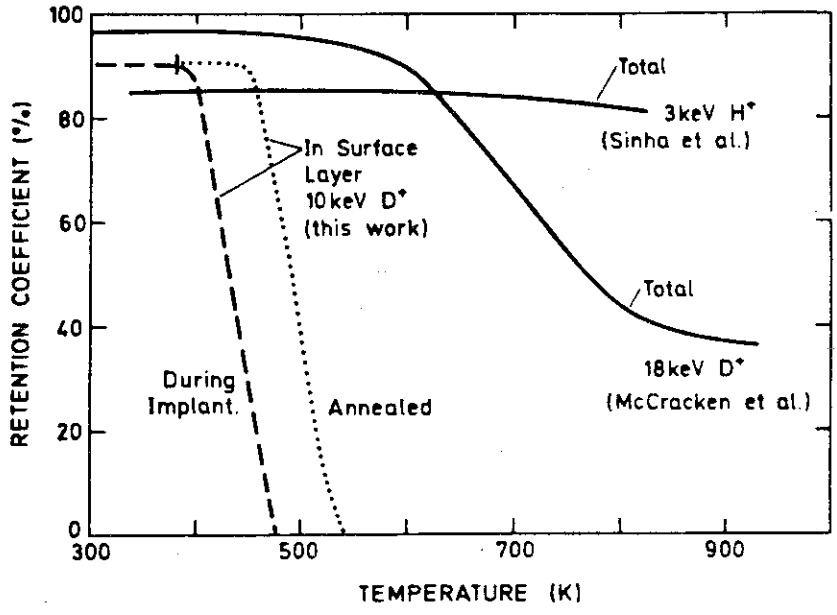

Fig. 6. Retention coefficient η as a function of implantation temperature and annealing temperature (dotted line). Total doses: present study, $\lesssim 2 \times 10^{18}$ ions/cm^2; Sinha et al. [3], 7.5×10^{19} ions/cm^2; McCracken et al. [4], 5×10^{18} ions/cm^2.

RT-33

Title	Burial of 60 keV Deuterium Ions in Stainless Steel and Titanium
Reference	Nature, 212 (1966) 1346
Authors	N.J. Freeman, I.D. Latimer, N.R. Daly
Institution	Atomic Weapons Establishment, UK

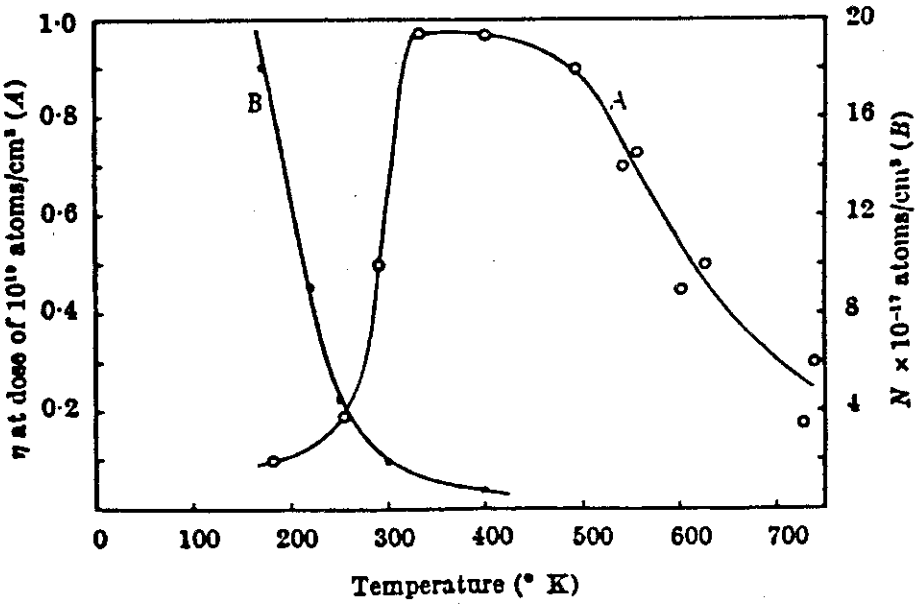

Fig. 2. *A*, Plot of trapping coefficient, η, at a dose of 10^{19} atoms/cm^2 against temperature (T) for titanium. *B*. Plot of total number of particles trapped in the metal per cm^3 (N) against temperature for stainless steel.

RT-51

Title	Temperature Dependence of Trapping and Depth Profiles of 6 to 15 keV Deuterium in Carbon
Reference	J. Nucl. Mat., 63 (1976) 100
Authors	B.M.U. Scherzer, R. Behrish, W. Eckstein, U. Littmark, J. Roth, M.K. Sinha
Institution	Max-Plank-Institut für Plasmaphysik, F.R.G.

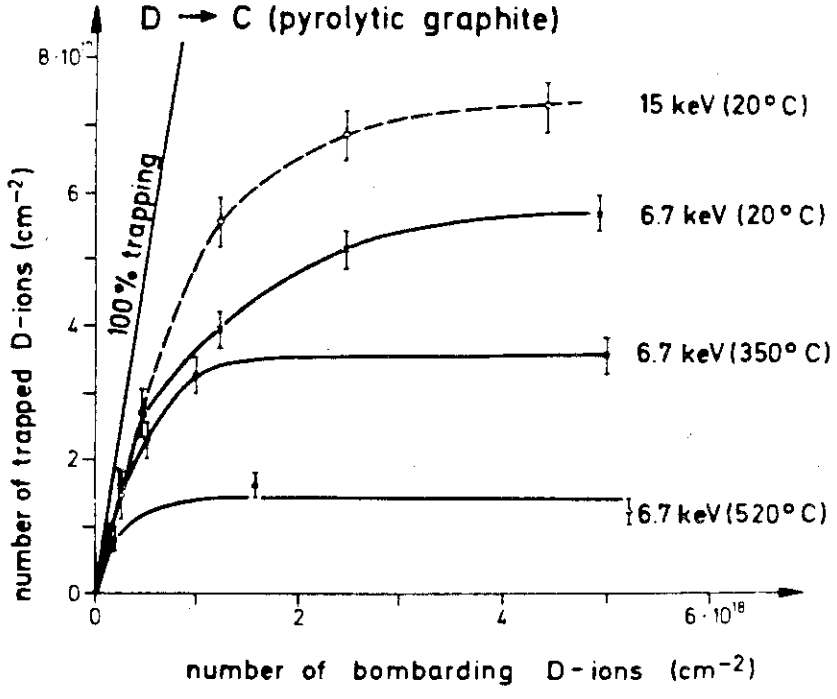

Fig. 3. Amount of deuterium trapped in a surface layer of ~4000 Å (range of sensitivity for the nuclear reaction) as a function of primary ion dose.

RT-52

Title	Behavior of Implanted D and He in Pyrolytic Graphite
Reference	J. Nucl. Mat., 76 & 77 (1978) 313
Authors	R.A. Langley, R.S. Blewer(a) J. Roth(b)
Institution	(a) Sandia Laboratories, Albuquerque, USA (b) Max-Plank-Institut für Plasmaphysik, Garching, F.R.G.

R.A. Langley et al. / Behavior of implanted D and He in pyrolitic graphite

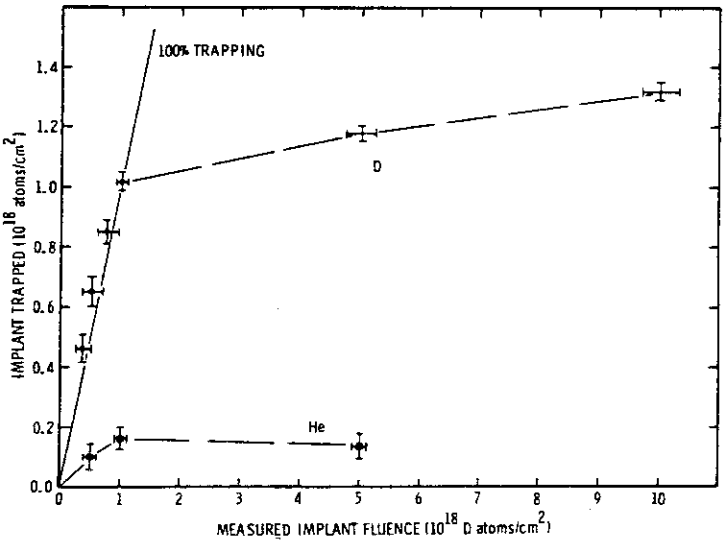

Fig. 3. Implant trapped as a function of implant fluence at room temperature. Dashed lines are included to guide the eye.

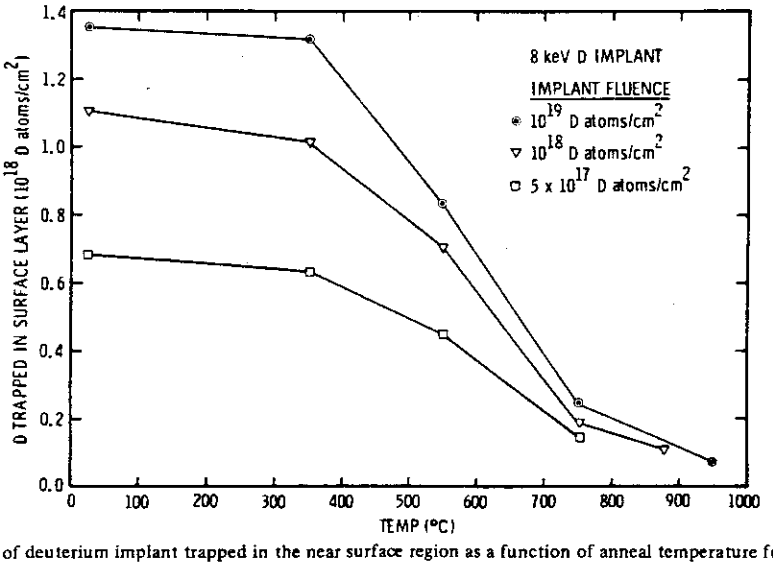

Fig. 5. Amount of deuterium implant trapped in the near surface region as a function of anneal temperature for different fluences.

RT-53

Title	The Trapping of Thermal Atomic Hydrogen on Pyrolytic Grophite
Reference	J. Nucl. Mat., 93 & 94 (1980) 558
Authors	P. Hucks, K. Flaskamp, E. Vietzke
Institution	Institut für Chemie 1 (Nuklearchemie), Kernforshungsanlage, Jülich GmbH, F.R.G.

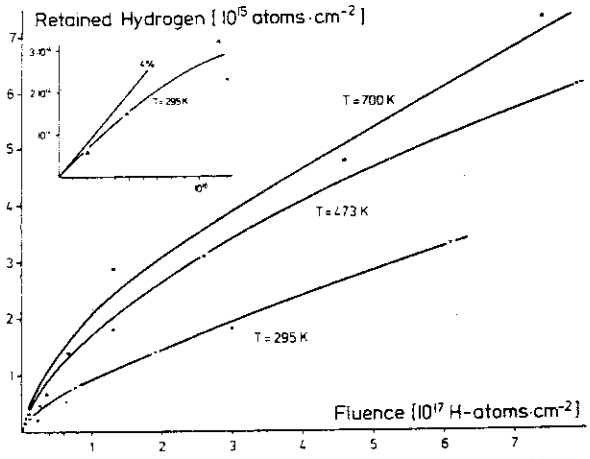

Fig. 2. Retention of hydrogen as a function of the irradiation fluence for different temperatures. Most of these results were obtained in one series except for (Δ), where another source tube and also another selector arrangement was used. The mixing ratio between hydrogen and tritium was 820:1.

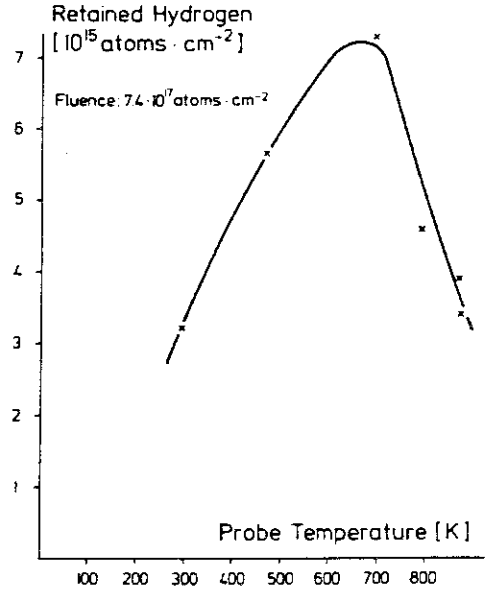

Fig. 4. The temperature dependence of the retention of hydrogen at an irradiation fluence of $7.4 \times 10^{17}\,cm^{-2}$ ([H]:[T] = 820:1).

RT-54

Title	A simple Model for the Trapping of Deuterons in Carbon Target
Reference	Nucl. Instr. Methods, 170 (1980) 449
Authors	S.K. Erents and E.S. Hotston
Institution	Culham Laboratory, UK

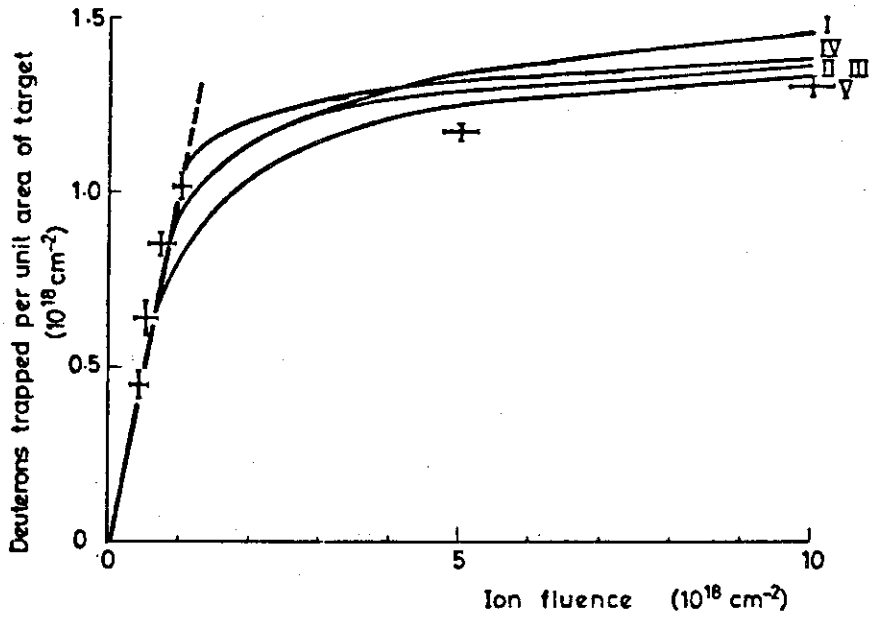

Fig. 2. Deuterons trapped per unit area of carbon target as a function of incident ion influence, for normal bombardment with 8 keV deuterons. The solid lines are the predictions of the model and the experimental points are from ref. 9. The values of A and N_1 used are:

RT-55

Title	The effect of Radiation of Damage on Deuteron Re-Emission and Trapped in Carbon
Reference	J. Nucl. Mat., 111 & 112 (1982) 606
Authors	K. Sone, G.M. McCracken
Institution	UKAEA Culham Laboratory, UK

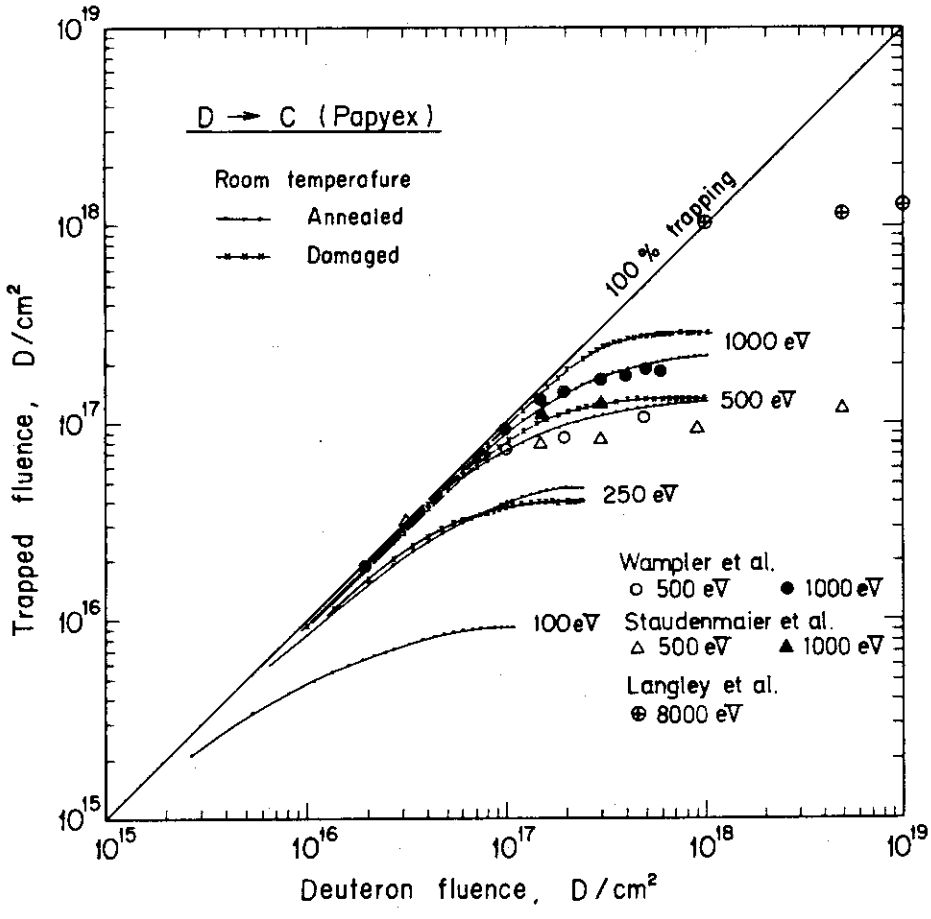

Fig. 2. The amount of deuterons in annealed and damaged carbon samples as a function of fluence for different energies. The data from figs. 1a and 1b have been replotted. Data by Staudenmaier et al. [13], by Langley et al. [14] and by Wampler et al. [15] are plotted for comparison.

RT-56

Title	Ion-Induced Release of Deuterium from Carbon
Reference	J. Nucl. Mat., 111 & 112 (1982) 616
Authors	W.R. Wampler, S.M. Myers
Institution	Sandia National Laboratories, Albuquerque, USA

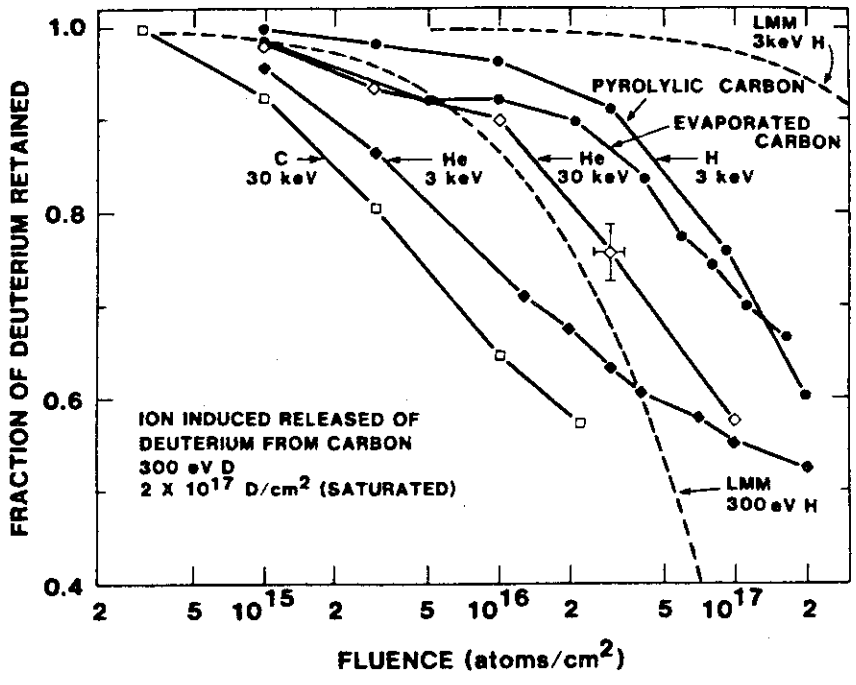

Fig. 2. The fraction of deuterium retained as a function of bombarding ion fluence for carbon samples initially implanted with 2×10^{17} D cm^{-2} incident fluence of 300 eV deuterium. The type of ion and energy of the bombarding ions are indicated. The experimental uncertainty is indicated by the error bars on one of the data points. Except for the curve labeled pyrolytic carbon all the data were taken on evaporated carbon film samples. For comparison the dashed lines show D release curves calculated using the local mixing model (LMM).

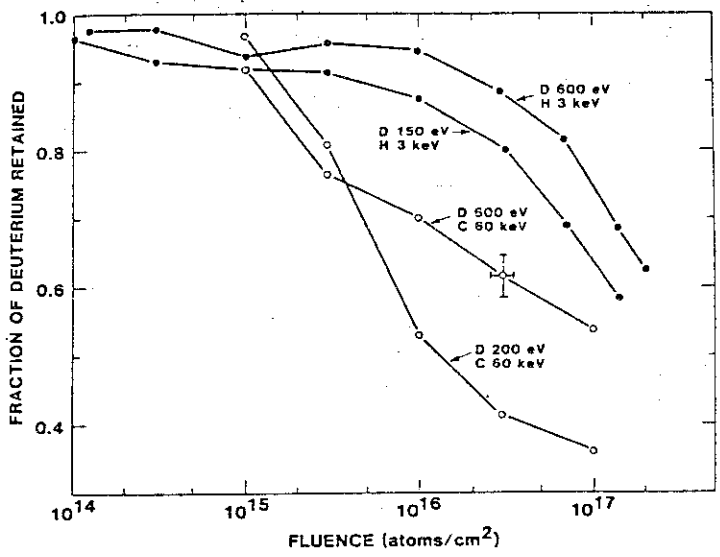

Fig. 3. The fraction of deuterium retained as a function of bombarding ion fluence showing the effects of varying the energy and therefore the depth of the implanted deuterium. Circles show the data for bombarding 60 keV carbon and dots show the data for 3 keV hydrogen. The energy of the implanted deuterium is indicated.

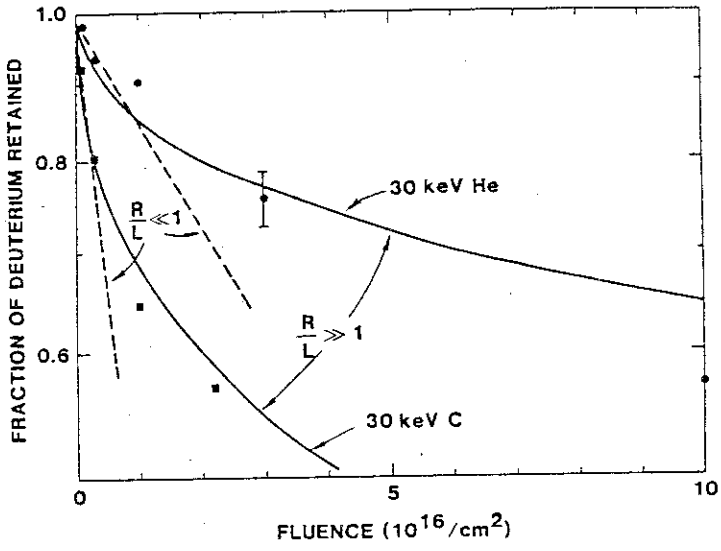

Fig. 4. The fraction of deuterium retained as a function of bombarding ion fluence for carbon implanted with 300 eV deuterium saturation. The dots show the measured data. The dashed lines show the fit for an exponential release curve (corresponding to no retrapping) to the low-fluence portion of the data. The solid lines show the fit for very strong trapping.

RT-57

Title	Temperature Dependence of H Saturation and Isotope Exchange
Reference	J. Nucl. Mat., 103 & 104 (198]) 513
Authors	B.L. Doyle, W.R. Wampler and D.K. Brice
Institution	Sandia National Laboratories, Albuquerque, USA

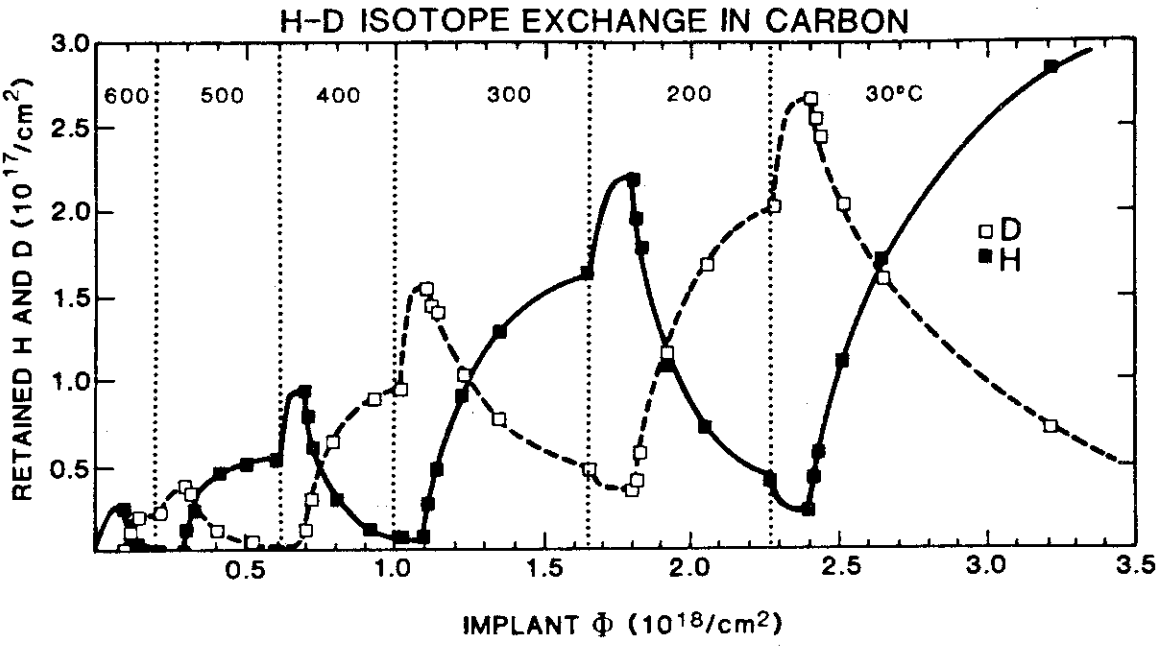

Figure 2. Saturation and isotope exchange of 1.5 keV D and H in carbon. See text for details. A gap is left to indicate where the sample is implanted to saturation at each new temperature. The solid (dashed) curves are intended to guide the eye through the H (D) data.

RT-71

Title	Saturation and Isotopic Replacement of Deuterium in Low-Z Materials
Reference	J. Nucl. Mat., 93 & 94 (1980) 551
Authors	B.L. Doyle, W.R. Wampler, D.K. Brice, S.T. Picraux
Institution	Sandia National Laboratories, Albuerque, USA

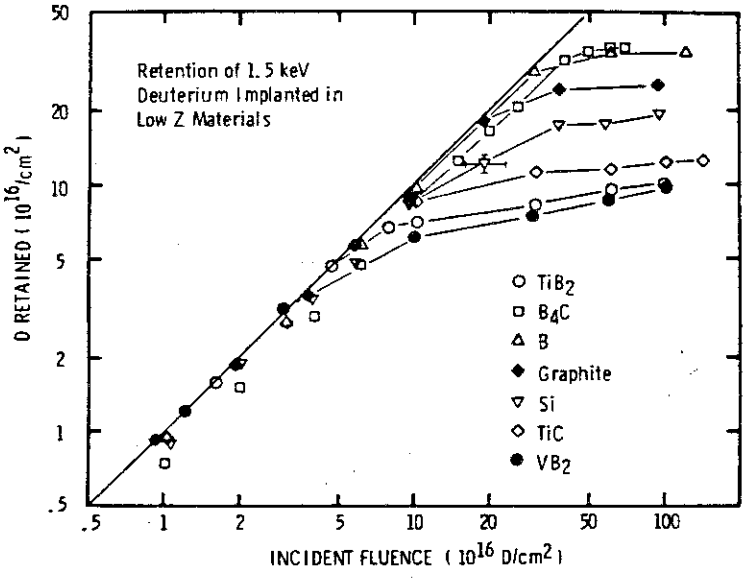

Fig. 2. D saturation curves for the materials in this study.

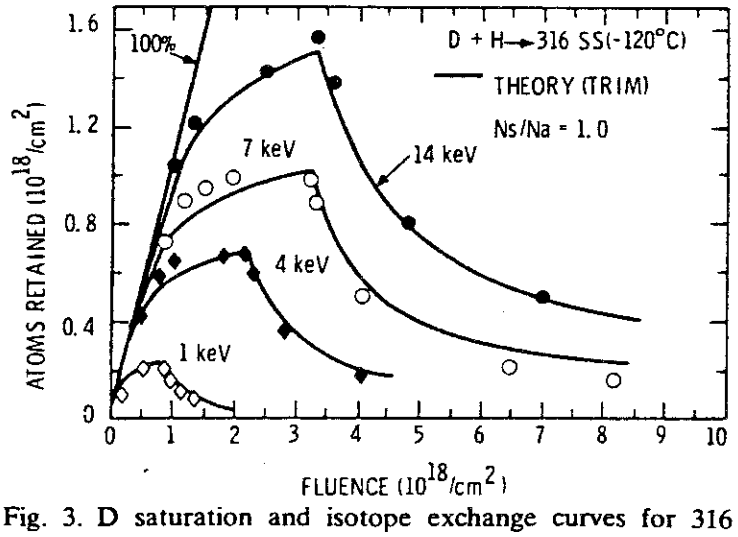

Fig. 3. D saturation and isotope exchange curves for 316 stainless steel at several incident energies. See text for details.

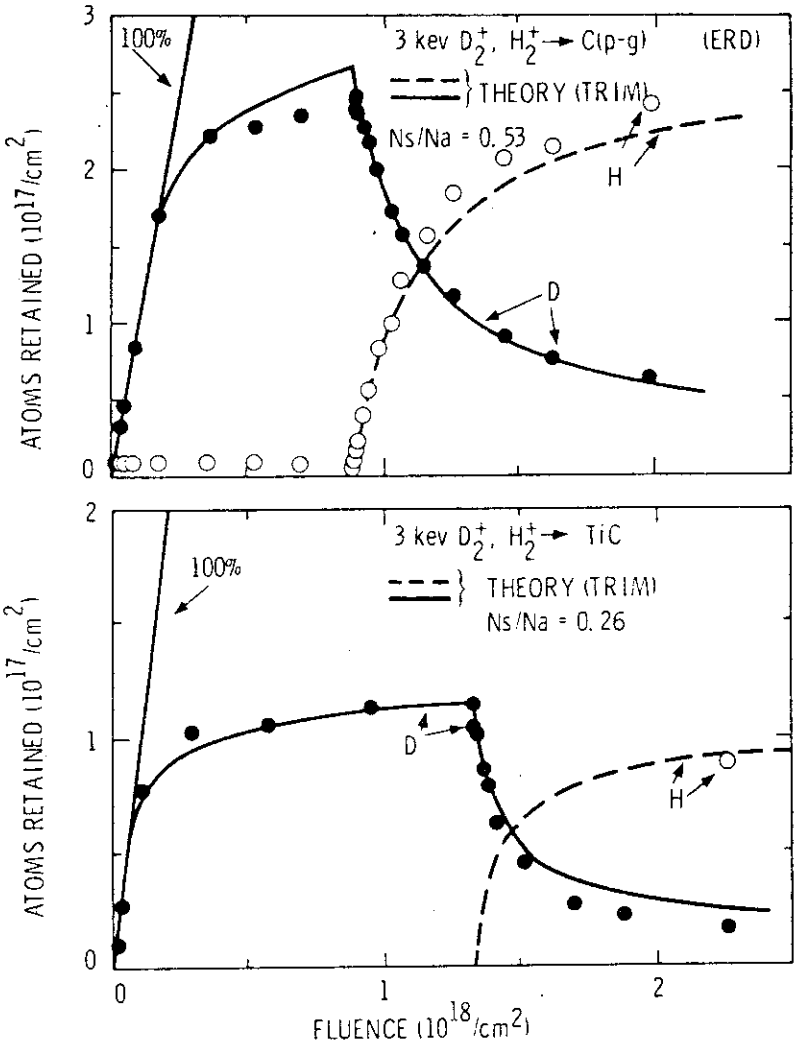

Fig. 4. D saturation and isotopic replacement curves for 3 keV D_2^+ and H_2^+ on pyrolytic graphite (top) and TiC (bottom).

RT-72

Title	Deuterium Trapping and Release in Titanium-Based Coating for TFTR
Reference	J. Nucl. Mat., 93 & 94 (1980) 569
Authors	K.L. Wilson and A.E. Pontau
Institution	Sandia National Laboratories, Livermore, USA

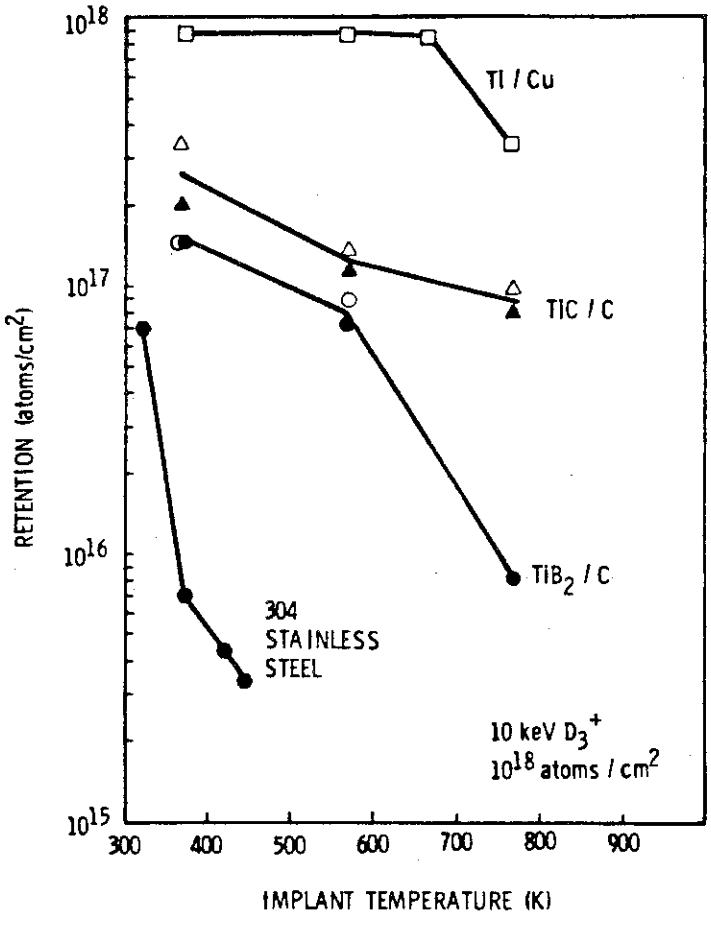

Fig. 6. A summary of the deuterium retention as a function of implant temperature for Ti/Cu, TiB_2/C, and TiC/C implanted with a standard fluence of 1×10^{18} D/cm^2. Data for 304 stainless steel [22] are included for comparison. Re-emission data – open symbols; desorption data – filled symbols. Solid lines are added to guide the eye.

RT-73

Title	Implantation of 5 keV Deuterium in BeO
Reference	Radiat. Eff., 48 (1980) 221
Authors	R. Behrisch, R.S. Blewer, J. Borders, R. Langley, J. Roth, B.M.U. Scherzer, R. Schulz
Institution	Max-Plank-Institut für Plasmaphysik, Garching, F.R.G.

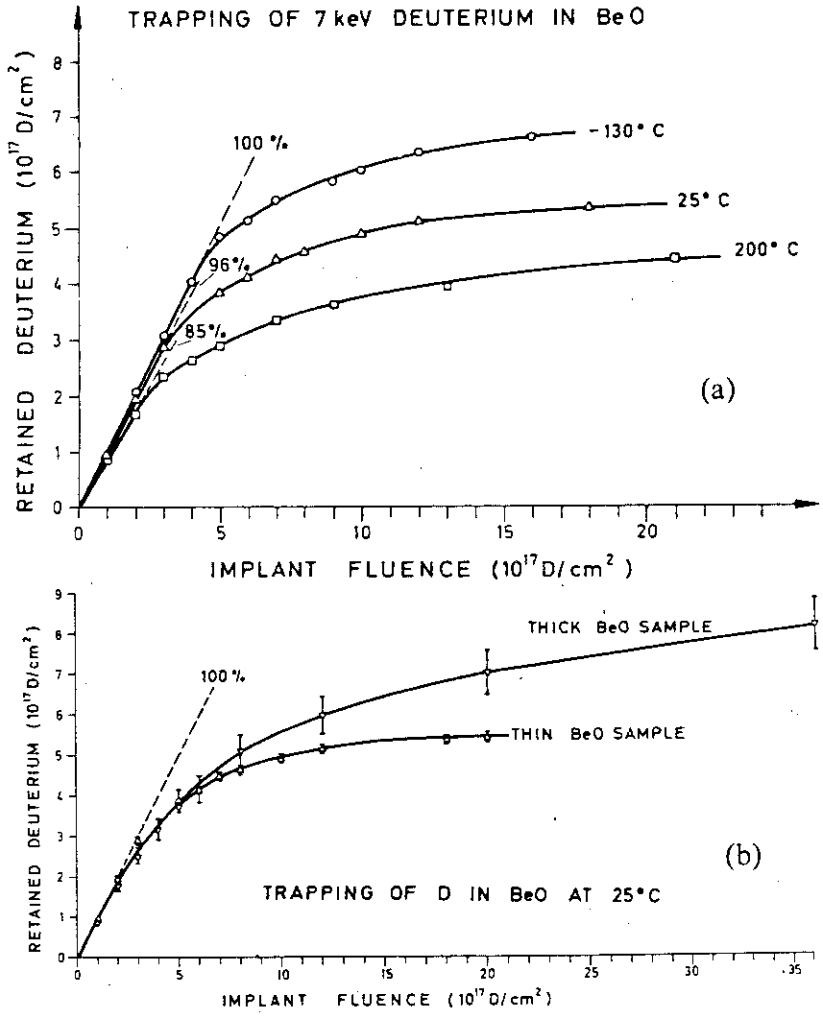

FIGURE 1 (a) Trapping curves for deuterium in a 165 nm layer of BeO as a function of implant fluence at three different temperatures. The fraction of the implant beam which is trapped before the onset of saturation is indicated by dashed lines. (b) Comparison of trapping behavior of 165 nm versus 4000 nm thick layers of BeO at room temperature.

RT-74

Title	Deuterium-Trapping Measurements on Boron Coatings for the TOKAMAK Fusion Test Reactors
Reference	Thin Solid Films, 83 (1981) 73
Authors	K.L. Wilson and A.E. Pontau
Institution	Sandia National Laboratories, Livermore, USA

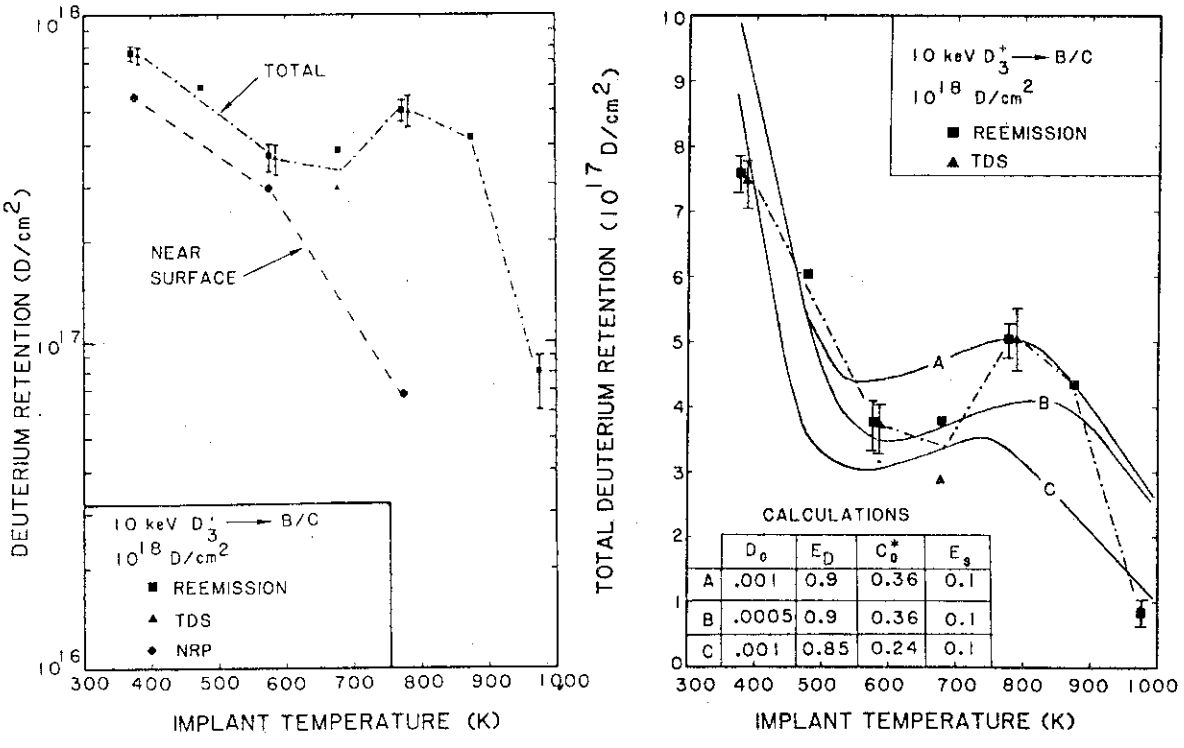

	D_0	E_D	C_0^*	E_S
A	.001	0.9	0.36	0.1
B	.0005	0.9	0.36	0.1
C	.001	0.85	0.24	0.1

Fig. 4. Deuterium retention as a function of implant temperature. The total retention in the sample is based on re-emission and TDS data. Near-surface retention to a depth of about 1 μm is determined from NRP. The lines are added to guide the eye. Error bars represent the variations in the values for multiple samples.

Fig. 5. DIFFUSE numerical calculations of the total retention as a function of implant temperature. The experimental data are from Fig. 4. D_0 is in square centimeters per second, E_D and E_S in electronvolts and C_0^* in atom fraction per (atmosphere)$^{1/2}$.

RT-75

Title	Temperature Dependence of H Saturation and Isotope Exchange
Reference	J. Nucl. Mat., 103 & 104 (1981) 513
Authors	B.L. Doyle, W.R. Wampler, D.K. Brice
Institution	Sandia National Laboratories, Albuquerque, USA

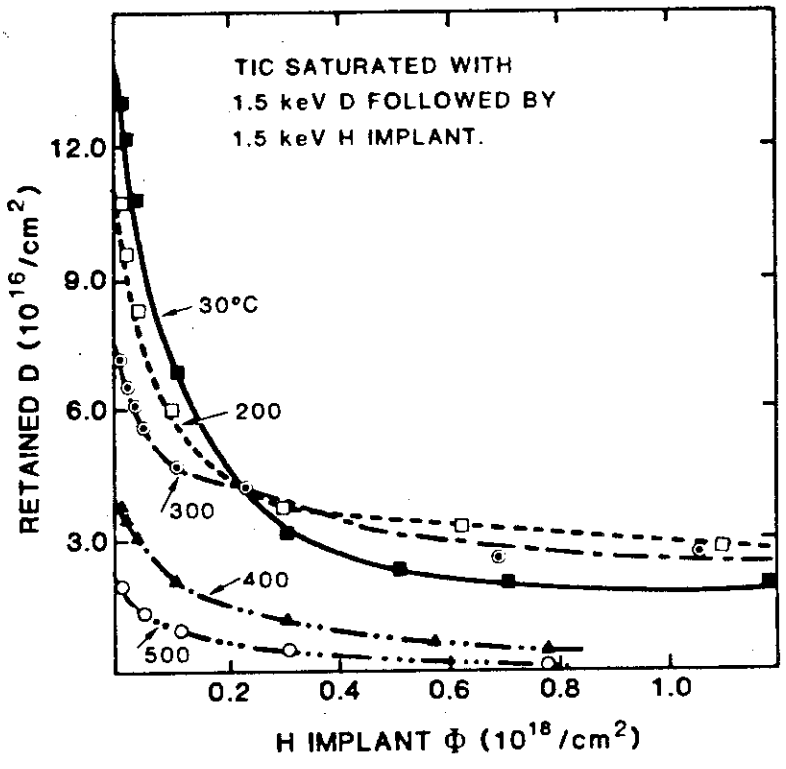

Figure 1. Temperature dependence of D saturation and isotope exchange in TiC. The samples were first saturated with 1.5 keV D and then 1.5 keV H was implanted. The curves are eye-guides.

RT-76

Title	Deuterium Trapping in Low-Z Coatings
Reference	J. Nucl. Mat., 111 & 112 (1982) 590
Authors	S.K. Erents
Institution	Culham Laboratory, UK

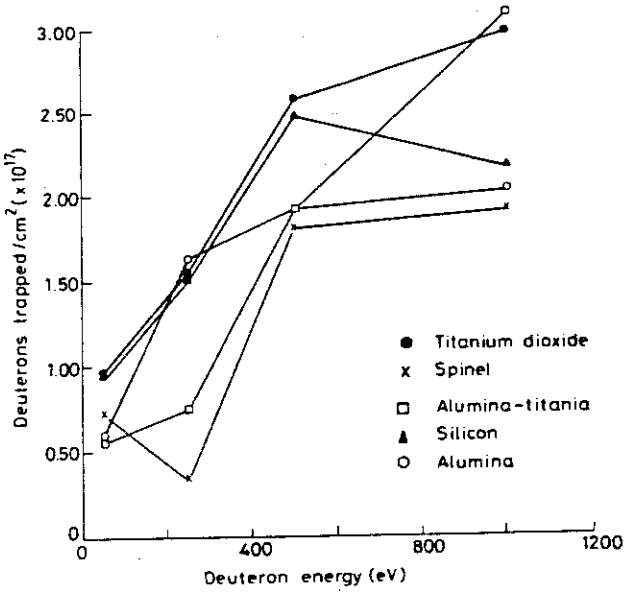

Fig. 4. Total number of deuterons trapped in coatings as a function of deuteron energy. 300 K bombardments.

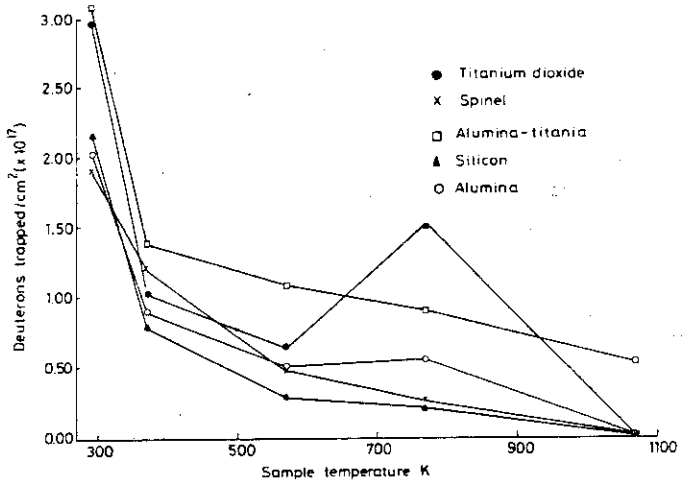

Fig. 7. Total number of deuterons trapped in coatings as a function of implant temperature. 2 keV D_2^+.

References

RT-01 J. Altstetter, R. Behrisch, J. Bøttiger, P. Pohl and B.M.U. Scherzer : Depth Profiling of Deuterium Implanted into Stainless Steel, Nucl. Instr. Methods, 149 (1978) 59.

RT-02 C.J. Altstetter, R. Behrisch and B.M.U. Scherzer : Trapping of Deuteron Implanted into Stainless Steel and Low Temperature, J. Vac. Sci. Tech., 15 (1978) 706.

RT-03 R.S. Blewer, R. Behrisch, B.M.U. Scherzer and R. Schule : Trapping and Replacement of 1-14 keV Hydrogen and Deuterium in 316 Stainless Steel, J. Nucl. Mat., 76 & 77 (1978) 305.

RT-04 K.L. Wilson, A.E. Pontau, L.G. Haggmark, M.I. Maskes, J. Bohdansky and J. Roth : Trapping and Deuterium in Helium-Damaged Steel, He^+ Fluence Dependence, J. Nucl. Mat., 103 & 104 (1981) 493.

RT-05 K.L. Wilson, A.E. Pontau, L.G. Haggmark and M.I. Baskes : Combined Depth Profiling and Thermal Desorption of Implanted Deuterium in 304LN Stainless Steel, J. Nucl. Mat., 93 & 94 (1980) 594.

RT-06 N.J. Freeman, I.D. Latimer and N.R. Daly : Burial of 60 keV Deuterium Ions in Stainless Steel and Titanium, Nature, 212 (1966) 1346.

RT-11 F. Besenbacher, J. Bøttiger, T. Laursen and W. Möller : Hydrogen Trapping in Ion-Implanted Nickel, J. Nucl. Mat., 93 & 94 (1980) 617.

RT-12 R. Schulz, R. Behrisch and B.M.U. Scherzer : D and ^3He Trapping and Mutual Replacement in Molybdenum, Nucl. Instr. Methods, 168 (1980) 295.

RT-13 S.T. Picraux, J. Bøttiger and N. Rud : Enhanced Hydrogen Trapping due to He Ion Damage, J. Nucl. Mat., 63 (1976) 110.

RT-14 R. Schulz, R. Behrisch and B.M.U. Scherzer : Trapping and Mutual Release of D and ^3He in Molybdenum, J. Nucl. Mat., 93 & 94 (1980) 608.

RT-15 S.T. Picraux, J. Bøttiger and N. Rud : Profile Studies of Hydrogen Trapping in Metals due to Ion Damage, Appl. Phys. Lett., 28 (1976) 179.

RT-16 J. Bøttiger, S.T. Picraux, N. Rud and T. Laursen : Trapping of Hydrogen Isotopes in Molybdenum and Niobium Predamaged by Ion Implantation, J. Appl. Phys., 48 (1979) 920.

RT-17 S.M. Myers, S.T. Picraux and R.E. Stoltz : Deep Deuterium Traps in Y Implanted Fe, Appl. Phys. Lett., 37 (1980) 168.

RT-31 J. Bohdansky, J. Roth, M.K. Sinha and W. Ottenberger : Trapping Coefficients of Energetic Hydrogen (0.3 - 0.8 keV) in Ti at High Doses, J. Nucl. Mat., 63 (1976) 115.

RT-32 W. Möller, P. Børgesen and J. Bøttiger : Temperature-Dependent Depth Profiles of Deuterons Implanted into Zirconium, J. Nucl. Mat., 76 & 77 (1978) 289.

RT-33 See RT-06.

RT-51 B.M.U. Scherzer, R. Behrish, W. Eckstein, U. Littmark, J. Roth and M.K. Sinha : Temperature Dependence of Trapping and Depth Profiles of 6 to 15 keV Deuterium in Carbon, J. Nucl. Mat., 63 (1976) 100.

RT-52 R.A. Langley, R.S. Blewer and J. Roth : Behavior of Implanted D and He in Pyrolytic Graphite, J. Nucl. Mat., 76 & 77 (1978) 313.

RT-53 P. Hucks, K. Flaskamp and E. Vietzke : The Trapping of Thermal Atomic Hydrogen on Pyrolytic Graphite, J. Nucl. Mat., 93 & 94 (1980) 558.

RT-54 S.K. Erents and E.S. Hotston : A Simple Model for the Trapping of Deuterons in Carbon Target, Nucl. Instr. Methods, 170 (1980) 449.

RT-55 K. Sone and G.M. McCraken : The Effect of Radiation of Damage on Deuteron Re-Emission and Trapped in Carbon, J. Nucl. Mat., 111 & 112 (1982) 606.

RT-56 W.R. Wampler and S.M. Myers : Ion-Induced Release of Deuterium from Carbon, J. Nucl. Mat., 111 & 112 (1982) 616.

RT-57 See RT-75.

RT-71 B.L. Doyle, W.R. Wampler, D.K. Brice and S.T. Picraux : Saturation and Isotopic Replacement of Deuterium in Low-Z Materials, J. Nucl. Mat., 93 & 94 (1980) 551.

RT-72 K.L. Wilson and A.E. Pontau : Deuterium Trapping and Release in Titanium-Based Coating for TFTR, J. Nucl. Mat., 93 & 94 (1980) 569.

RT-73 R. Behrisch, R.S. Blewer, J. Border, R. Langley, J. Roth, B.M.U. Scherzer and R. Schulz : Radiat. Eff., 48 (1980) 221.

RT-74 K.L. Wilson and A.E. Pontau : Deuterium Trapping Measurements on Boron Coatings for the TOKAMAK Fusion Test Reactors, Thin Solid Films, 83 (1981) 73-78.

RT-75 B.L. Doyle, W.R. Wampler and K.K. Brice : Temperature Dependence of H Saturation and Isotope Exchange, J. Nucl. Mat., 103 & 104 (1981) 513-518.

RT-76 S.K. Erents : Deuterium Trapping in Low-Z Coatings, J. Nucl. Mat., 111 & 112 (1982) 590.

3.2.2 Depth Profile in the Materials

Depth profile of hydrogen isotopes implanted in the materials are summarized. DP-01 through 07 show the results with stainless steel, DP-11 through 16, with Ni and Mo, DP-31, with Zr, DP-51 through 54, with graphite, DP-61 through 67, with Si and DP-71 and 74, with other low mass number materials, respectively.

DP-01, 05, 52, 53, 64 and 65 show the measured depth profile for different implanted fluence. There can be observed the tendency where the concentration increases near the surface, as implantation comes close to saturation in case of graphite and Si. DP-05, 12, 14, 31, 51, 72 and 73 show the measured depth profile for H implantation at different temperature. Profile at higher temperature is similar to the profile of lower concentration.

DP-02, 03, 07 and 13 show the results of hydrogen isotopes implantation with He pre-irradiation. In this case, trap is formed by both He and hydrogen isotopes implantation.

DP-04, 53 and 54 show the experiments where D is implanted first, then H is implanted that causes re-emission of D. DP-15 shows the experiments where ions implanted prior to the others are re-emitted by the ions of post implantation, for example, hydrogen isotopes implantation is applied first, then He is irradiated that causes re-emission of the former and vice versa. DP-51 and 53 show the depth profiles for different energy. DP-51 shows that the concentration near the surface agrees with the distribution of irradiation defects and the inner profile corresponds with the distribution of ranges.

DP-14, 31, 61 and 62 show the variation in density near the surface. In case of those metals as Zr and Ti that form hydrides, hydrogen isotopes can reach in deeper region, as shown in DP-31 and 71.

DP-01

Title	Trapping of Deuteron Implanted into Stainless Steel at Low Temperatures
Reference	J. Vac. Sci. Tech., 15 (1978) 706
Authors	C.J. Altstetter, R. Behrish, B.M.U. Scherzer
Institution	Max-Plank-Institut für Plasmaphysik, Garching, F.R.G.

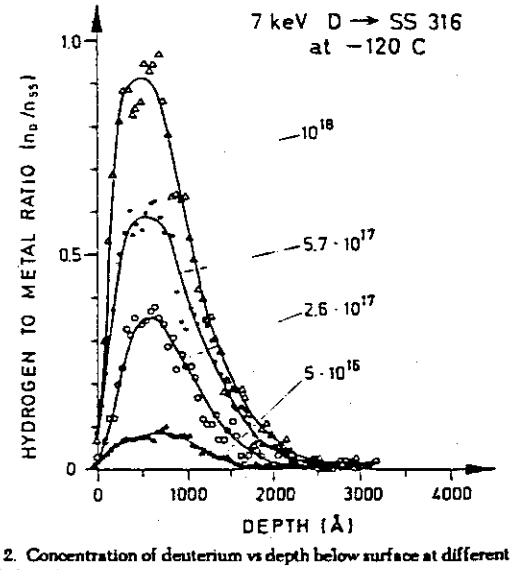

FIG. 2. Concentration of deuterium vs depth below surface at different dose levels for 7 keV implantation of 316 stainless steel at −120° C.

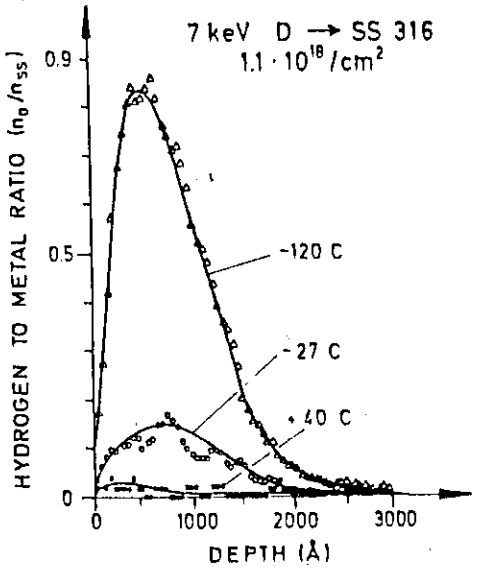

FIG. 5. Change of concentration profile as a result of warming from −120° C.

DP-02

Title	Trapping and Surface Permeation of Deuterium in Helium-Implanted Stainless Steel
Reference	J. Nucl. Mat., 111 & 112 (1982) 579
Authors	S.M. Myers, W.R. Wampler
Institution	Sandia National Laboratories, Albuquerque, USA

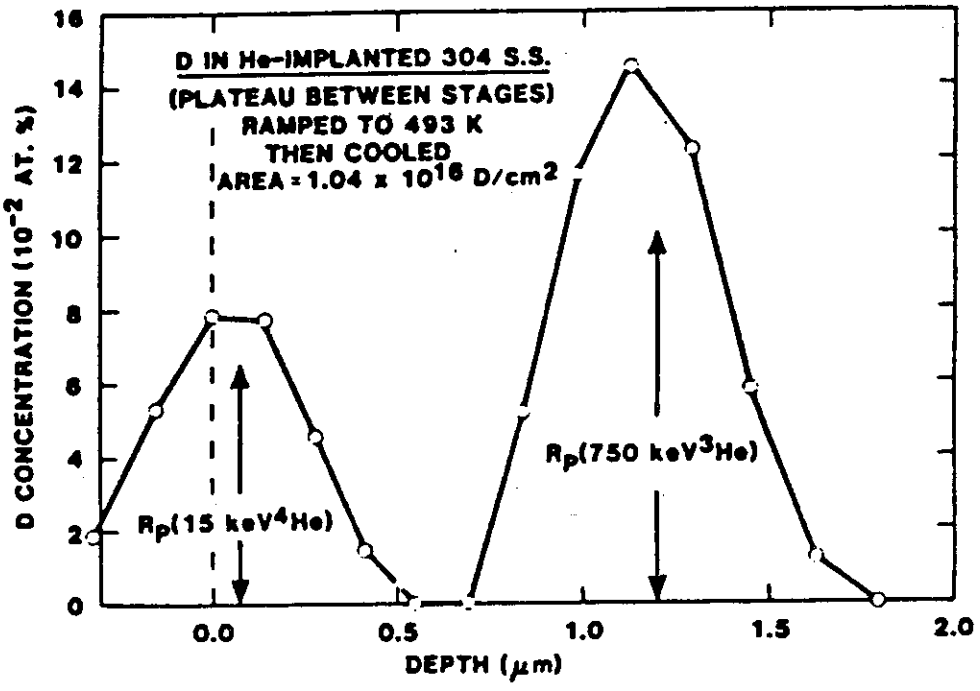

Fig. 3. Depth profile of D in the plateau between release stages. The implanted D fluence was 1×10^{16} atoms cm^{-2}.

DP-03

Title	Trapping of Deuterium in Helium-Damaged Steel: He^+ Fluence Dependence
Reference	J. Nucl. Mat., 103 & 104 (1981) 493
Authors	K.L. Wilson, A.E. Pontau, L.G. Haggmark, M.I. Baskes(a) J. Bohdansky, J. Roth(b)
Institution	(a) Sandia National Laboratories, Livermore, USA (b) Max-Plank-Institut für Plasmaphysik, Garching, F.R.G.

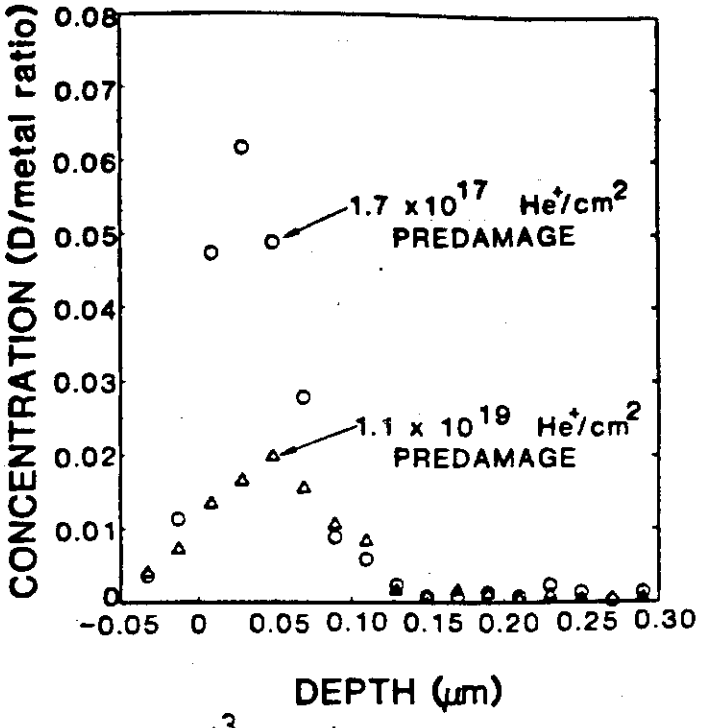

Figure 2. $D(^3He, \alpha)H$ nuclear reaction profiling data for two 304 LN stainless steel samples predamaged with 8 keV He^+, followed by the standard D implant, and held for 1800 s at 296 K prior to profiling. The calculated depth resolution (full width half maximum) is ≈30 nm at the surface. Hence negative depths reflect the finite depth resolution of the profiling technique.

DP-04

Title	Trapping and Replacement of 1-14 keV Hydrogen and Deuterium in 316 Stainless Steel
Reference	J. Nucl. Mat., 76 & 77 (1978) 305
Authors	R.S. Blewer, R. Behrish, B.M.U. Scherzer, R. Schulz
Institution	Max-Plank-Institut für Plasmaphysik, Garching. F.R.G.

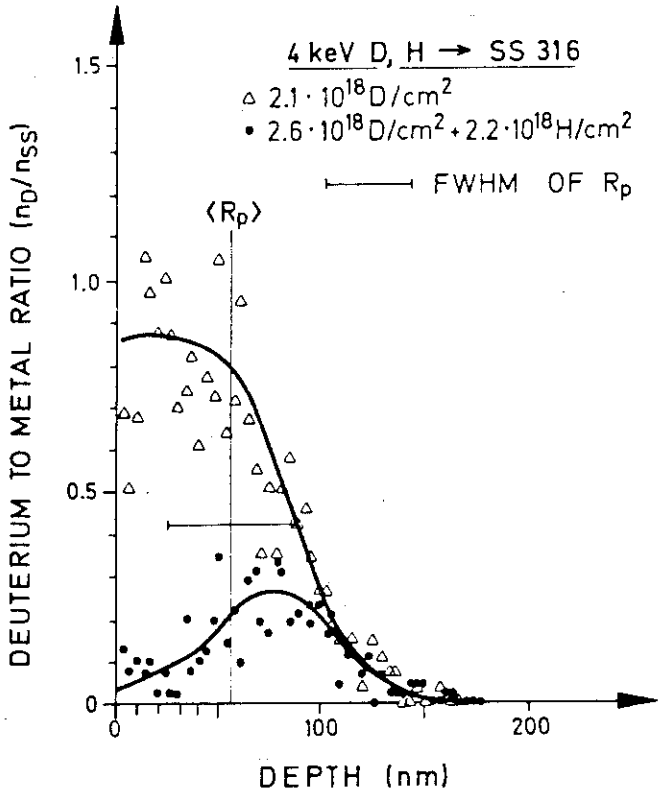

Fig. 4. 4 keV deuterium depth profiles at saturation (upper curve) and at an advanced stage of replacement (lower curve). The measured mean projected range, $\langle R_p \rangle$ is also indicated.

DP-05

Title	Combined Depth Profiling and Thermal Desorption of Implanted Deuterium in 304 LN Stainless Steel
Reference	J. Nucl. Mat., 93 & 94 (1980) 594
Authors	J. Bohdansky(a) K.L. Wilson, A.E. Pontau, L.G. Haggmark, M.I. Baskes(b)
Institution	(a) Max-Plank-Institut für Plasmaphysik, Garching, F.R.G. (b) Sandia National Laboratories, Livermore, USA

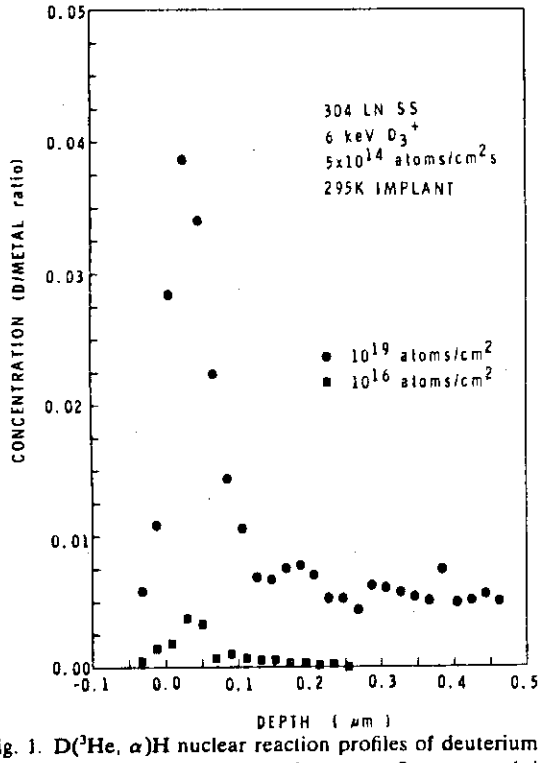

Fig. 1. D(^{3}He, α)H nuclear reaction profiles of deuterium in 304LN stainless steel implanted to two fluences and immediately quenched to 77 K at ≈0.25 K/s.

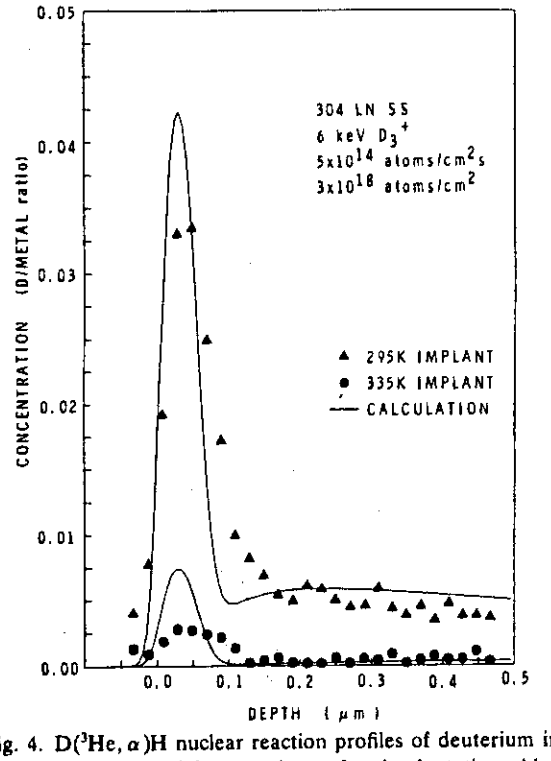

Fig. 4. D(^{3}He, α)H nuclear reaction profiles of deuterium in 304LN stainless steel for two times after implantation. Also shown are convoluted DIFFUSE profiles for the two isothermal anneal times.

DP-06

Title	Dynamic Measurements of Implanted Deuterium Retention and Release in Stainless Steel and Carbon
Reference	J. Nucl. Mat. 111 & 112 (1982) 654
Authors	E.W. Thomas, M. Braun
Institution	Research Institute of Physics, Association Euratom-NE, Sweden

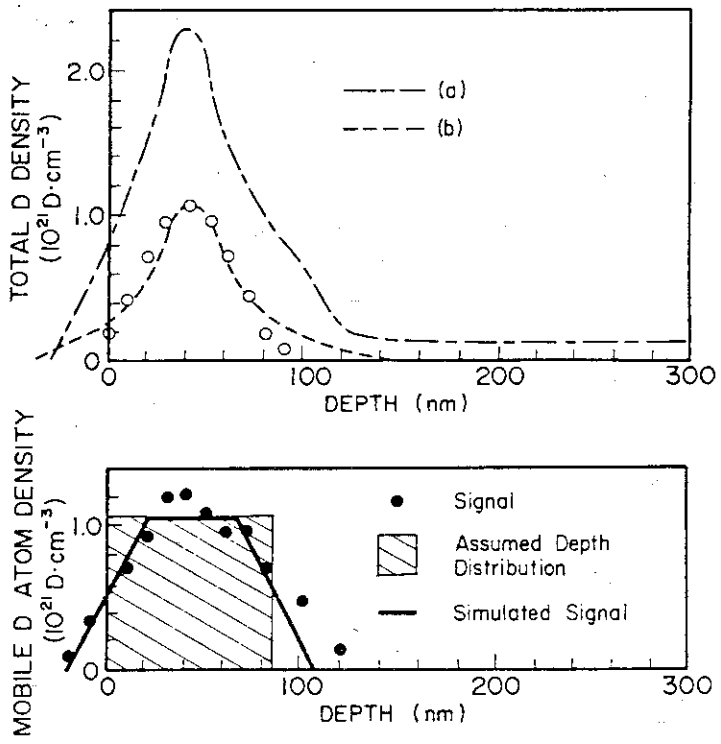

Fig. 1. Depth distributions of implanted deuterium for 5 keV D^+ ions into a stainless steel target held at 60°C. The upper set of curves are the measured depth distributions. Line (a) is obtained after a dose of about 1.5×10^{17} D cm^{-2}, where re-emission has saturated. Line (b) is taken 1000 s after cessation of bombardment and after the decay of the RGA signal back to zero. The open circles shown on line (b) are simulated signals for the trapped deuterium using a Gaussian depth distribution (see text). In the lower part of the figure is shown the difference between curves (a) and (b) representing (by points) the apparent depth distribution of the mobile deuterium. The cross-hatched area is an assumed depth distribution with a concentration of 1.06×10^{21} D cm^{-3} to a depth of 850 Å, and the trapezoidal line is a simulated signal using a detector with a triangular response function of 20 keV width (FWHM).

DP-07

Title	Deuterium Retention in Helium-Damaged Stainless Steel: Detrapping Energy
Reference	J. Nucl. Mat., 111 & 112 (1982) 651
Authors	A.E. Pontau, M.I. Baskes, K.L. Wilson, L.G. Haggmark(a) J. Bohdansky, B.M.U. Scherzer, J. Roth(b)
Institution	(a) Sandia National Laboratories, Livermore, USA (b) Max-Plank-Institut für Plasmaphysik, Garching, F.R.G.

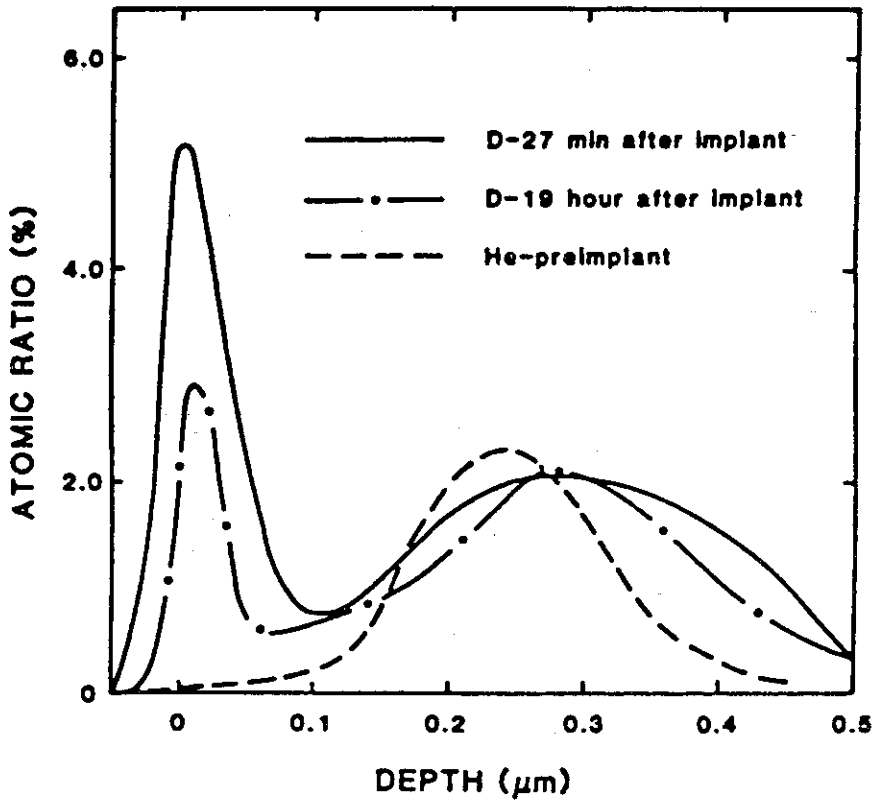

Fig. 1. Depth profiles of ^{3}He and D in 304LN stainless steel. The sample was prebombarded with 100 keV ^{3}He to $\sim 3.4\times10^{16}$ He cm^{-2}. 10^{18} D cm^{-2} was implanted as 6 keV D_3^+ at room temperature. The portion retained after 27 min was 7.1×10^{16} D cm^{-2}, and decreased to 5.5×10^{16} D cm^{-2} after 19 h.

DP-11

Title	Defect Trapping of Ion-Implanted Deuterium in Nickel
Reference	J. Appl. Phys., 53 (1982) 3536
Authors	F.Besenbacher, J. Bøttiger(a) S.M. Myers(b)
Institution	(a) University of Aarhus, Denmark (b) Sandia Laboratories, Albuquerque, USA

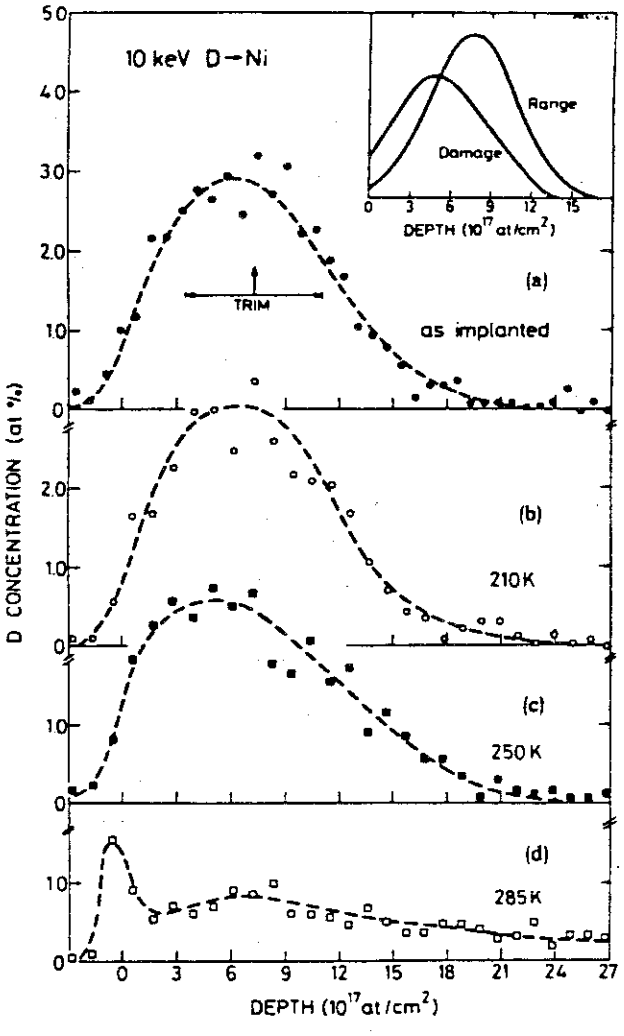

FIG. 2. The evolution of the *D*-depth profiles for 4.2×10^{16} *D*/cm^2 implanted into Ni at 10 keV and $T = 80$ K during linear-ramp annealing at a rate of 10^{-2} K/s. Dashed curves are drawn to guide the eye only. In the inset are shown the theoretical damage and range profiles obtained from the TRIM Monte-Carlo code. In case (a), the mean and FWHM for the TRIM range profile are compared with the experimental depth profile. Polycrystalline Ni foils were used here, whereas single crystals were employed otherwise.

DP-12

Title	Hydrogen Trapping in Ion-Implanted Nickel
Reference	J. Nucl. Mat., 93 & 94 (1980) 617
Authors	F. Bestembacher, J. Bøttiger, T. Laursen, W. Möller
Institution	Institute of Physics, University of Aarhus, Denmark

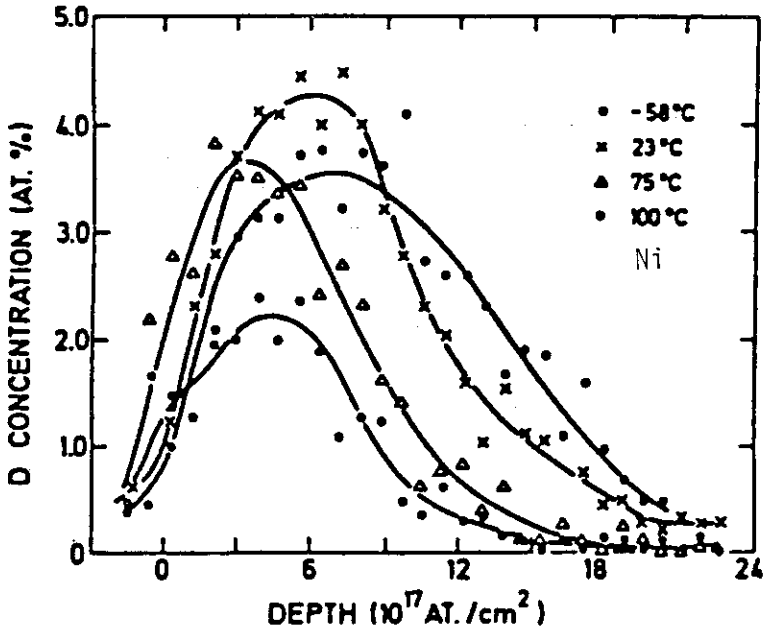

Fig. 5. The D-depth distributions at different stages of the annealing for a 10-keV He-preimplanted sample (cf. fig. 4).

DP-13

Title	Enhanced Hydrogen Trapping due to He Ion Damage
Reference	J. Nucl. Mat., 63 (1976) 110
Authors	S.T. Picraux(a) J. Bøttiger, N. Rud(b)
Institution	(a) Sandia Laboratories, Albuquerque, USA (b) University of Aarhus, Denmark

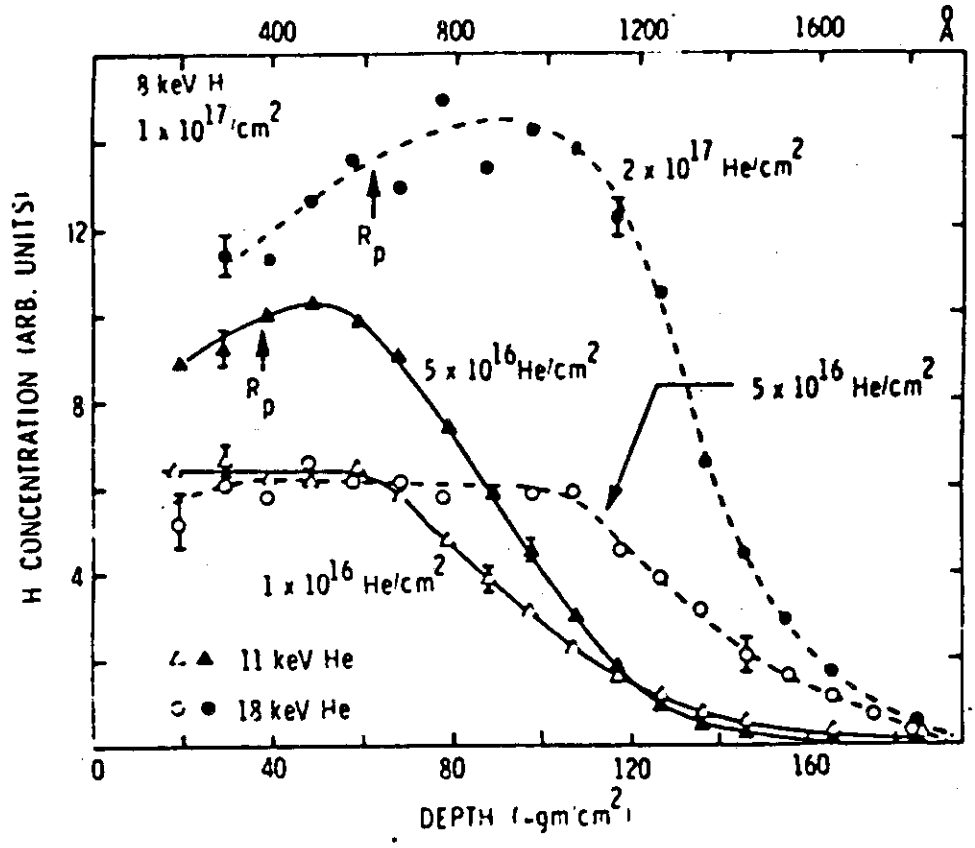

Fig. 1. Hydrogen depth profiles in Mo single-crystal samples predamaged by ^{4}He bombardment at the energies and fluences indicated and followed by 8 keV H injection to a fluence of 1 X 10^{17}/cm^2.

DP-14

Title	Interaction of Hydrogen with Radiation Defects in Metals
Reference	J. Nucl. Mat., 93 & 94 (1980) 588
Authors	A.E. Gorodetsky, A.P. Zakharov, V.M. Sharapov, V.Kh. Alimov
Institution	Institute of Physical Chemistry, Academy of Science, USSR

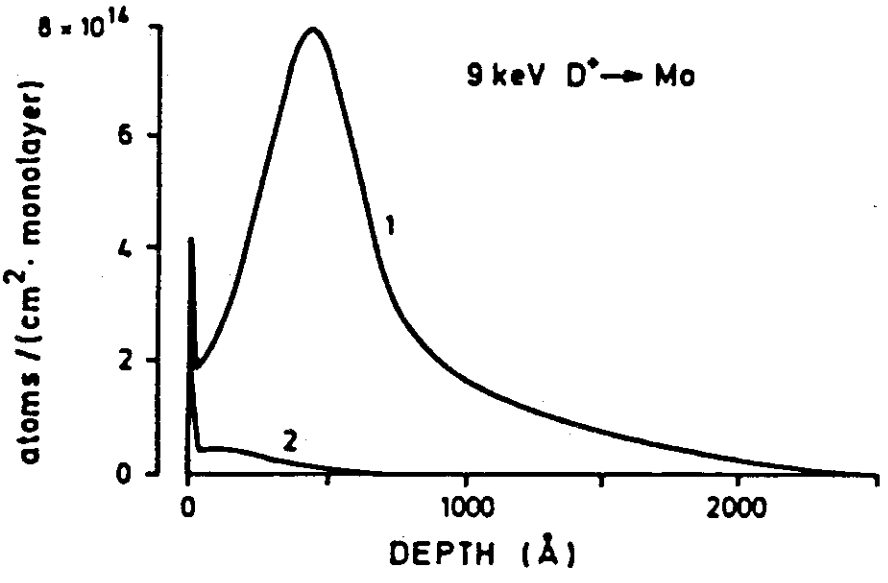

Fig. 2. Distribution of implanted 9 keV D^+ in Mo: 1 – Φ = 2×10^{17} cm^{-2}, 77 K; 2 – $\Phi = 10^{17}$ cm^{-2}, 300 K.

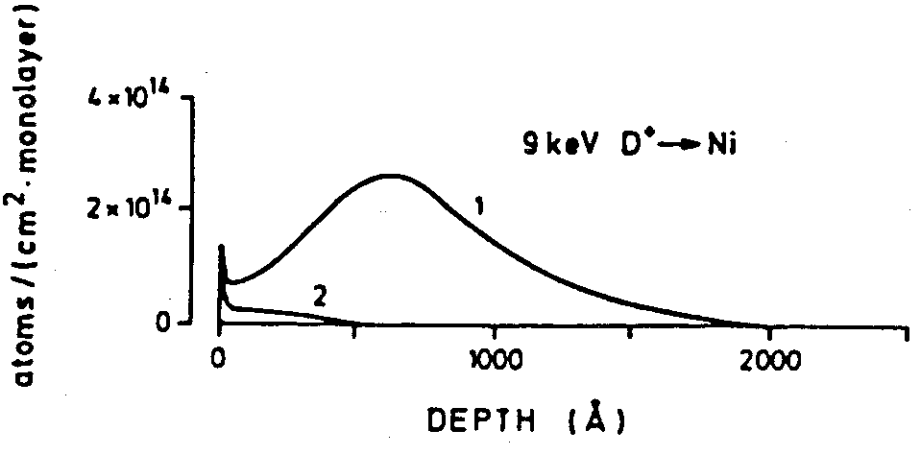

Fig. 3. Distribution of implanted 9 keV D^+ in Ni, Φ = 2×10^{17} cm^{-2}, 1 – 77 K; 2 – 300 K.

DP-15

Title	Trapping and Mutual Release of D and ^{3}He in Molybdenum
Reference	J. Nucl. Mat., 93 & 94 (1980) 608
Authors	R. Schulz, R. Behrisch, B.M.U. Scherzer
Institution	Max-Plank-Institut für Plasmaphysik, Garching, F.R.G.

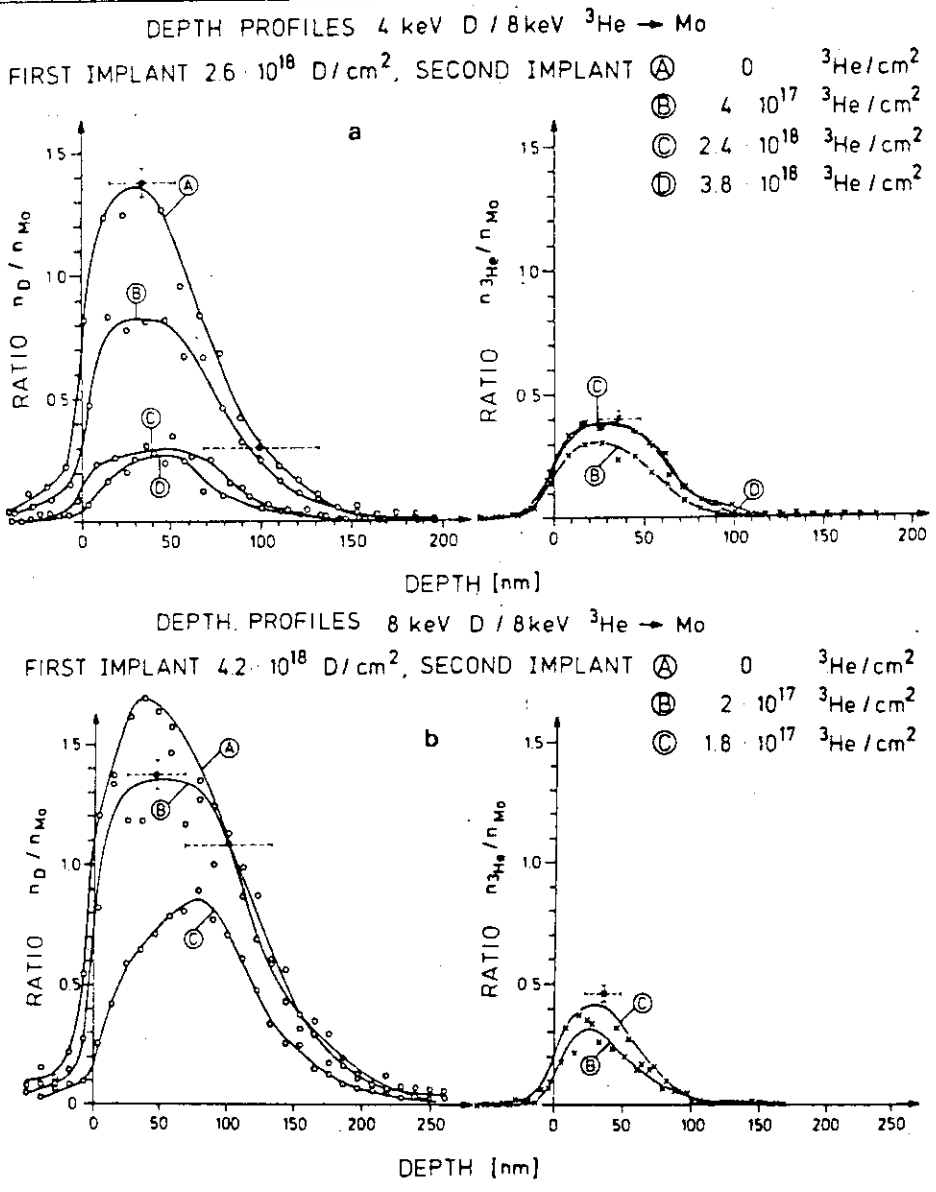

Fig. 5. (a) Concentration profiles of 4 keV D and 8 keV ^{3}He at different fluences of the postbombarded ^{3}He ions. (b) Concentration profiles of 8 keV D and 8 keV ^{3}He at different fluences of the postbombarded ^{3}He ions.

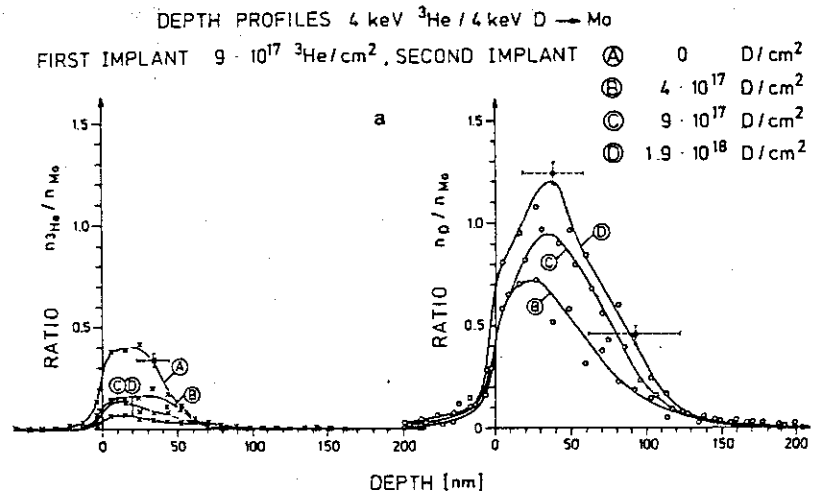

Fig. 6a. Concentration profiles of 4 keV ^{3}He and 4 keV D at different fluences of the postimplanted D ions in polycrystalline Mo.

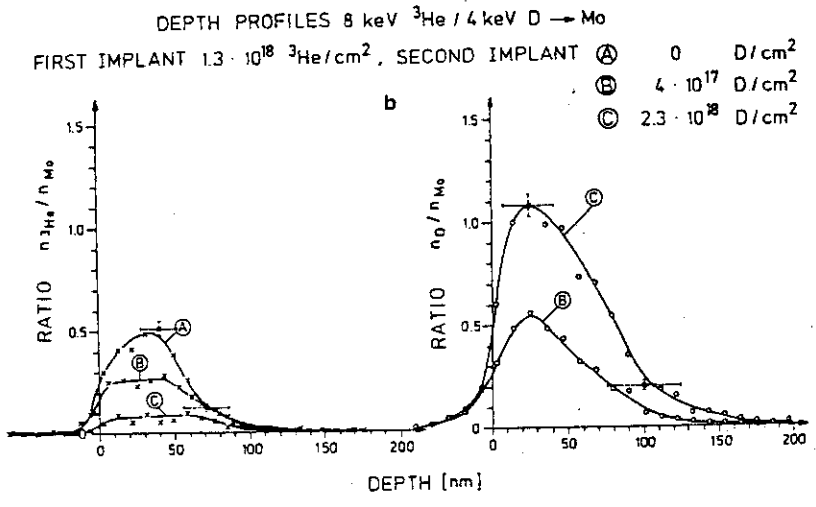

Fig. 6b. Concentration profiles of 8 keV ^{3}He and 4 keV D at different fluences of the postimplanted D ions.

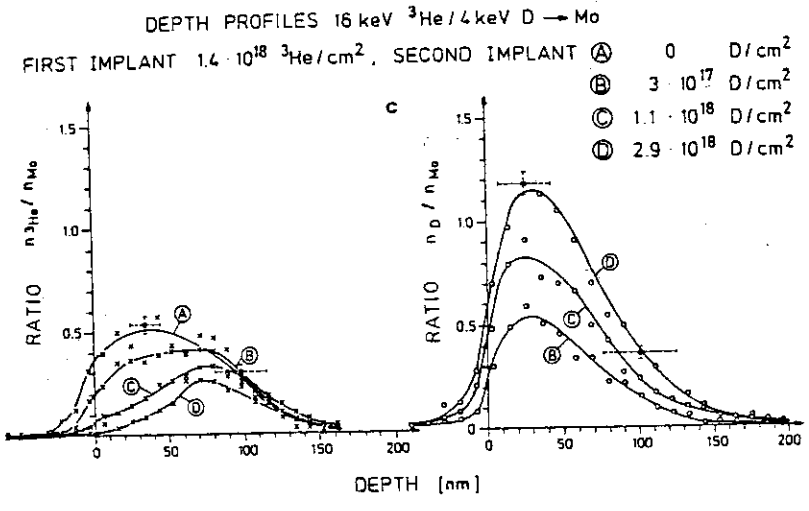

Fig. 6c. Concentration profiles of 16 keV ^{3}He and 4 keV D at different fluences of the postimplanted D ions. The letters A, B, etc. give the fluences also indicated in fig. 2.

DP-16

Title	Large Depth Profile Measurements of D, ^{3}He and Li by Deuteron Induced Nuclear Reactions
Reference	Nucl. Instr. Methods, 140 (1977) 157
Authors	W. Möller, M. Hufschomidt, D. Kamke
Institution	Institut für Experimentalphysik I der Ruhr-Universität Bochum, F.R.G.

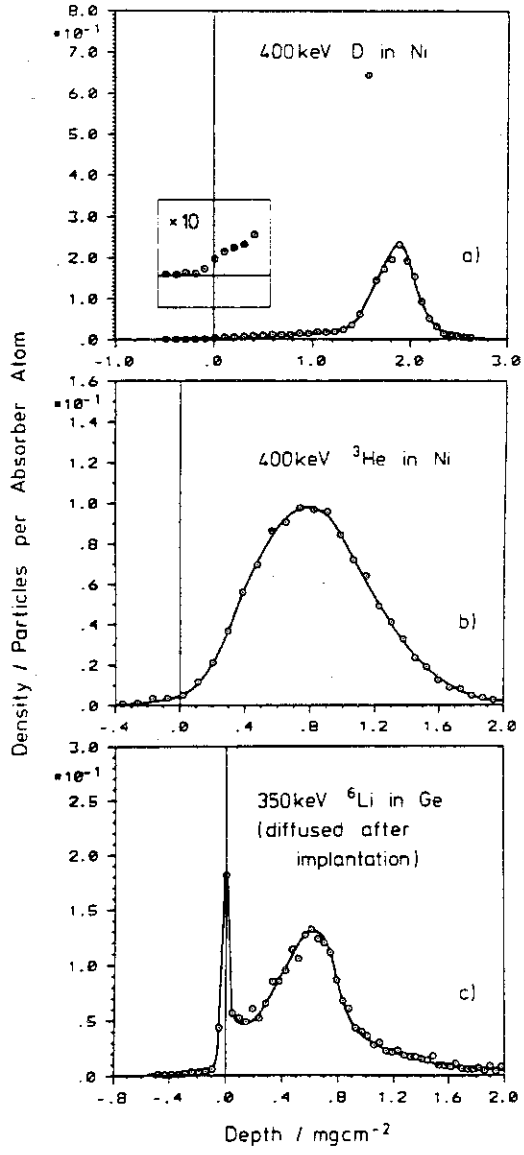

Fig. 11. Depth profiles computed from the energy spectra plotted in fig. 10.

DP-21

Title	New Precision Technique for Measuring the Concentration versus Depth of Hydrogen in Solids
Reference	Appl. Phys. Lett., 28 (1976) 566
Authors	W.A. Lanford, H.P. Trautvetter(a) J.F. Ziegler, J. Keller(b)
Institution	(a) Wright Nuclear Structure Laboratory, Yale University, USA (b) IBM Watson Research Laboratory, USA

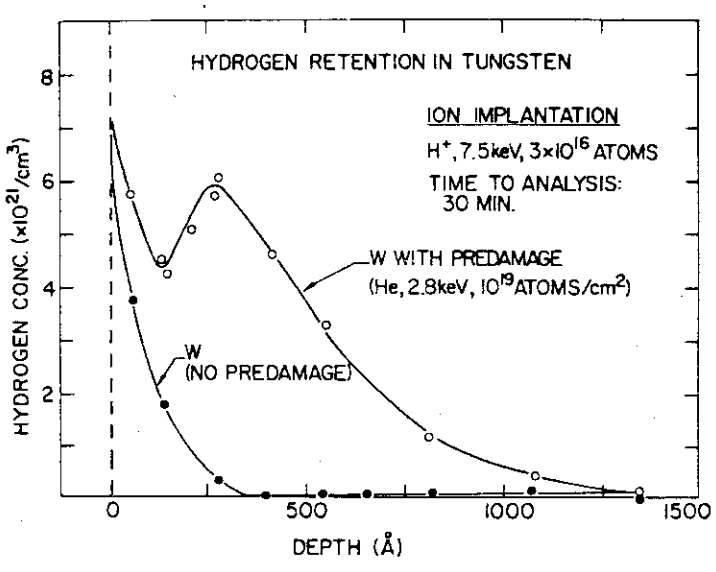

FIG. 4. Hydrogen profiles of two tungsten samples implanted with 7.5-keV hydrogen. One sample had been predamaged with 2.8-keV He and one had not.

DP-31

Title	Temperature-Dependent Depth Profiles of Deuterons Implanted into Zirconium
Reference	J. Nucl. Mat., 76 & 77 (1978) 289
Authors	W. Möller, P. Børgesen, J. Bøttiger
Institution	Institute of Physics, University of Aahus, Denmark

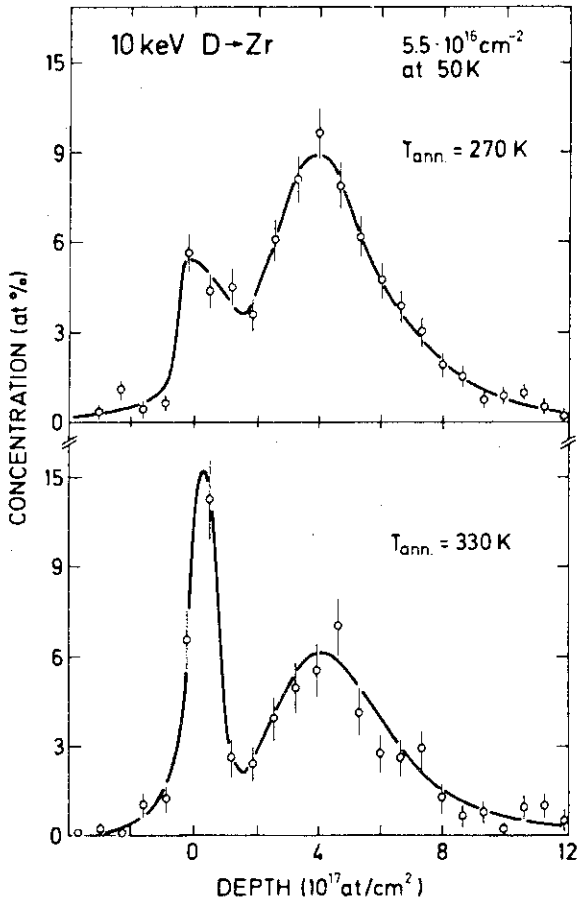

Fig. 2. Depth profiles for 10 keV D^+ implanted into Zr at 50 K, followed by subsequent heating to 270 and 330 K, respectively. The target was held at each temperature for 10 min before starting the analysis; typical analysis times were 30 min. The concentration scale gives the D/Zr atomic ratio.

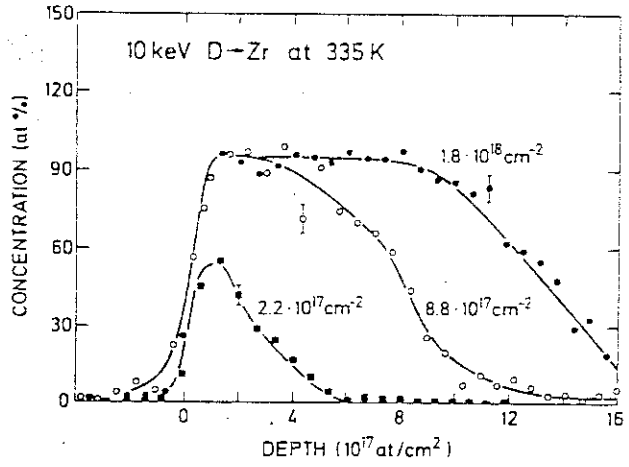

Fig. 3. Depth profiles for 10 keV D^+ implanted into Zr kept at 335 K for different implantation doses.

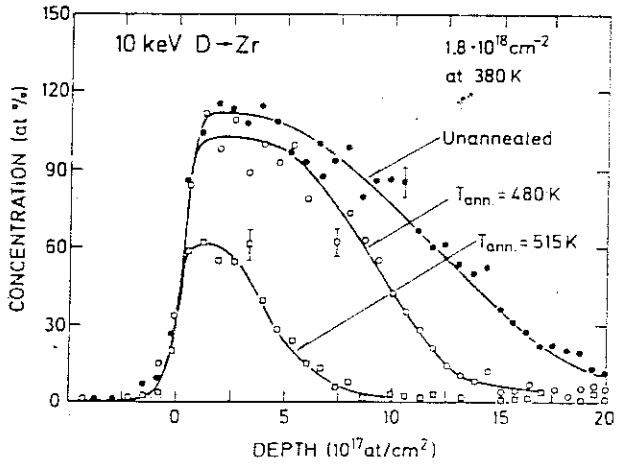

Fig. 4. Depth profile for 10 keV D^+ implanted into Zr at 380 K together with profiles measured after heating.

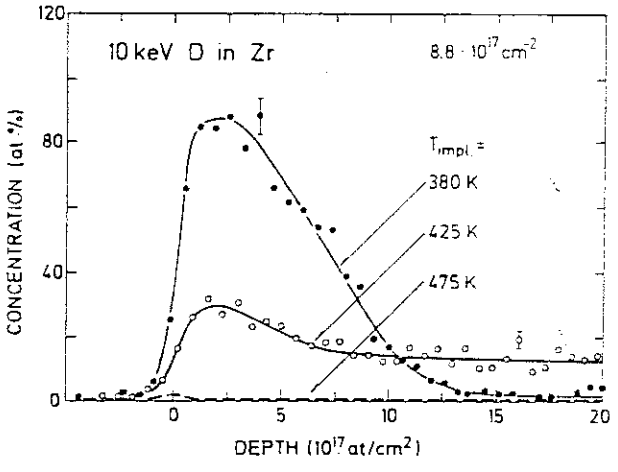

Fig. 5. Depth profiles for 10 keV D^+ implanted into Zr, kept at different temperatures.

DP-51

Title	Temperature Dependence of Trapping and Depth Profiles of 6 to 15 keV Deuterium in Carbon
Reference	J. Nucl. Mat., 63 (1976) 100
Authors	B.M.U. Scherzer, R. Behrish, W. Eckstein, U. Littmark, J. Roth, M.K. Sinha
Institution	Max-Plank-Institut für Plasmaphysik, Garching, F.R.G.

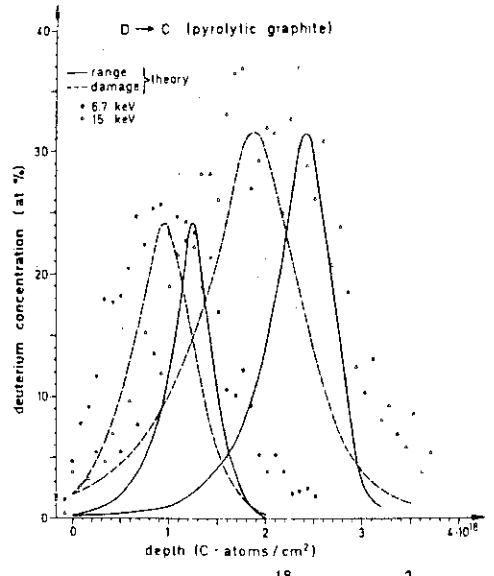

Fig. 4. Depth profiles of 1.5×10^{18} deuterons/cm^2 implanted with 6.7 keV and 3×10^{18} deuterons/cm^2 implanted with 15 keV at room temperature. Range (full drawn lines) and damage profiles (broken lines) are calculated from Boltzmann transport theory [15].

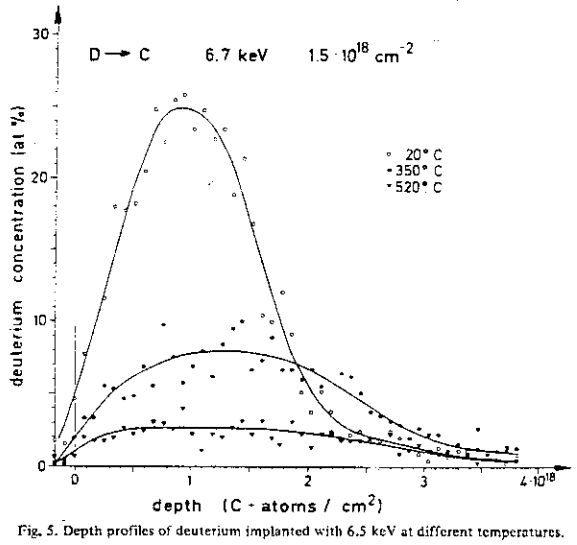

Fig. 5. Depth profiles of deuterium implanted with 6.5 keV at different temperatures.

DP-52

Title	Behavior of Implanted D and He in Porolytic Graphite
Reference	J. Nucl. Mat., 76 & 77 (1978) 313
Authors	R.A. Langley, R.S. Blewer(a) J. Roth(b)
Institution	(a) Sandia Laboratories, Albuquerque, USA (b) Max-Plank-Institut für Plasmaphysik, Garching, F.R.G.

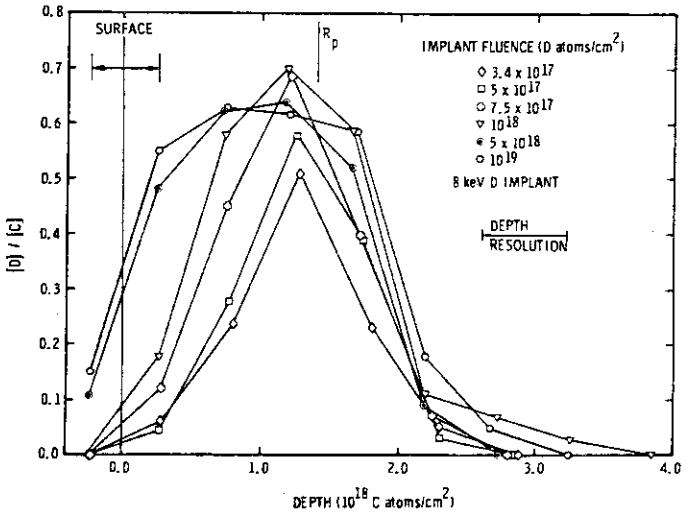

Fig. 1. Depth profiles for implanted 8 keV D as a function of implant fluence

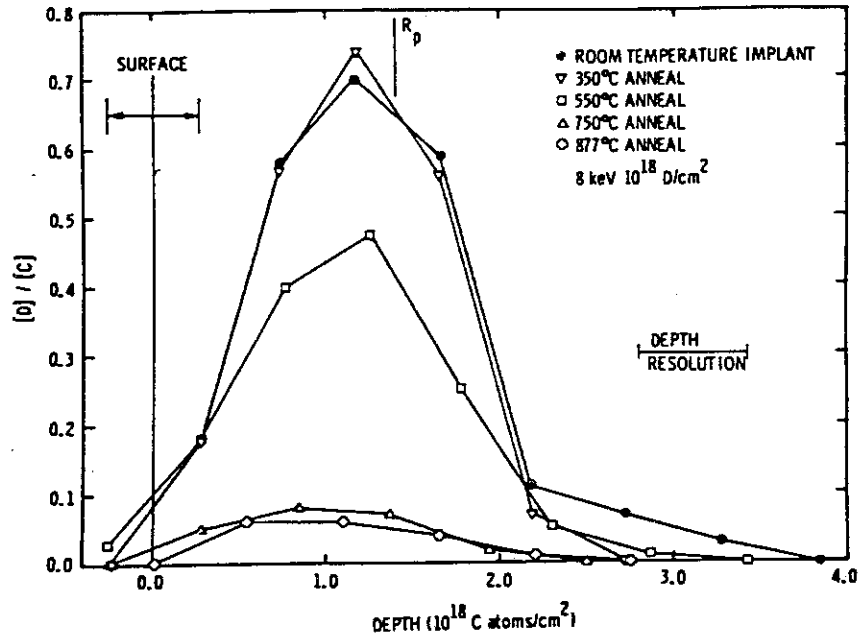

Fig. 4. Deuterium profile change as a function of anneal temperature.

DP-53

Title	Depth Resolved Measurement of Hydrogen Isotope Exchange in Carbon
Reference	J. Nucl. Mat., 103 & 104 (1981) 509
Authors	W.R. Wampler(a) C.W. Magee(b)
Institution	(a) Sandia National Laboratories, Albuquerque, USA (b) RCA Laboratories, USA , USA

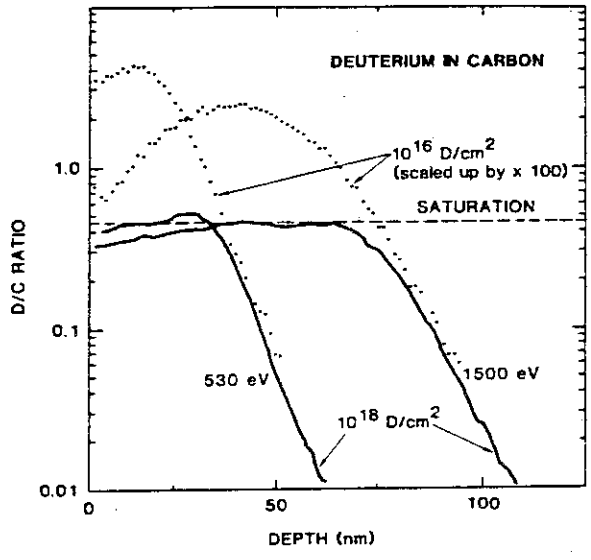

Figure 1: Concentration versus depth measured by SIMS for 530 eV and 1500 eV D implanted in carbon to an incident fluence of 10^{18}D/cm^2 (solid curves) and 10^{16}D/cm^2 (dotted curves).

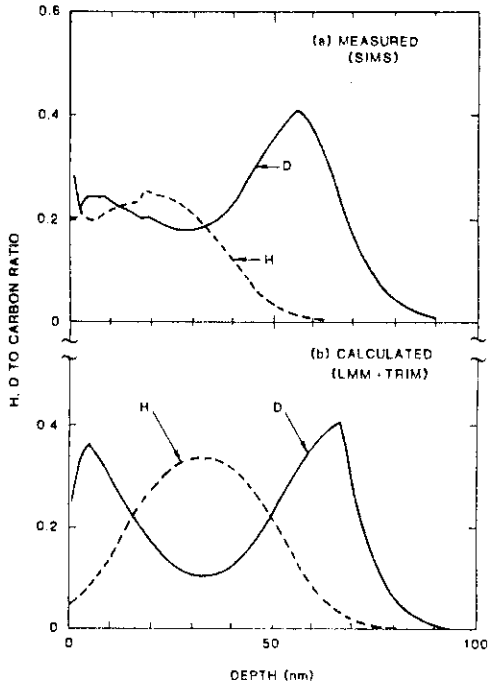

Figure 3: H and D profiles in carbon implanted with 10^{18}D/cm^2 followed by 2 x 10^{17}H/cm^2 both at 1.5 keV showing isotope exchange of the D by the H.

DP-54

Title	Dynamic Measurements of Implanted Deuterium Retention and Release in Stainless Steel and Carbon
Reference	J. Nucl. Mat., 111 & 112 (1982) 654
Authors	E.W. Thomas, M. Braun
Institution	Research Institute of Physics, Association Euratom-NE, Sweden

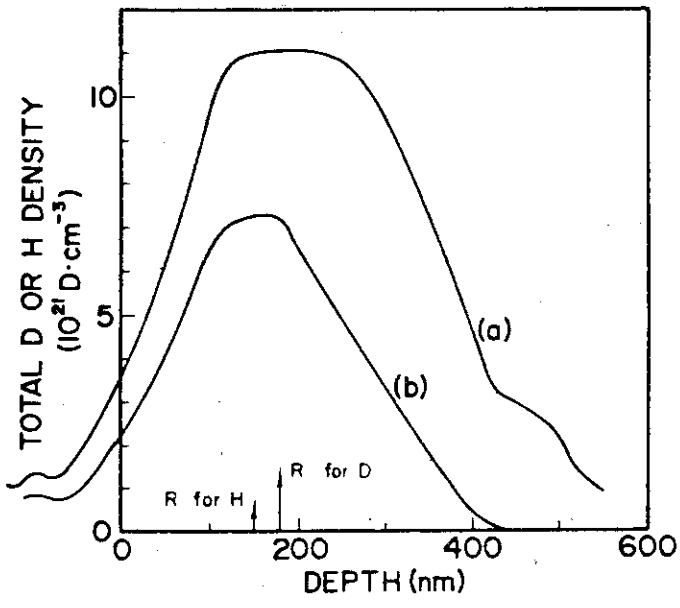

Fig. 2. Line (a) is the measured depth distribution of D after bombardment of room temperature Papyex by 5 keV D^+ fluence of 4.93×10^{18} D cm^{-2}. Line (b) is the *change* in D density after subsequent bombardment by 5 keV H^+ to a fluence of 1.08×10^{18} H cm^{-2}; this line presumably represents the depth distribution of implanted H. Indicated on the depth scale are the ranges of D and H.

DP-61

Title	The Application of Nuclear Reactions for Quantitative Hydrogen Analysis in a Variety of Different Materials Problems
Reference	Nucl. Instr. Methods, 149 (1978) 9
Authors	G.J. Clark, C.W. White, D.D. Allred, B.R. Appleton(a) F.B. Kock(b) C.W. Magee(c)
Institution	(a) ORNL, USA (b) Bell Laboratories, USA (c) RCA Laboratories, USA

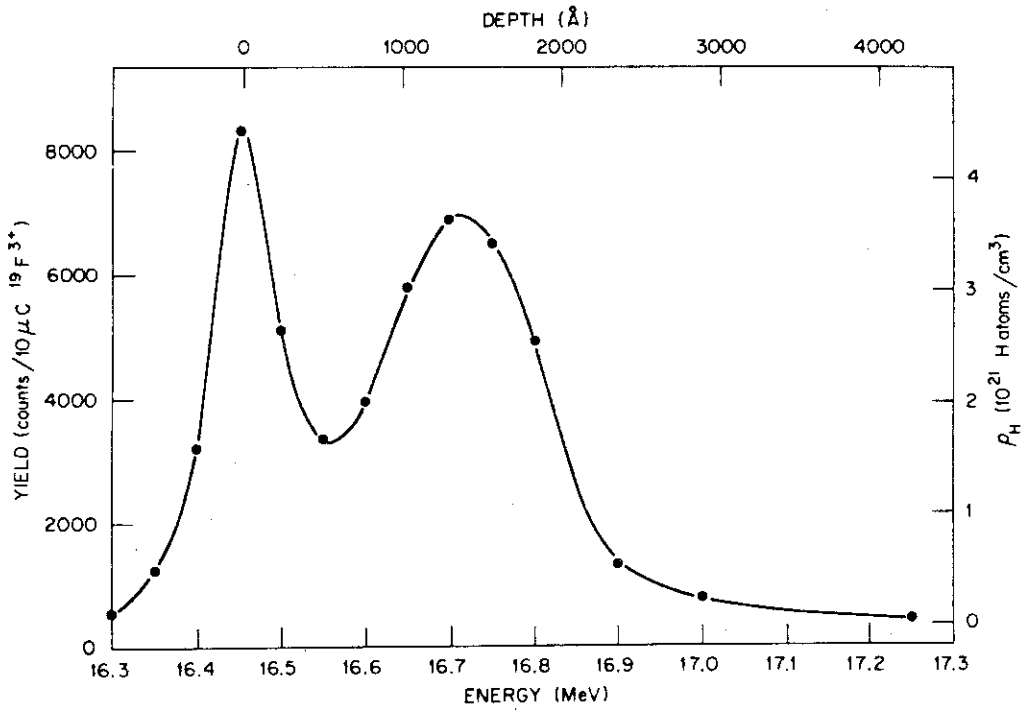

H^+ (10 keV, $4 \times 10^{16}/cm^2$) in Si.

Fig. 2. Hydrogen profile of H^+ implanted Si wafer.

DP-62

Title	Profiling Hydrogen in Materials Using Ion Beams
Reference	Nucl. Instr. Methods, 149 (1978) 19
Authors	J.F. Ziegler et al.
Institution	IBM Research etc. , USA

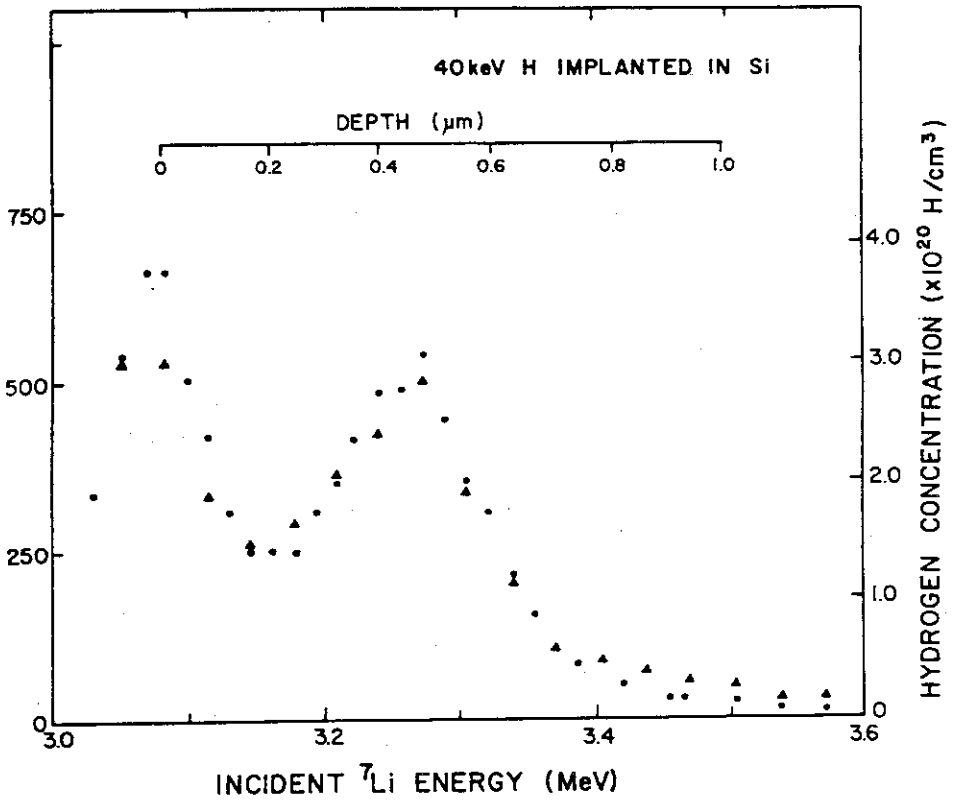

Fig. 8. Experimental yield curve of the $^{1}H + ^{7}Li$ (3.07 MeV) → γ-ray from the proton round-robin sample. Results are shown for two separate measurements calibrated with different sets of hydrogen-in-titanium standards. The resonance width of the reaction, a depth resolution of 170 nm, has not been extracted from the profile.

DP-63

Title	Technique for Profiling ^{1}H with 2.5-MeV Van de Graaff Accelerators
Reference	Appl. Phys. Lett. 34 (1979) 811
Authors	B.L. Doyle and P.S. Peercy
Institution	Sandia Laboratories, Albuquerque, USA

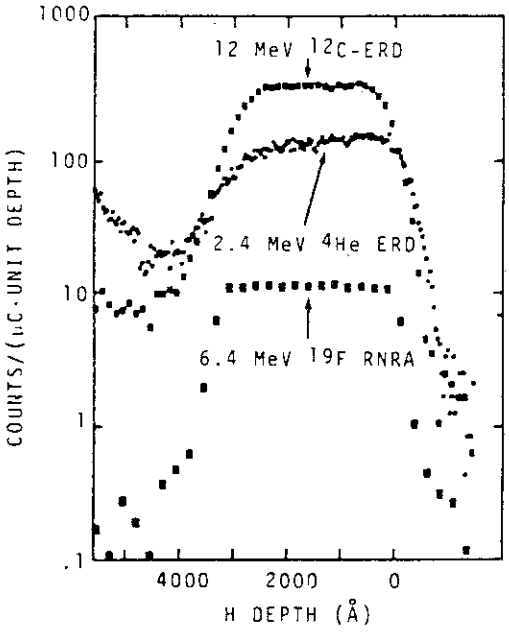

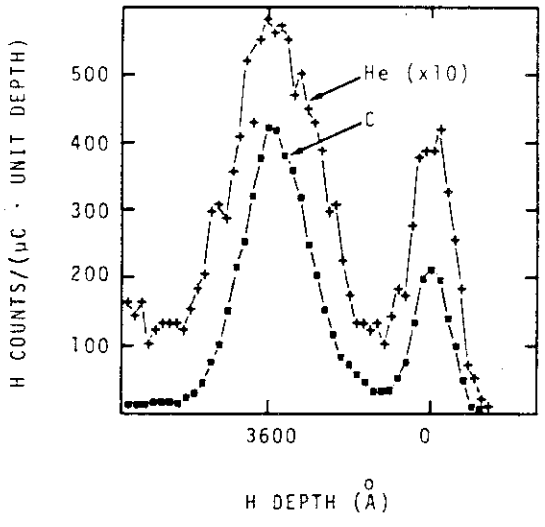

FIG. 2. Comparison between ^{1}H profiles in Si_3N_4 measured by nuclear-reaction analysis using the $^{1}H(^{19}F,\alpha\gamma)\,^{16}O$ resonance at 6.4- and 12-Mev ^{12}C ERD and 2.4-Mev ^{4}He ERD. The measured yields are plotted on a log scale in units such that the yield differences are inversely proportional to the time required to collect the spectra.

FIG. 3. Comparison of the measured profile of implanted ^{1}H in silicon measured by ERD using 12-MeV ^{12}C and 2.4-MeV ^{4}He.

DP-64

Title	Volume Expansion and Oxygen Incorporation in Deuteron-Bombarded Silicon
Reference	J. Nucl. Mat., 93 & 94 (1980) 581
Authors	K. Wittmaack(a) G. Staudenmaier(b)
Institution	(a) Gesellschaft fur Strahlem-und Umweltforshung mbH, F.R.G. (b) Max-Plank-Institut für Plasmaphysik, Garching, F.R.G.

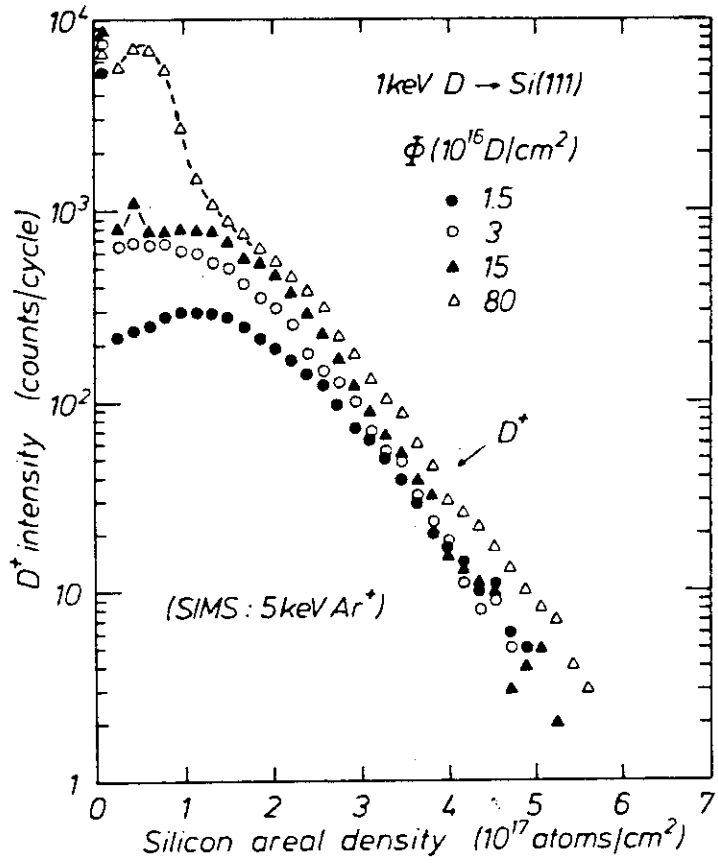

Fig. 1. SIMS depth profiles of 1 keV deuterium implanted in silicon. Parameter is the implantation fluence.

DP-65

Title	A Trap Activation Model for Hydrogen Retained and Isotope Exchange in Some Refractory Materials
Reference	J. Nucl. Mat., 103 & 104 (1981) 503
Authors	K.D. Brice, B.L. Doyle
Institution	Sandia National Laboratories, Albuquerque, USA

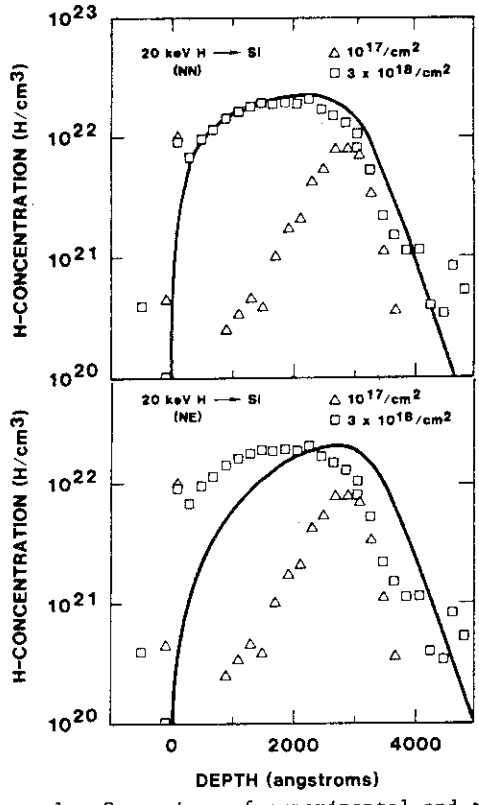

Figure 1. Comparison of experimental and theoretical hydrogen saturation depth profiles in Si (E=20 keV). Theoretical profiles are best fits obtained with Eq.3 and the parameters in Table I. a) (k,k') = N,N). b) (k,k') = (N,E).

DP-66

Title	New Precision Technique for Measuring the Concentration versus Depth of Hydrogen in Solids
Reference	Appl. Phys. Lett. 28 (1976) 566
Authors	W.A. Lanford, H.P. Trautvetter(a) J.F. Ziegler, J. Keller(b)
Institution	(a) Wright Nuclear Structure Laboratory, Yale University, USA (b) IBM Watson Research Laboratory, USA

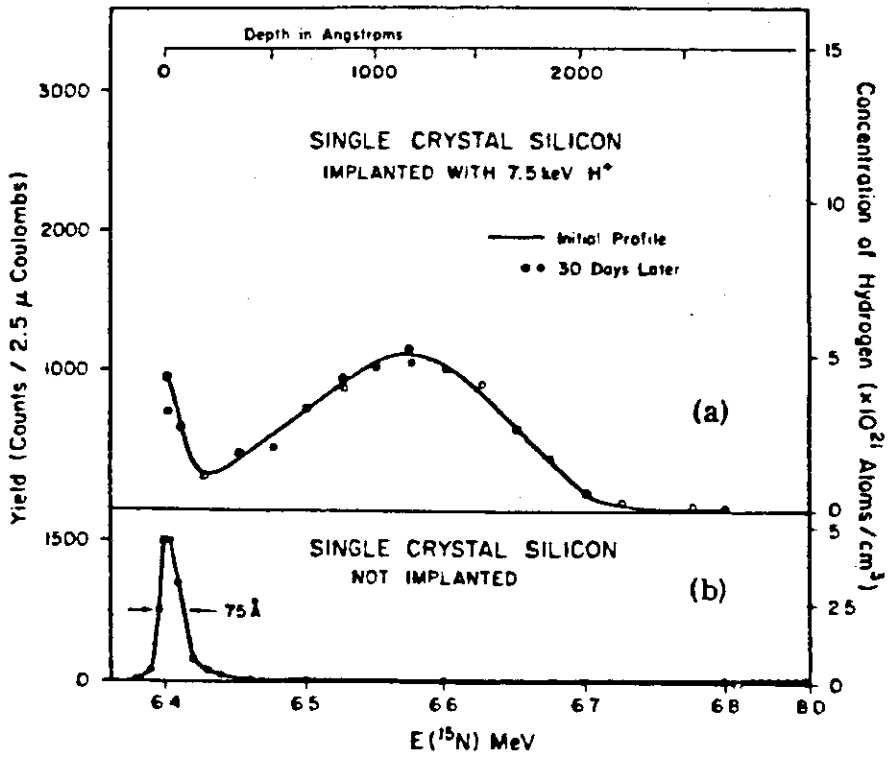

FIG. 3. (a) Hydrogen profile of a single-crystal silicon wafer implanted with 3×10^{16} H^+ ions at 7.5 keV. The solid black data points and the line are the profile as measured immediately after the implantation. The open circles are from a profile taken 30 days later. (b) Hydrogen profile of a single-crystal silicon wafer, similar to the one shown in (a) but with no implantation.

DP-67

Title	Depth Distribution of Low Energy Deuterium Implanted into Silicon as Determined by SIMS
Reference	Nucl. Instr. Methods, 168 (1980) 383
Authors	C.M. Magee(a) S.A. Cohen(b) D.E. Voss, D.K. Brice(c)
Institution	(a) RCA Laboratories, USA (b) Plasma Physics Laboratory, Princeton University, USA (c) Sandia National Laboratories, Albuquerque, USA

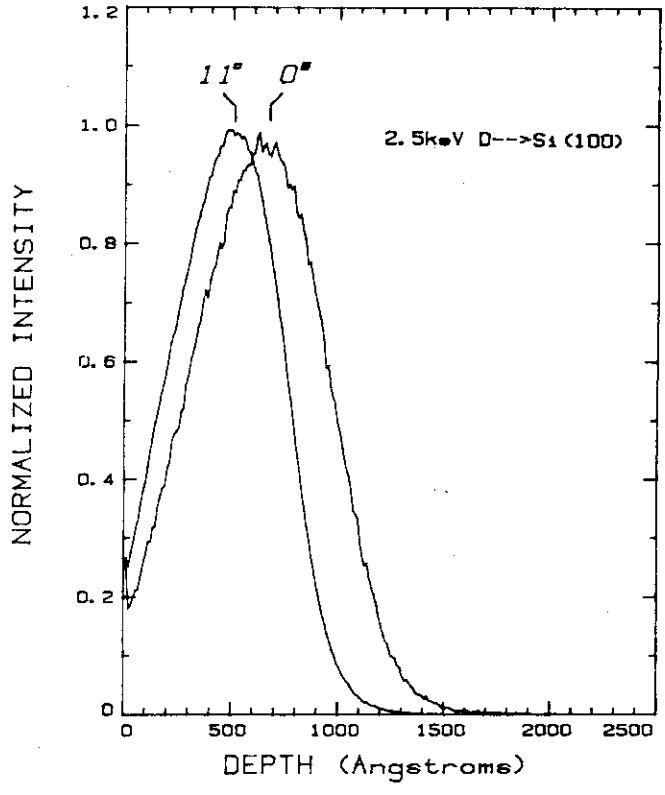

Fig. 2. Deuterium depth profiles of two (100) silicon samples ion implanted with 2.5 keV D at 0° and 11° off the surface normal.

DP-71

Title	Deuterium Trapping and Release in Titanium-Based Coating for TFTR
Reference	J. Nucl. Mat., 93 & 94 (1980) 569
Authors	K.L. Wilson, A.E. Pontau
Institution	Sandia National Laboratories, Livermore, USA

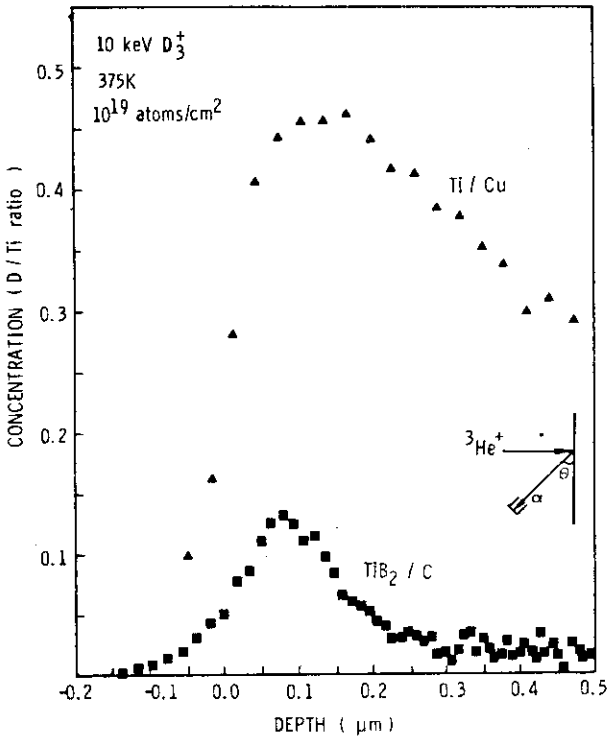

Fig. 3. D(^{3}He, α)H nuclear reaction profiling data for deuterium trapped in the first 0.5 μm of a Ti/Cu cladding and a TiB_2/C coating implanted at 375 K to 1×10^{19} D/cm^2 fluence. The Ti/Cu cladding was analyzed with 800 keV $^3He^+$ at $\theta = 15°$; the TiB_2/C coating was analyzed with 550 keV $^3He^+$ at $\theta = 75°$ because of surface roughness. Negative depths reflect the resolution of the profiling technique.

DP-72

Title	Implantation of 5 keV Deuterium in BeO
Reference	Radiat. Eff., 48 (1980) 221
Authors	R. Behrisch, R.S. Blewer, J. Borders, R. Langley, J. Roth, B.M.U. Scherzer, R. Schulz
Institution	Max-Plank-Institut für Plasmaphysik, Garching, F.R.G.

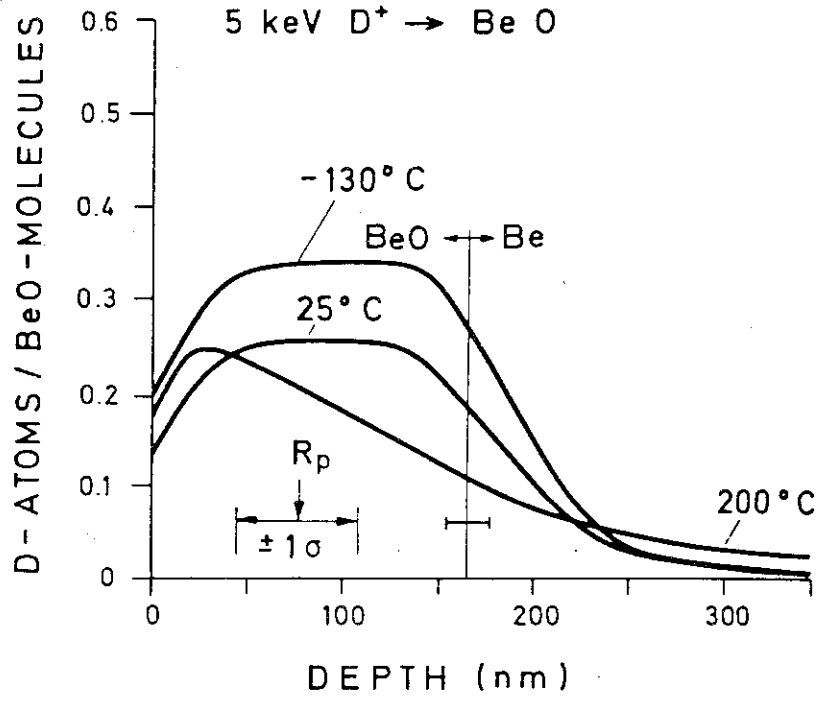

FIGURE 2 Depth profiles of deuterium implanted in a 165 nm BeO film for three different temperatures. The projected range, R_p, and the range straggling, σ, are also indicated.

DP-73

Title	Deuterium-Trapping Measurements on Boron Coatings for the TOKAMAK Fusion Test Reactors
Reference	Thin Solid Films, 83 (1981) 73
Authors	K.L. Wilson and A.E. Pontau
Institution	Sandia National Laboratories, Livermore, USA

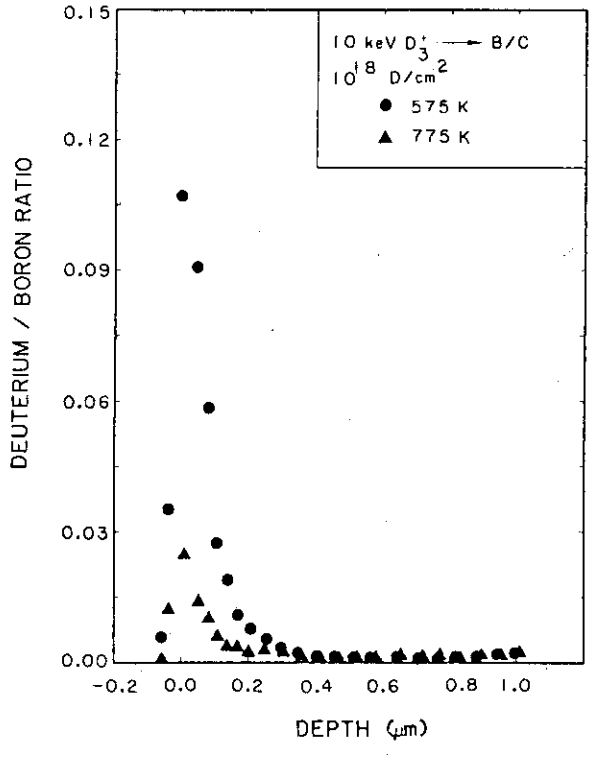

Fig. 3. D(^{3}He, α)H nuclear reaction profiles for deuterium implanted into boron coatings at two temperatures.

DP-74

Title	Hydrogen Retention and Release in First-Wall Coatings for TOKAMAKS
Reference	Thin Solid Films, 63 (1979) 277
Authors	B.L. Doyle, F.L. Vook
Institution	Sandia National Laboratories, Albuquerque, USA

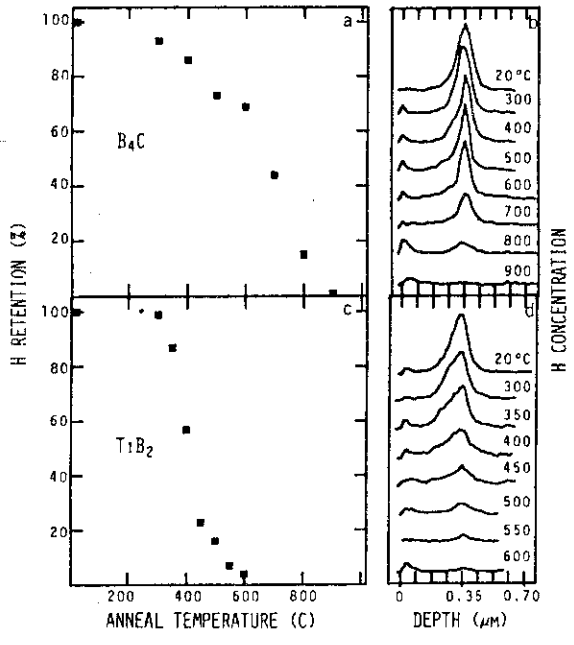

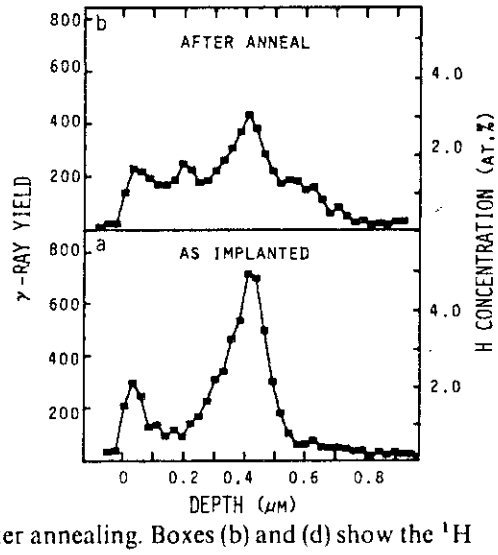

Fig. 1. ^{1}H profiles and retention curves for B_4C and TiB_2 after annealing. Boxes (b) and (d) show the ^{1}H profiles as measured by nuclear reaction analysis for ^{1}H implanted into B_4C and TiB_2, respectively. These samples were annealed isochronally at the indicated temperatures. The profiles have been displaced vertically for clarity. Boxes (a) and (c) show the respective retention curves for B_4C and TiB_2.

Fig. 2. ^{1}H profiles of ^{1}H implanted (10^{17} cm^{-2}, 30 keV) helium-predamaged (10^{17} cm^{-2}, 20 and 100 keV) B_4C: (a) as implanted; (b) after a 20 min anneal at 700 °C.

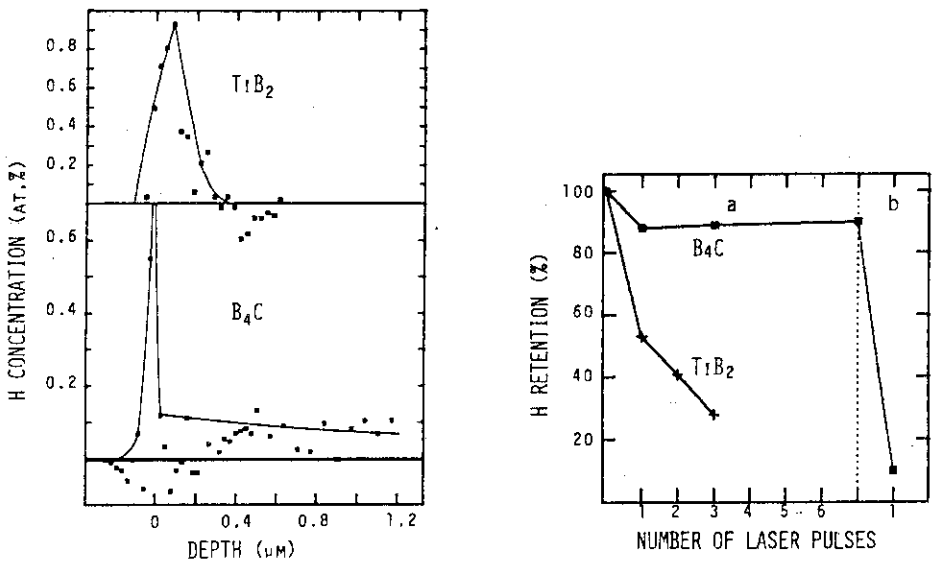

Fig. 3. Hydrogen profiles of TiB_2 and B_4C after exposure to intense low energy (250 eV) atomic hydrogen beams.

Fig. 4. Hydrogen retention in B_4C and TiB_2 after annealing with a Q-switched neodymium glass laser ($\lambda \approx 1$ μm, $\tau \approx 20$ ns). In box (a) the energy flux was 1.5 J cm^{-2} while in box (b) it was 3.0 J cm^{-2}.

References

DP-01 C.J. Altstetter, R. Behrish and B,M.U. Scherzer : Trapping of Deuteron Implanted into Stainless Steel at Low Temperatures, J. Vac. Sci. Tech., 15 (1978) 706.

DP-02 S.M. Myers and W.R. Wampler : Trapping and Surface Permeation of Deuterium in Helium-Implanted Stainless Steel, J. Nucl. Mat., 111 & 112 (1982) 579.

DP-03 K.L. Wilson, A.E. Pontau, L.G. Haggmark, M.I. Baskes, J. Bohdansky and J. Roth : Trapping of Deuterium in Helium-Damaged Steel: Helium Fluence Dependence, J. Nucl. Mat., 103 & 104 (1981) 493.

DP-04 R.S. Blewer, R. Behrisch, B.M.U. Scherzer and R. Schulz : Trapping and Replacement of 1-14 keV Hydrogen and Deuterium in 316 Stainless Steel, J. Nucl. Mat., 76 & 77 (1978) 305.

DP-05 J. Bohdansky, K.L. Wilson, A.E. Pontau, L.G. Haggmark and M.I. Baskes : Combined Depth Profiling and Thermal Desorption of Implanted Deuterium in 304LN Stainless Steel, J. Nucl. Mat., 93 & 94 (1980) 594.

DP-06 E.W. Thomas and M. Braun : Dynamic Measurements of Implanted Deuterium Retention and Release in Stainless Steel and Carbon, J. Nucl. Mat., 111 & 112 (1982) 654.

DP-07 A.E. Pontau, M.I. Baskes, K.L. Wilson, L.G. Haggmark, J. Bohdansky, B.M.U. Scherzer and J. Roth : Deuterium Retention in Helium-Damaged Stainless Steel Detrapping Energy, J. Nucl. Mat., 111 & 112 (1982) 651.

DP-11 F. Besenbacher, J. Bøttiger and S.M. Myers : Defect Trapping of Ion-Implanted Deuterium in Nickel, J. Appl. Phys., 53 (1982) 3536.

DP-12 F. Bestembacher, J. Bøttiger, T. Lauersen and W. Möller : Hydrogen Trapping in Ion-Implanted Nickel, J. Nucl. Mat., 93 & 94 (1980) 617.

DP-13 S.T. Picraux, J. Bøttiger and N. Rud : Enhanced Hydrogen Trapping due to the Ion Damage, J. Nucl. Mat., 63 (1976) 110.

DP-14 A.E. Gorodetsky, A.P. Zakharov, V.M. Sharapov and V. Kh. Alimov : Interaction of Hydrogen with Radiation Defects in Metals, J. Nucl. Mat., 93 & 94 (1980) 588.

DP-15 R. Schulz, R. Behrisch and B.M.U. Scherzer : Trapping and Mutual Release of D and ^{3}He in Molybdenum, J. Nucl. Mat., 93 & 94 (1980) 608.

DP-16 W. Möller, M. Hufschmidt and D. Kamke : Large Depth Profile Measurements of D, ^{3}He and Li by Deuteron Induced Nuclear Reactions, Nucl. Instr. Methods, 140 (1977) 157.

DP-21 W.A. Lanford, H.P. Tautvetter, J.F. Ziegler and J. Keller : New Precision Technique for Measuring the Concentration Versus Depth of Hydrogen in Solids, Appl. Phys. Lett., 28 (1976) 566.

DP-31 W. Möller, P. Børgesen and J. Bøttiger : Temperature-Dependent Depth Profiles of Deuterons Implanted into Zirconium, J. Nucl. Mat., 76 & 77 (1978) 289.

DP-51 B.M.U. Scherzer, R. Behrish, W. Eckstein, U. Littmark, J. Roth and M.K. Sinha : Temperature Dependence of Trapping and Depth Profiles of 6 to 15 keV Deuterium in Carbon, J. Nucl. Mat., 63 (1967) 100.

DP-52 R.A. Langley, R.S. Blewer and J. Roth : Behavior of Implanted D and He in Porolytic Graphite, J. Nucl. Mat., 76 & 77 (1978) 313.

DP-53 W.R. Wampler and C.W. Magee : Depth Resolved Measurement of Hydrogen Isotope Enhanced in Carbon, J. Nucl. Mat., 103 & 104 (1981) 509.

DP-54 See DP-06.

DP-61 G.J. Clark, C.W. White, D.D. Allred, B.R. Appleton, F.B. Kock and C.W. Magree : The Application of Nuclear Reactors for Quantitative Hydrogen Analysis in a Variety of Different Materials Problems, Nucl. Instr. Methods, 149 (1978) 9.

DP-62 J.F. Ziegler, et al. : Profiling Hydrogen in Materials Using Ion Beams, Nucl. Instr. Methods, 149 (1978) 19.

DP-63 B.L. Doyle and P.S. Peercy : Technique for Profileing ^{1}H with 2.5 MeV Van de Graaff Accelerators, Appl. Phys. Lett., 34 (1979) 811.

DP-64 K. Wittmaack and G. Staudenmaier : Volume Expansion and Oxygen Incorporation in Deuteron-Bombarded Silicon, J. Nucl. Mat., 93 & 94 (1980) 581.

DP-65 K.D. Brice and B.L. Doyle : A Trap Activation Model for Hydrogen Retained and Isotope Exchange in Some Refractory Materials, J. Nucl. Mat., 103 & 104 (1981) 503.

DP-66 See DP-21.

DP-67 C.M. Magee, S.A. Cohen, D.E. Voss and D.K. Brice : Depth Distribution of Low Energy Deuterium Implanted into Silicon as Determined by SIMS, Nucl. Instr. Methods, 168 (1980) 383.

DP-71 K.L. Wilson and A.E. Pontau : Deuterium Trapping and Release in Titanium-Based Coating for TFTR, J. Nucl. Mat., 93 & 94 (1980) 569.

DP-72 R. Behrisch, R.S. Blewer, J. Border, R. Langley, J. Roth, B.M.U. Scherzer and R. Schulz : Implantation of 5 keV Deuterium in BeO, Radiat. Eff., 48 (1980) 221.

DP-73 K.L. Wilson and A.E. Pontau : Deuterium-Trapping Measurements on Boron Coatings for the TOKAMAK Fusion Test Reactors, Thin Solid Films, 83 (1981) 73.

DP-74 B.L. Doyle and F.L. Vook : Hydrogen Retention and Release in First-Wall Coatings for TOKAMAKs, Thin Solid Films, 63 (1979) 277.

3.2.3 Thermal Desorption Spectroscopy

TD-01 through 05 show the results of thermal desorption spectroscopy of stainless steel, TD-11 through TD-13, of Ni and Mo, TD-51, of graphite, TD-71 and 72, of other low mass number materials, respectively.

In TD-01, two peaks are shown for SS 321 but only one peak for SS304, and it is understood that the peak of SS321 for higher temperature may be caused by impurities. In TD-02, are shown two peaks for different binding energies. In TD-04, peaks for lower temperature are different but those for higher temperature are same in case different waiting time elapses. If oxygen concentration on the surface increases, the peak for higher temperature rises up. In TD-05, when hydrogen implantation is applied with He pre-irradiation, the sample with only surface traps shows higher peak for higher temperature than that with both surface and inner traps.

In TD-11, when hydrogen isotopes are implanted in Ni and Li with and without pre-irradiation, both cases show simillar spectra but in case of He, spectrum is shifted toward higher temperature side.

In TD-51, comparision is made for graphite implanted with D and H. D_2 spectrum shows wider spread than H_2 spectrum.

TD-01

Title	Thermal Desorption and Bombardment-Induced Release of Deuterium Implanted into Stainless Steel
Reference	J. Nucl. Mat., 76 & 77 (1978) 322
Authors	G. Farrell, S.E. Donnelly
Institution	Department of Electrical Engineering, University of Salford, UK

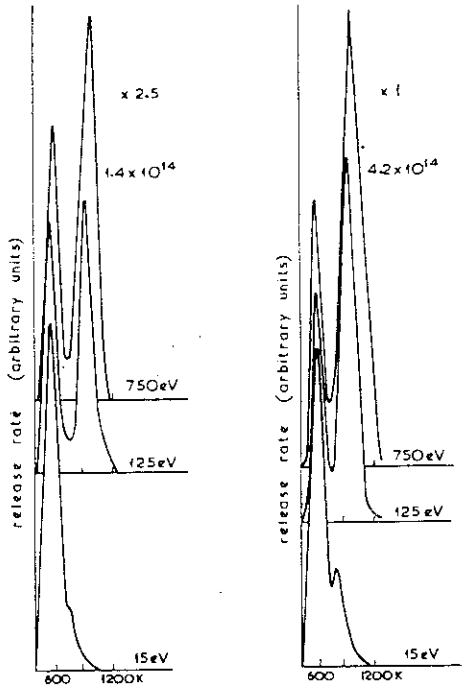

Fig. 2. Desorption spectra of deuterium from 321 stainless steel at various deuteron energies and fluences.

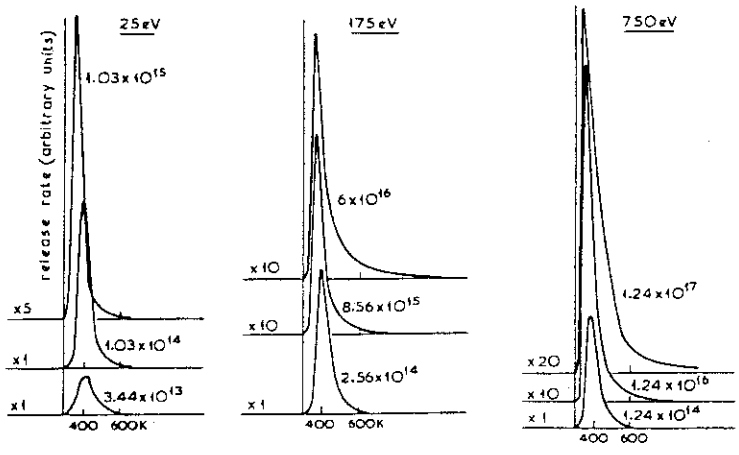

Fig. 5. Desorption spectra of deuterium from 304 stainless steel at various deuteron energies and fluences.

TD-02

Title	Deuterium Trapping in Irradiated 316 Stainless Steel
Reference	J. Nucl. Mat., 76 & 77 (1978) 291
Authors	K.L. Wilson, M.I. Baskes
Institution	Sandia Laboratories, Livermore, USA

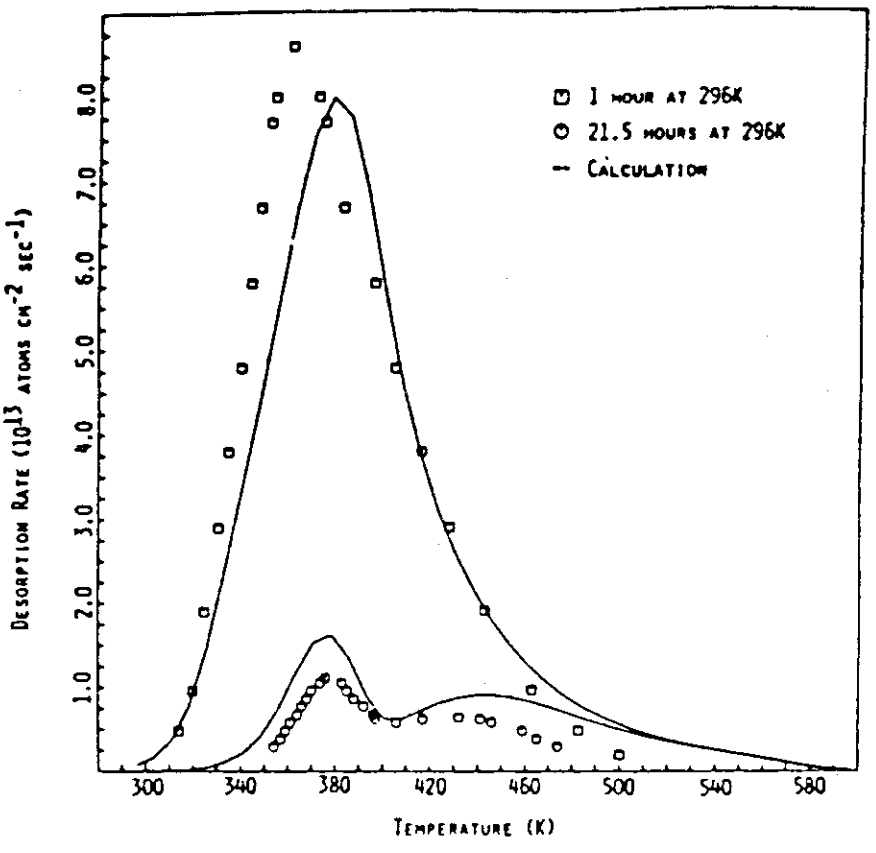

Fig. 1. Experimental and theoretical plots of desorption rate as a function of ramping temperature for two samples retained for 1 and 21.5 h at 296 K after 1 keV D^+ bombardment at 10^{18} D^+/cm^2. The ramp rate was 0.8 K/s.

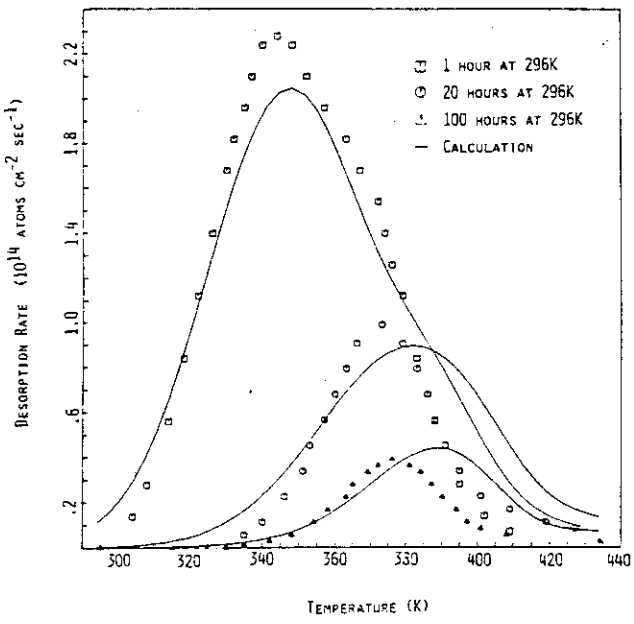

Fig. 4. Experimental and theoretical plots of desorption rate as a function of ramping temperature for three samples retained for 1, 20, or 100 h at 296 K after 10 keV D^+ implantation ot 10^{18} D^+/cm^2. Ramp rate was 0.09 K/s for the 1 h sample and 0.14 K/s for the 20 and 100 h samples.

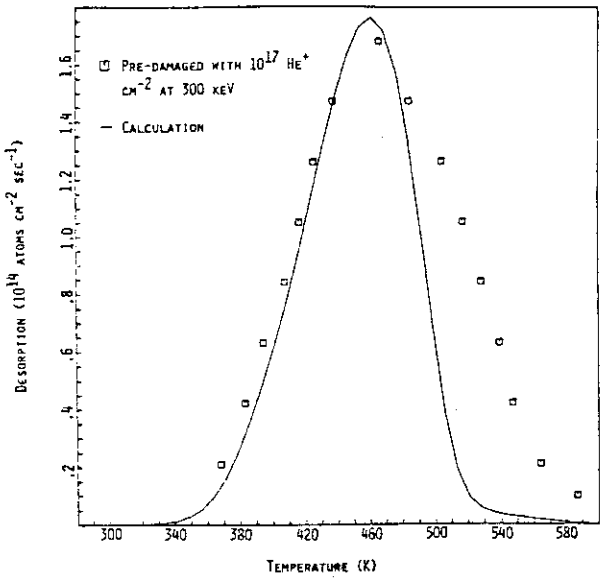

Fig. 5. Experimental and theoretical plots of desorption rate as a function of ramp temperature for a sample pre-bombarded with 300 keV $^3He^+$ to a fluence of 10^{17} He^+/cm^2, implanted with 1 keV D^+ to 10^{18} D^+/cm^2, and held at 296 K for 21.5 h prior to linear ramping. Ramp rate was 0.8 K/s.

TD-03

Title	Combined Depth Profiling and Thermal Desorption of Implanted Deuterium in 304 LN Stainless Steel
Reference	J. Nucl. Mat., 93 & 94 (1980) 594
Authors	J. Bohdansky(a) K.L. Wilson, A.E. Pontau, L.G. Haggmark, M.I. Baskes(b)
Institution	(a) Max-Plank-Institute für Plasmaphysik, Garching, F.R.G. (b) Sandia National Laboratories, Livermore, USA

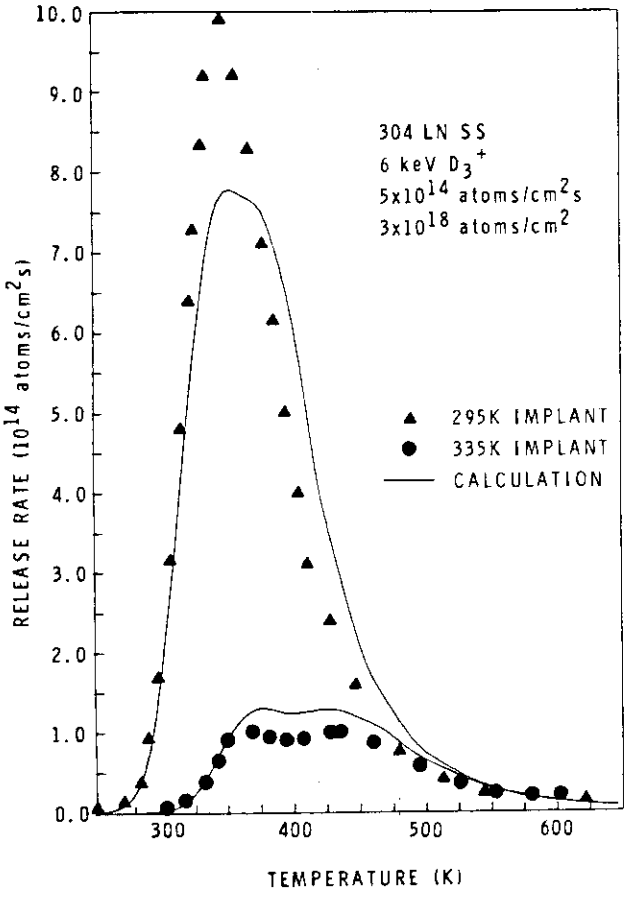

Fig. 6. Linear temperature ramp thermal desorptions of deuterium implanted into 304LN stainless steel at two temperatures and then quenched at ≈0.25 K/s. The ramp rate was 1.2 K/s. Also shown are DIFFUSE calculations of the release rate as a function of ramp temperature for the two sets of conditions.

TD-04

Title	Some Factors Affecting the Dynamics of a Plasma-Wall Interaction Simulator
Reference	J. Nucl. Mat., 111 & 112 (1982) 636
Authors	R.E. Clausing, L. Heatherly, L.C. Emerson
Institution	Oak Ridge National Laboratory, USA

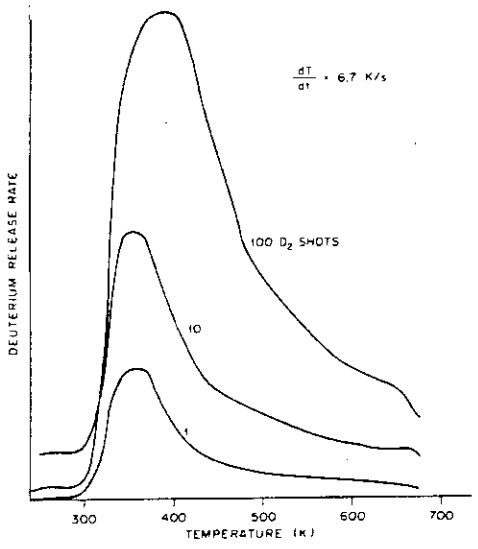

Fig. 2. Thermal desorption of deuterium from the wall sample after 1, 10, and 100 plasma pulses. The sample was outgassed to 675 K or higher before each set of plasma exposures. The temperature during plasma pulses was 300 K. The 10 shot series was made at 1 min intervals. The first 90 shots of the 100 shot series were made at 20 s intervals and the last 10 were at 1 min intervals. The thermal desorption began 4 min after the final plasma pulse in each series.

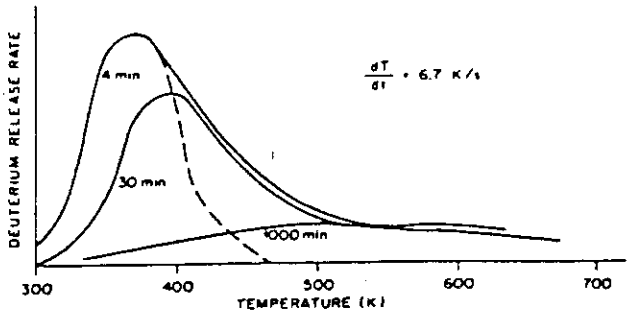

Fig. 3. Effect of waiting time on thermal desorption spectra. The dotted line indicates schematically the shape of a curve which would result from desorption of a surface species having a single activation energy for desorption and no subsurface diffusion.

TD-05

Title	Trapping and Surface Permeation of Deuterium in Helium-Implanted Stainless Steel
Reference	J. Nucl. Mat., 111 & 112 (1982) 579
Authors	S.M. Myers, W.R. Wampler
Institution	Sandia National Laboratories, Albuquerque, USA

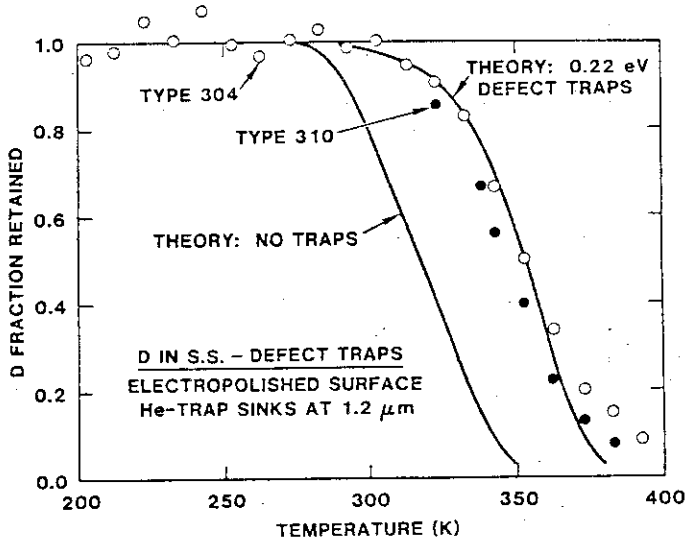

Fig. 4. Deuterium retention versus temperature under conditions reflecting defect trapping. The implanted D fluence was 1×10^{16} atoms cm^{-2}.

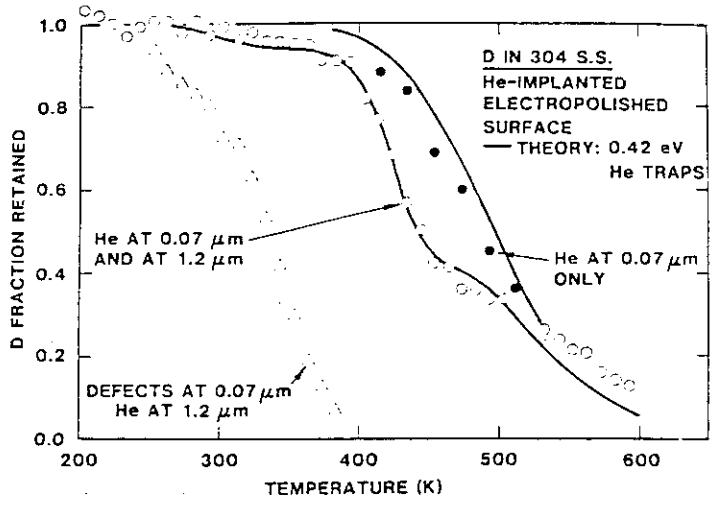

Fig. 2. Deuterium retention versus temperature for stainless steel implanted with He and D. The implanted D fluence was 2×10^{16} atoms cm^{-2}, the ramp rate 2 K min^{-1}.

TD-11

Title	Hydrogen Trapping in Ion-Implanted Nickel
Reference	J. Nucl. Mat., 93 & 94 (1980) 617
Authors	F. Bestembacher, J. Bøttiger, T. Laursen, W. Möller
Institution	Institute of Physics, University of Aarhus, Denmark

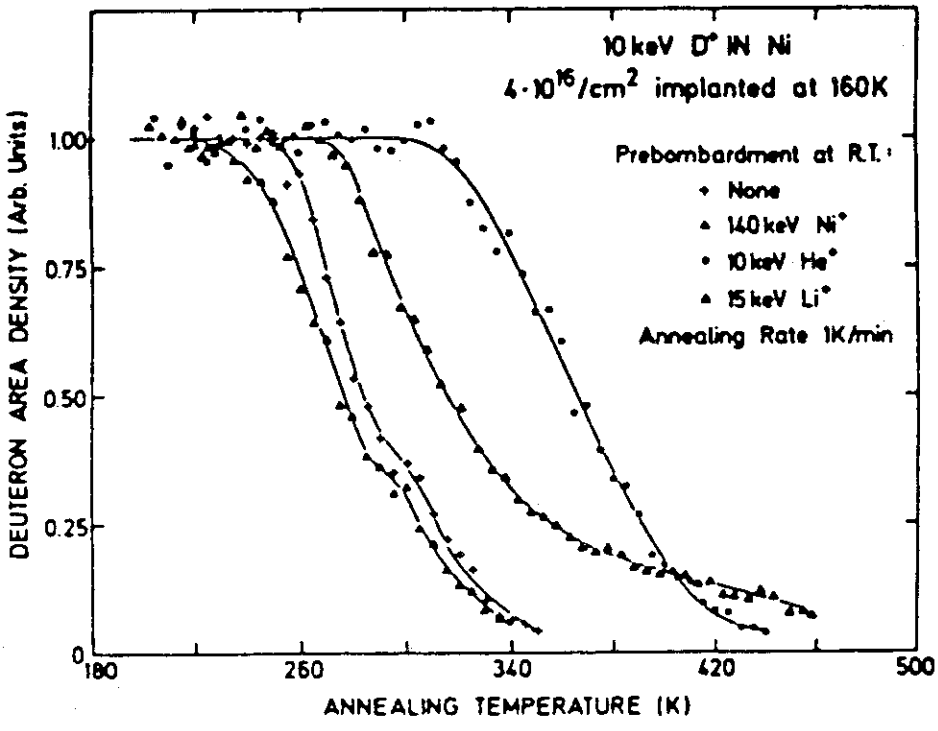

Fig. 4. Linear-ramp annealing curves. Annealing rate 1 K/min (cf. table 1).

TD-12

Title	Defect Trapping of Ion-Implanted Deuterium in Nickel
Reference	J. Appl. Phys. 53 (1982) 3536
Authors	F. Besenbacher, J. Bøttiger(a) S.M. Myers(b)
Institution	(a) University of Aarhus, Denmark (b) Sandia Laboratories, Albuquerque, USA

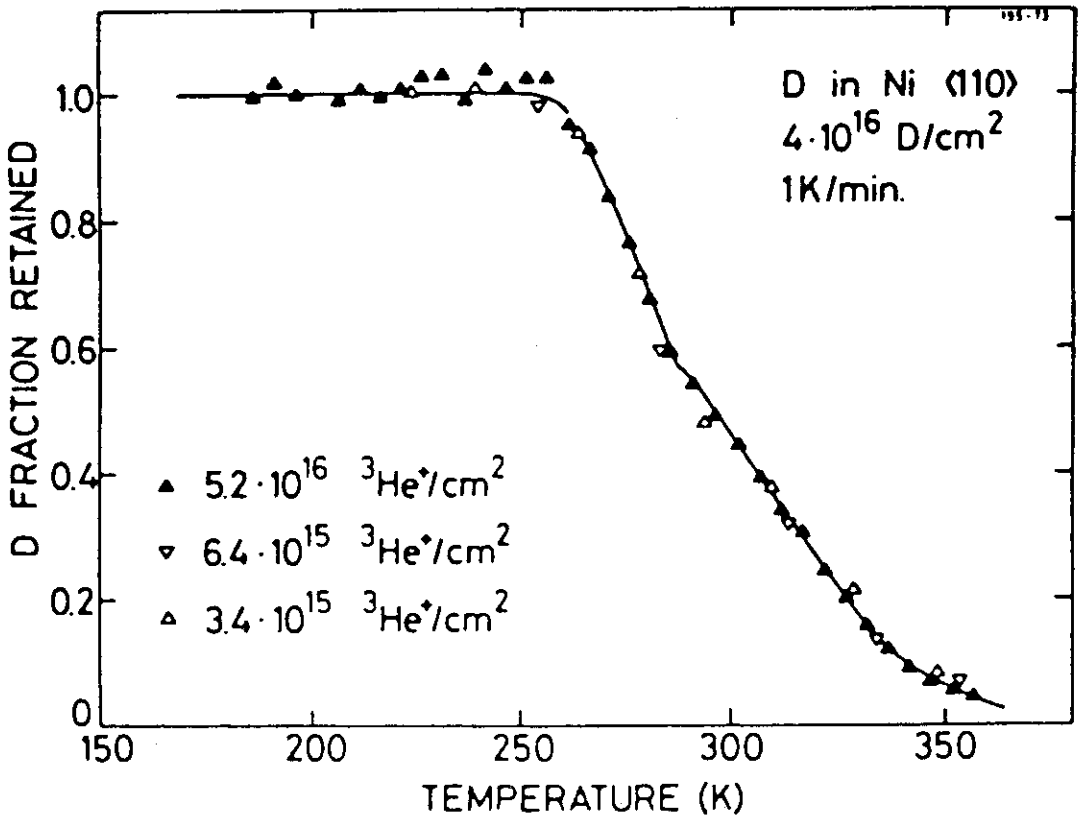

FIG. 3. Release of 4×10^{16}/cm² *D* implanted at 10 keV and 100 K into Ni during linear ramping of temperature. The release was measured for three different beam spots on the same target, corresponding to total accumulated ^{3}He fluences of $\sim5\times10^{16}$/cm² (▲), 6×10^{15}/cm² (▽), and 3×10^{15}/cm² (△). The solid curve through the release data is drawn to guide the eye only.

TD-13

Title	Trapping and Re-Emission of Deuterium from Molybdenum Following Bombardment at 77K
Reference	Vacuum, 24, 445
Authors	S.K. Erents
Institution	Culham Laboratory, UK

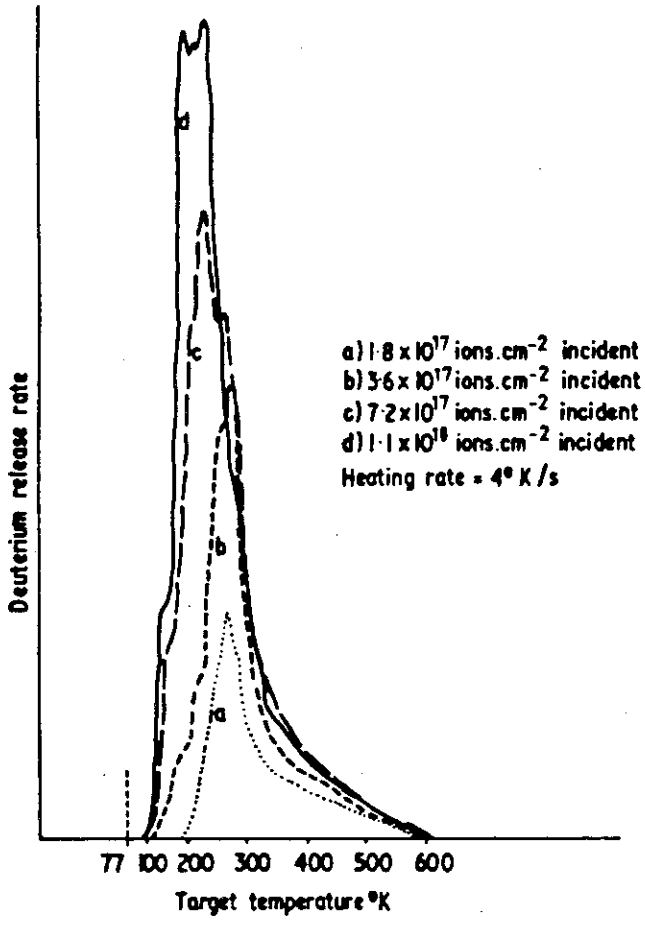

Figure 3a. Thermal spectra following 7 keV D^+ bombardment of Mo.

TD-51

Title	Behavior of Implanted D and He in Pyrolytic Graphite
Reference	J. Nucl. Mat., 76 & 77 (1978) 313
Authors	R.A. Langley, R.S. Blewer(a) J. Roth(b)
Institution	(a) Sandia Laboratories, Albuquerque, USA (b) Max-Plank-Institute für Plasma Physik, Garching, F.R.G.

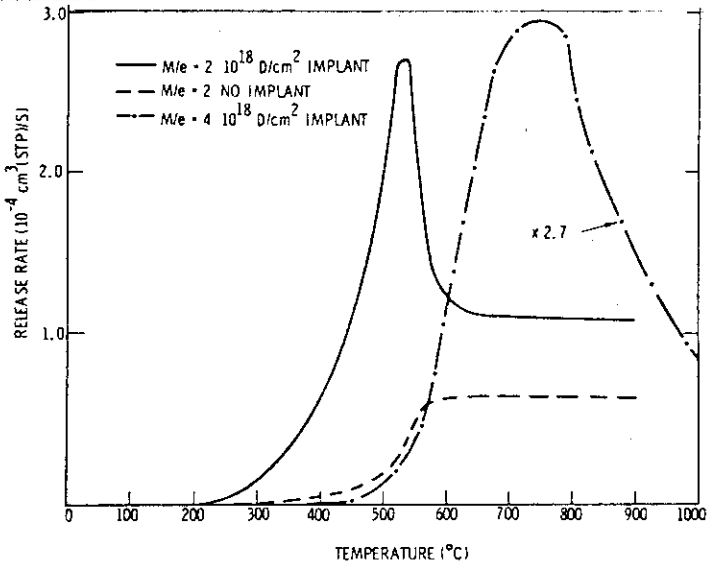

Fig. 6. Release rate for H_2 and D_2 as a function of temperature for both implanted and unimplanted samples. Temperature ramp rate was 5°C/s.

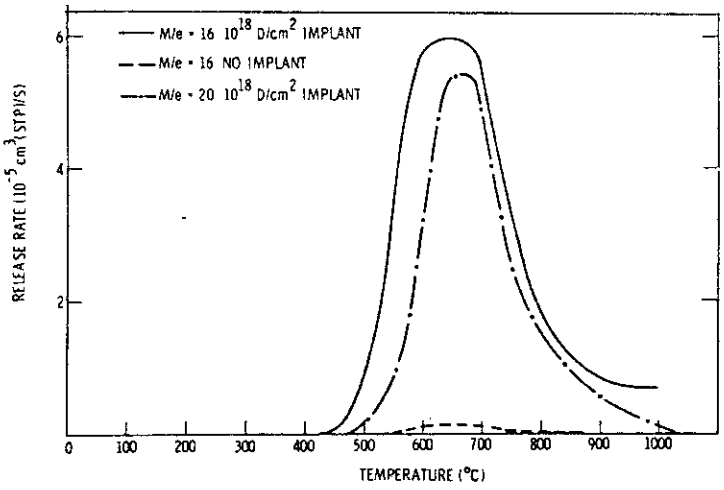

Fig. 7. Release rate for CH_4 and CD_4 as a function of temperature for both implanted and unimplanted samples. Temperature ramp rate was 5°C/s.

TD-71

Title	Deuterium-Trapping Measurements on Boron Coatings for the TOKAMAK Fusion Test Reactors
Reference	Thin Solid Films, 83 (1981) 73
Authors	K.L. Wilson and A.E. Pontau
Institution	Sandia National Laboratories, Livermore, USA

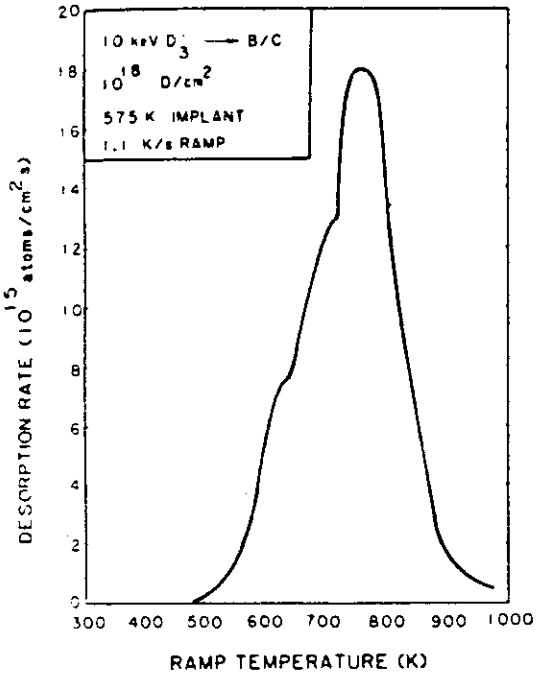

Fig. 2. A linear ramp thermal desorption spectrum for a boron coating implanted at 575 K.

TD-72

Title	Deuterium Trapping and Release in Titanium-Based Coating for TFTR
Reference	J. Nucl. Mat., 93 & 94 (1980) 569
Authors	K.L. Wilson, A.E. Pontau
Institution	Sandia National Laboratories, Livermore, USA

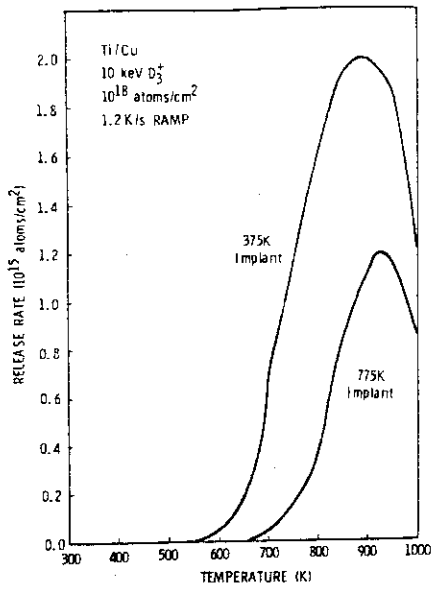

Fig. 2. Thermal desorption spectra for Ti/Cu claddings implanted to 1×10^{18} D/cm^2 fluence at 375 and 775 K. A linear temperature ramp rate of 1.2 K/s was used.

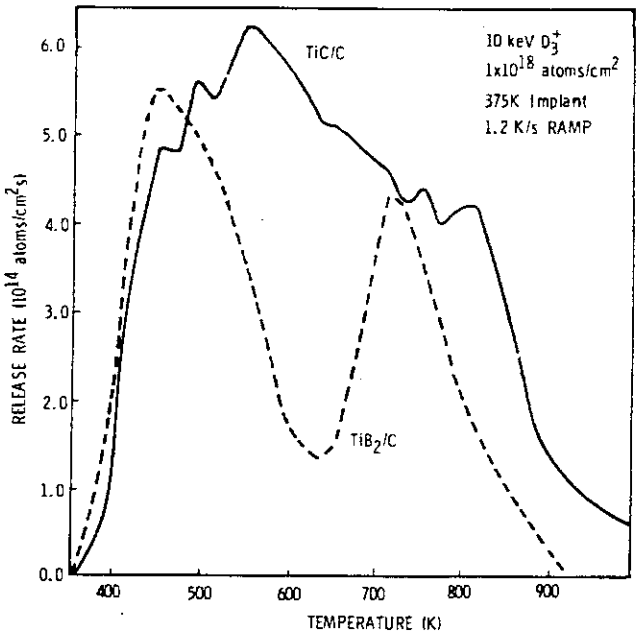

Fig. 5. Thermal desorption spectra for TiB_2/C and TiC/C coatings implanted to 1×10^{18} D/cm^2 fluence at 375 K. A linear temperature ramp rate of 1.2 K/s was used.

References

TD-01 G. Farrell and S.E. Donnelly : Thermal Desorption and Bombardment-Induced Release of Deuterium Implanted into Stainless Steel, J. Nucl. Mat., 76 & 77 (1978) 322.

TD-02 K.L. Wilson and M.I. Baskes : Deuterium Trapping in Irradiated 316 Stainless Steel, J. Nucl. Mat., 76 & 77 (1978) 291.

TD-03 J. Bohdansky, K.L. Wilson, A.E. Pontau, L.G. Haggmark and M.I. Baskes : Combined Depth Profiling and Thermal Desorption of Implanted Deuterium in 304LN Stainless Steel, J. Nucl. Mat., 93 & 94 (1980) 594.

TD-04 R.E. Clausing, L. Heatherly and L.C. Emerson : Some Factors Affecting the Dynamics of a Plasma-Wall Interaction Simulator, J. Nucl. Mat., 111 & 112 (1982) 636.

TD-05 S.M. Myers and W.R. Wampler : Trapping and Surface Permeation of Deuterium in Helium-Implanted Stainless Steel, J. Nucl. Mat., 111 & 112 (1982) 579.

TD-11 F. Bestenbacher, J. Bøttiger, T. Laursen and W. Möller : Hydrogen Trapping in Ion-Implanted Nickel, J. Nucl. Mat., 93 & 94 (1980) 617.

TD-12 F. Bestenbacher, J. Bøttiger and S.M. Myers : Defect Trapping of Ion-Implanted Deuterium in Nickel, J. Appl. Phys., 53 (1982) 3536.

TD-13 S.K. Erents : Trapping and Re-Emission of Deuterium from Molybdenum Following Bombardment at 77K, Vacuum, 24, 445.

TD-51 R.A. Langley, R.S. Blewer and J. Roth : Behavior of Implanted D and He in Pyrolytic Graphite, J. Nucl. Mat., 76 & 77 (1978) 313.

TD-71 K.L. Wilson and A.E. Pontau : Deuterium-Trapping Measurements on Boron Coatings for the TOKAMAK Fusion Test Reactors, Thin Solid Films, 83 (1981) 73.

TD-72 K.L. Wilson and A.E. Pontau : Deuterium Trapping and Release in Titanium-Based Coating for TFTR, J. Nucl. Mat., 93 & 94 (1980) 569.

3.3 Permeation

In this section, data are collected on permeation. PM-01, 02 and 03 show researches on stainless steel, PM-11 through 13, on Ni and Mo, PM-21, on Ceramvar-Cu-Ceram multilayer, respectively. Among these, PM-02, 11 and 12 are concerned with irradiation experiments. In PM-11, permeation decreases first then turns to increase as the temperature rises. In PM-12, permeation increases as the time elapses and then decreases to reach equilibrium after passing the peak value. In PM-01, shown is the increase of permeation as oxygen concentration decreases. And in PM-21, more permeation of H_2 is shown than that of D_2.

PM-01

Title	Deuterium Permeation through 309S Stainless Steel with Thin, Characterized Oxides
Reference	J. Nucl. Mat., 53 (1974) 307
Authors	W.A. Swansiger, R.G. Musket, L.J. Weirick, W. Bauer
Institution	Sandia Laboratories, Livermore, USA

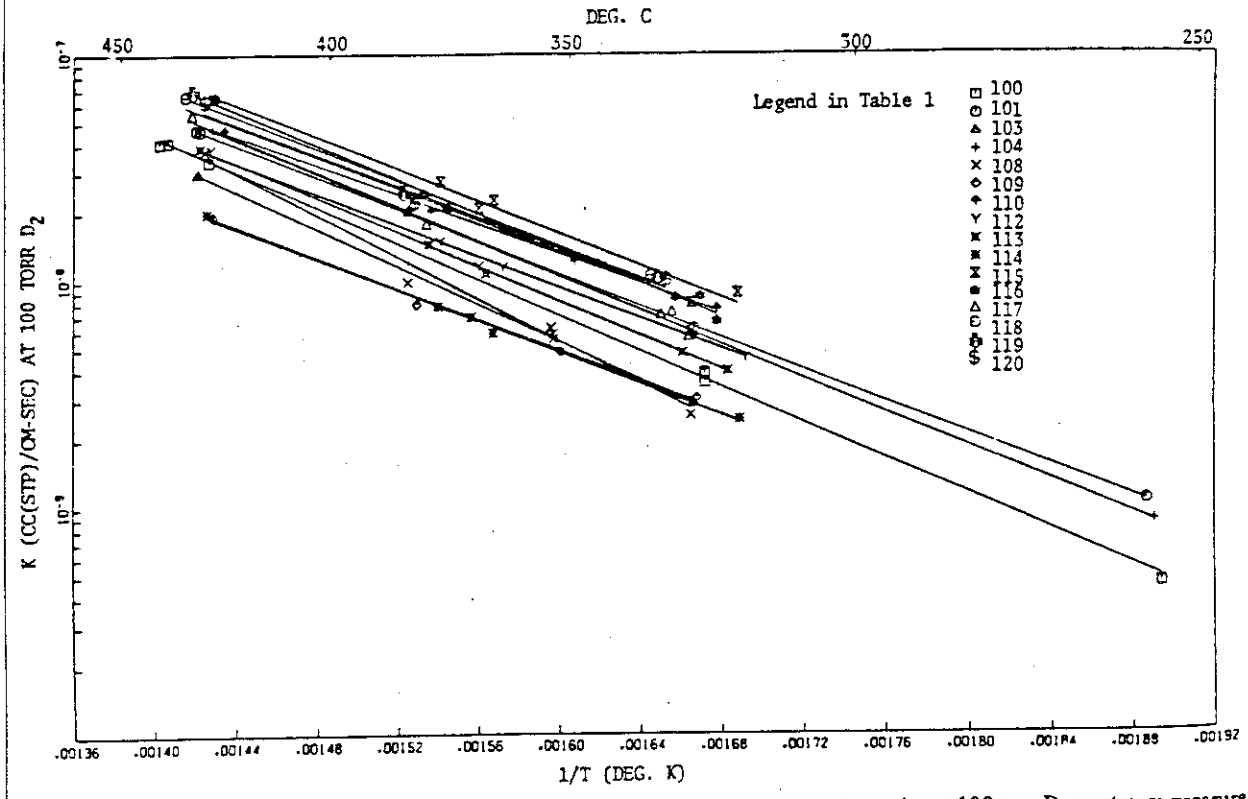

Fig. 1. Arrhenius plot showing range of permeabilities spanned by the 16 stainless steel samples at 100 torr D_2 upstream pressure.

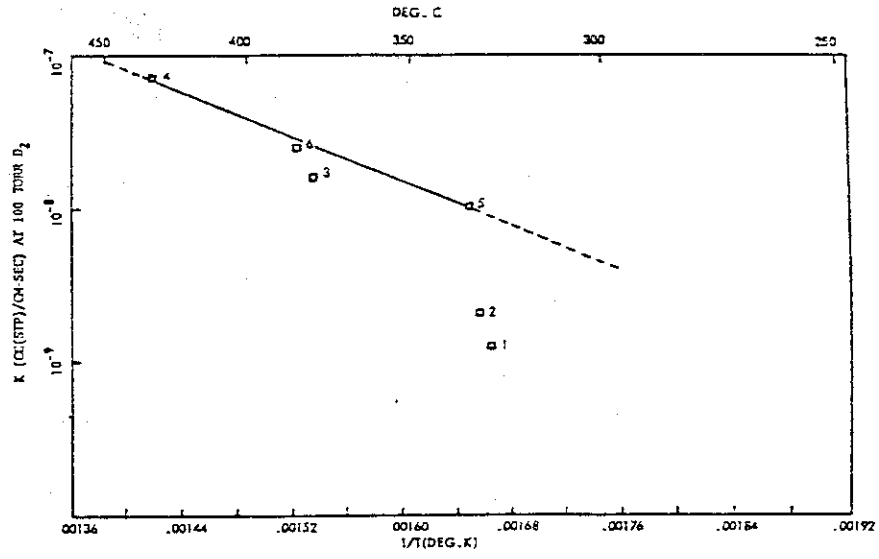

Fig. 3. Arrhenius plot depicting reduction of the oxide on sample 119 by permeating hydrogen. Points are numbered in the order in which data were taken.

Table I
Oxide preparation and characterization data for 10 mil 309S discs grouped according to surface treatment.

	Sample number	Oxide thickness (Å) weight gain	PIX	Oxide composition[b]	Substrate treatment	Surface treatment
I	100	–	180	Cr, Fe, Ni	BA	rinsed in methanol, air dried
	103	–	200	Cr, Fe	AR	rinsed in methanol, air dried
	104	–	180	Cr, Fe	BA	½ h at 900°C in 5 × 10^{-6} torr vacuum
	108	–	200	Cr, Fe	AR	cleaned ultrasonically in trichloroethylene, rinsed in methanol, air dried
II	113	–	–	Cr, Fe	BA	200°C, ambient air, 72 h
	112	–	–	Cr, Fe	BA	250°C, ambient air, 65 h
	120	270	–	Cr, Fe	VA2	360°C, ambient air, 0.7 h
	120 duplicate	–	–	Fe	VA2	360°C, ambient air, 0.7 h
	119[a]	310	–	U:Cr, Fe; D:Cr, Fe	VA2	360°C, ambient air, 7 h
	119 duplicate	–	–	Fe	VA2	360°C, ambient air, 7 h
	118	330	–	Cr, Fe	VA2	360°C, ambient air, 70 h
	118 duplicate	–	–	Fe	VA2	360°C, ambient air, 70 h
III	115	260	–	Fe, Cr	VA2	900°C at 9 × 10^{-6} torr for 15 min; 600°C at 0.2 torr O_2 for 2 h
	116[a]	640	–	Fe, Cr	VA2	900°C at 7 × 10^{-6} torr for 15 min; 700°C at 0.16 torr O_2 for 1 h
	117	1330	–	Fe, Cr	VA2	900°C at 9 × 10^{-6} torr for 15 min; 700°C at 0.14 torr O_2 for 26 h
	114	–	2200	Cr, Fe	AR	700°C, wet H_2, 3 h
	109	900	1400	Cr, Fe	AR	800°C at 2 × 10^{-5} torr O_2, 1 h
	110	> 1700	2700	Cr, Fe	BA	800°C at 2 × 10^{-4} torr O_2, 9 h
	101[a]	1700	1300	Cr, Fe	BA	800°C at 1 × 10^{-3} torr O_2, 1.2 h

Group I – unoxidized; Group II – air oxidized; Group III – high temperature oxidations: AR–as-received; BA–bright annealed; VA2–vacuum annealed twice: U – upstream side; D – downstream side.

a) Sputter-Auger analysis after permeation found significant differences in thickness and composition between upstream and downstream faces.

b) Underline indicates predominant metallic element.

PM-02

Title	The Application of Ion Beam Method to Diffusion and Permeation Measurements
Reference	Nucl. Instr. Methods, 168 (1980) 289
Authors	W. Möller, B.M.U. Scherzer, R.Behrisch
Institution	Max-Plank-Institut für Plasmaphysik, Garching, F.R.G.

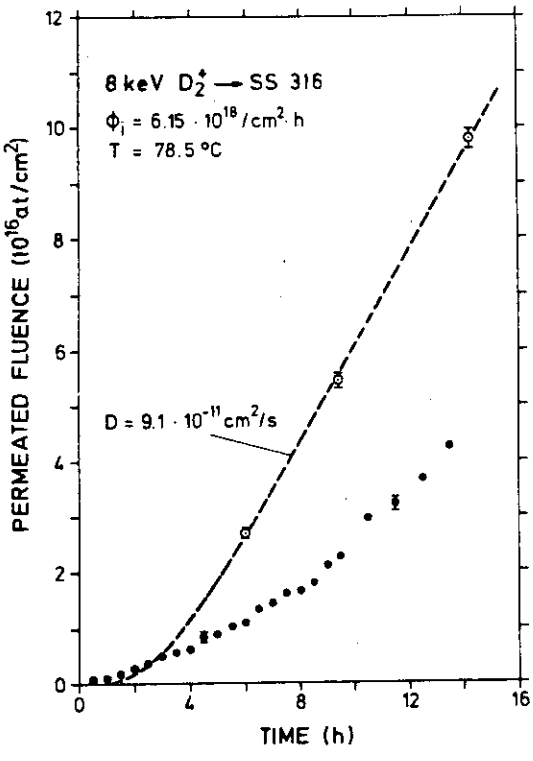

Fig. 3. Permeated fluence as function of time. Total analysing dose: $3\times2\,\mu$C (open symbols) and $23\times2\,\mu$C (filled circles). The error bars reflect the counting statistics.

PM-03

Title	The Rate of Hydrogen Release out of Clean Metallic Surfaces
Reference	J. Nucl. Mat., 76 & 77 (1978) 337
Authors	I. Ali-Khan, K.J. Dietz, F.G. Waelbroeck, P.Winehold
Institution	Institut für Plasmaphysik der Kernforshungsangle Jülich GmbH, F.R.G.

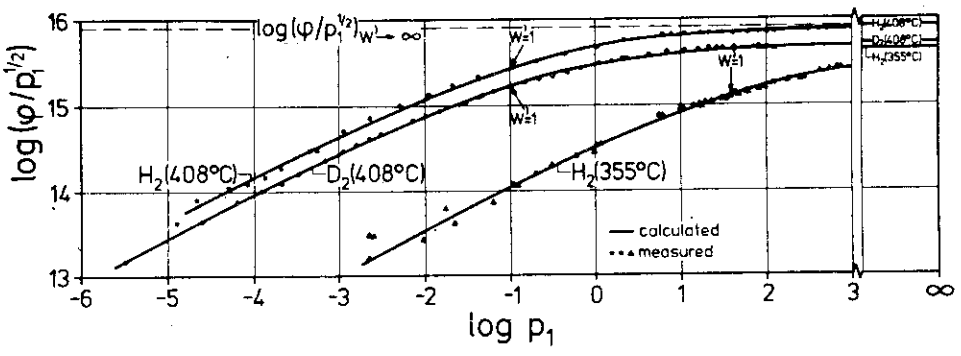

Fig. 2. Permeation in the stationary case. φ: permeation flux density ($H/cm^2 \cdot s$) p_1: upstream pressure (Torr); curves calculated according eq. (16) using the values of table 2. $(p_1)_{W'=1}$ = 40 Torr for H_2 at 355°C, 0.09 Torr for H_2 and D_2 at 408°C.

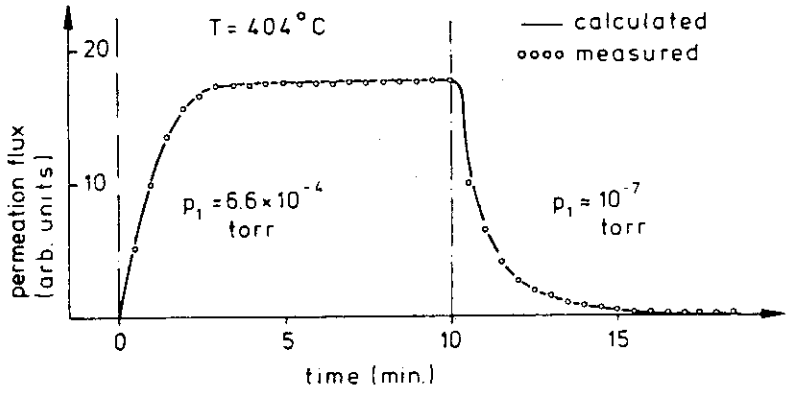

Fig. 3. Evolution of the permeation ($W' << 1$) in the non-stationary case. Curve calculated according to eqs. (21), and (22).

PM-11

Title	Interaction of Hydrogen with Radiation Defects in Metals
Reference	J. Nucl. Mat., 93 & 94 (1980) 588
Authors	A.E. Gorodetsky, A.P. Zakharov, V.M. Sharapov, V.Kh. Alimov
Institution	Institute of Physical Chemistry, Academy of Science, USSR

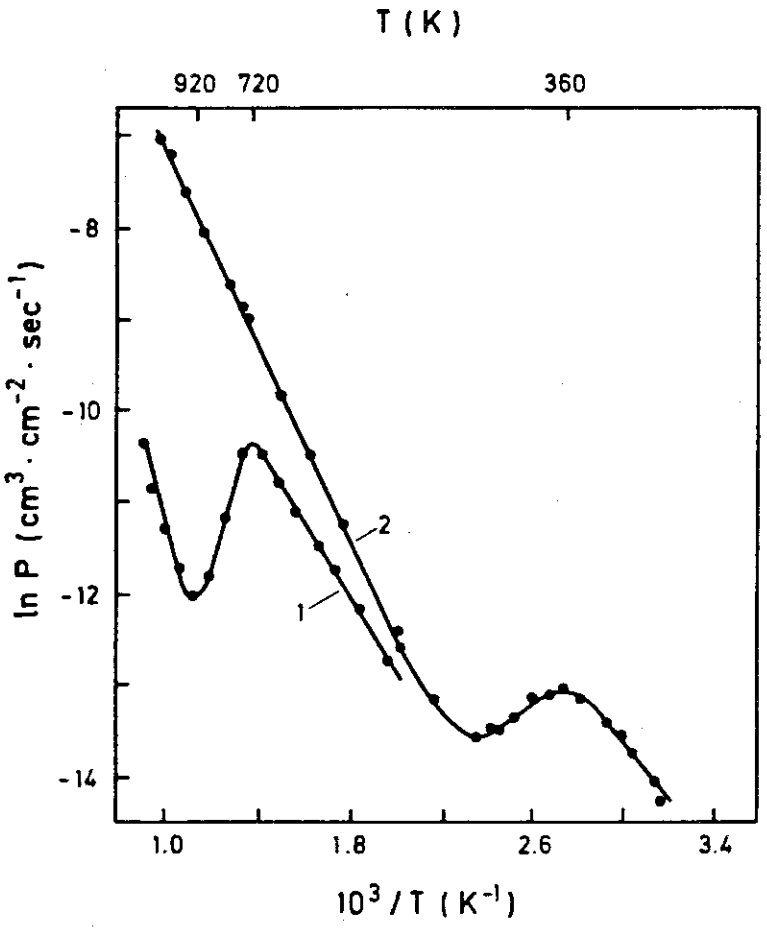

Fig. 1. The hydrogen permeation through Mo (1) and Ni (2) samples from a glow discharge plasma. Current densities are 5 mA/cm^2 for Mo and 2.5 mA/cm^2 for Ni, voltage 350 V. Sample thickness 0.1 mm.

PM-12

Title	Permeation and Reemission of Deuterium Implanted in Fast Wall Materials
Reference	J. Nucl. Mat., 103 & 104 (1981) 483
Authors	T. Tanabe, N. Saito, Y. Etoh, S. Imoto
Institution	Department of Nuclear Engineering, Osaka University, Japan

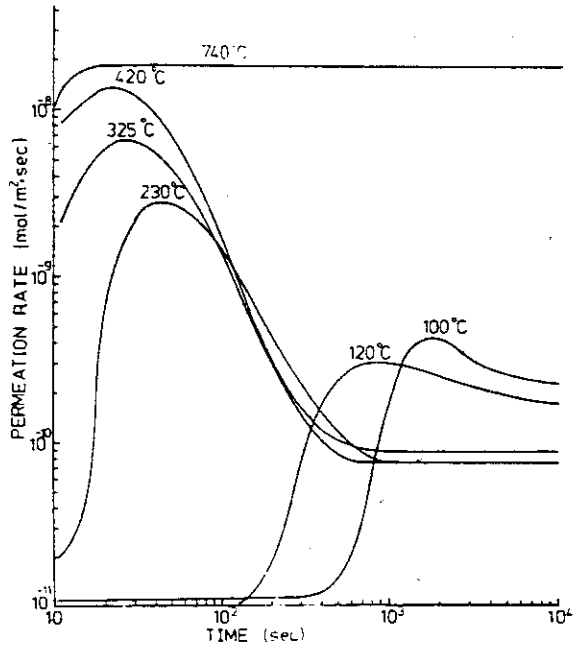

Fig.2 Permeation rate of deuterium through Ni during 20 keV D^+ implantation

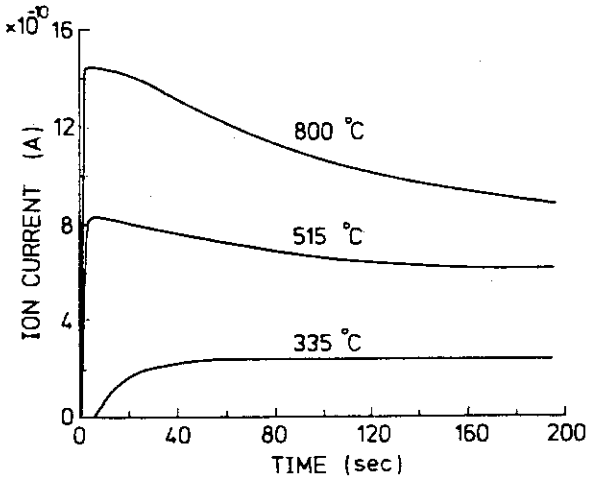

Fig.5 Permeation rate of deuterium through Mo during 20 keV D^+ implantation

PM-13

Title	Properties of Hydride-Forming Metals and of Multilayer Hydrogen Permeation Barriers
Reference	J. Nucl. Mat., 53 (1974) 313
Authors	J.W. Guthrie, L.C. Beavis, D.R. Begeal, W.G. Perkins
Institution	Sandia Laboratories, Albuquerque, USA

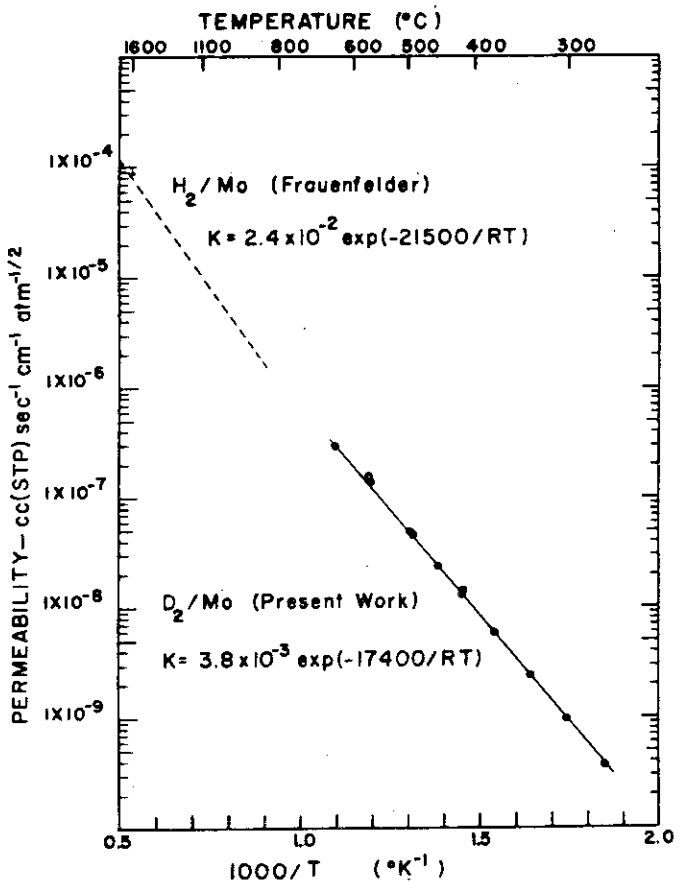

Fig. 7. Deuterium and hydrogen permeabilities for molybdenum.

PM-21

Title	Properties of Hydride-Forming Metals and of Multilayer Hydrogen Permeation Barriers
Reference	J. Nucl. Mat., 53 (1974) 313
Authors	J.W. Guthrie, L.C. Beavis, D.R. Begeal, W.G. Perkins
Institution	Sandia Laboratories, Albuquerque, USA

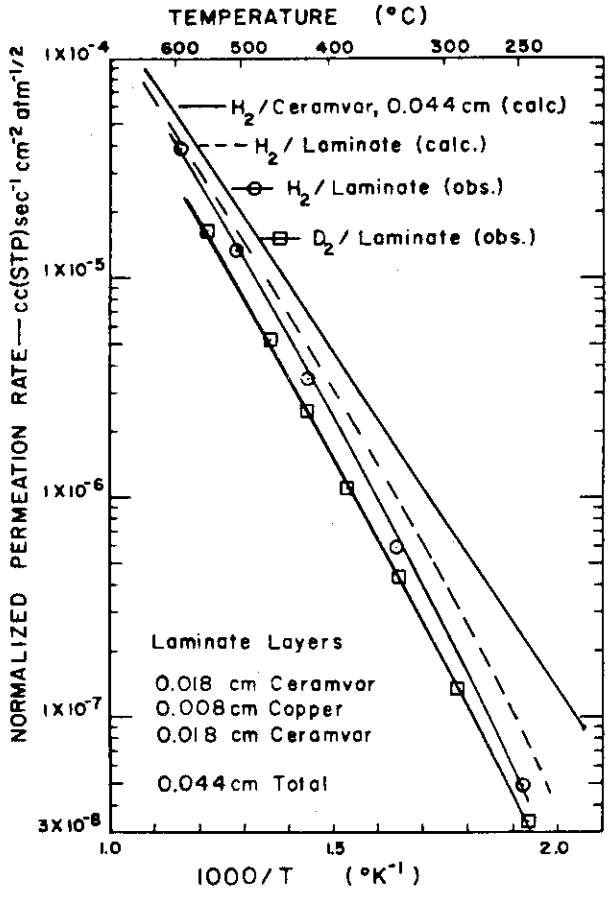

Fig. 6. Normalized permeation rates for hydrogen isotopes through Ceramvar–copper–Ceramvar laminate at 1 atm pressure.

References

PM-01 W.A. Swansiger, R.G. Musket, L.J. Weirick and W. Bauer : Deuterium Permeation through 309S Stainless Steel with Thin, Characterized Oxides, J. Nucl. Mat., 53 (1974) 307.

PM-02 W. Möller, B.M.U. Scherzer and R. Behrisch : The Application of Ion Beam Method to Diffusion and Permeation Measurements, Nucl. Instr. Methods, 168 (1980) 289.

PM-03 I. Ali-Khan, K.J. Dietz, F.G. Waelbroeck and P. Winehold : The Rate of Hydrogen Release out of Clean Metallic Surfaces, J. Nucl. Mat., 76 & 77 (1978) 337.

PM-11 A.E. Gorodetsky, A.P. Zakharov, V.M. Sharopov and V. Kh. Alimov : Interaction of Hydrogen with Radiation Defects in Metals, J. Nucl. Mat., 93 & 94 (1980) 588.

PM-12 T. Tanabe, N. Saito, Y. Etoh and S. Imoto : Permeation and Reemission of Deuterium Implanted in Fast Wall Materials, J. Nucl. Mat., 103 & 104 (1981) 483.

PM-13 J.W. Guthrie L.C. Beavis, D.R. Begeal and W.G. Perkins : Properties of Hydride-Forming Metals and of Multilayer Hydrogen Permeation Barriers, J. Nucl. Mat., 53 (1974) 313.

PM-21 See PM-13.

3.4 Ion Impact Desorption

ID-01 shows the data of ion impact desorption for stainless steel, ID-11, for Mo, ID-21 and 22, for W, ID-31, for Ti coated Cu, respectively. ID-01 shows D desorption cross section by H that decreases as the energy increases. ID-21 shows H desorption cross section by ^{3}He that stays constant for higher energy.

ID-01

Title	Ion Impact Desorption and Hydrogen Release
Reference	J. Nucl. Mat., 103 & 104 (1981) 499
Authors	R. Bastasz, L.G. Haggmark
Institution	Sandia National Laboratories, Livermore, USA

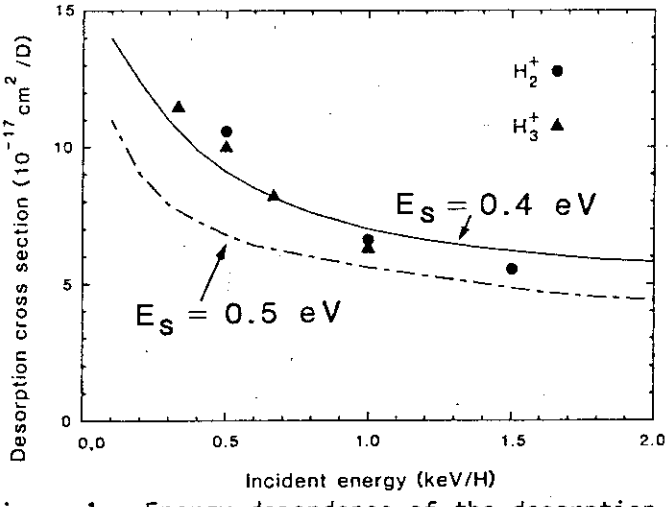

Figure 1 : Energy dependence of the desorption cross section for H → D (ads) on stainless steel at 30° incidence. TRIM results are shown for E_s of 0.4 and 0.5 eV.

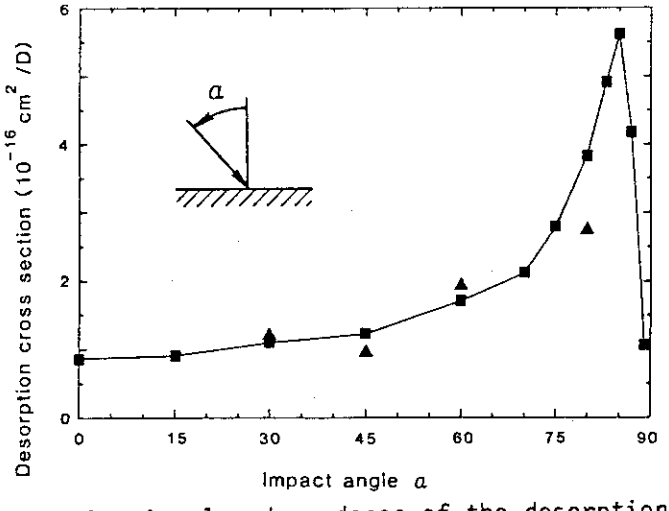

Figure 2 : Angular dependence of the desorption cross section. Experimental results are shown (triangles) for H → D (ads) on stainless steel at 333 eV. TRIM results (squares) are shown for E_s = 0.4 eV.

ID-11

Title	Desorption of Adsorbed and Condenced Bases on Metals by Deuterons
Reference	Vacuum, 24 (1974) 463
Authors	G. McCracken
Institution	Culham Laboratory, UK

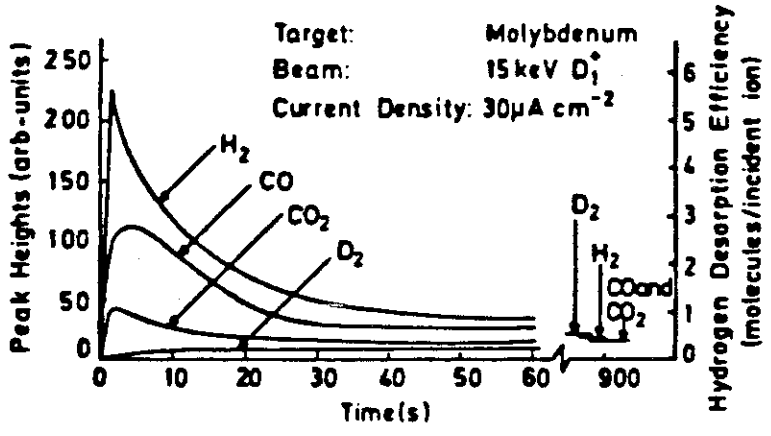

Figure 3. Desorption of adsorbed gas from a molybdenum surface by 15 keV D^+ ions. Current density 30 μA cm^{-2}.

ID-21

Title	Ion Impact Desorption Cross Sections of Hydrogen and Oxygen from Metals by Light Ion Bombardment
Reference	J. Nucl. Mat., 76 & 77 (1978) 328
Authors	E. Taglauer, W. Heiland
Institution	Max-Plank-Institut für Plasmaphysik, Garching, F.R.G.

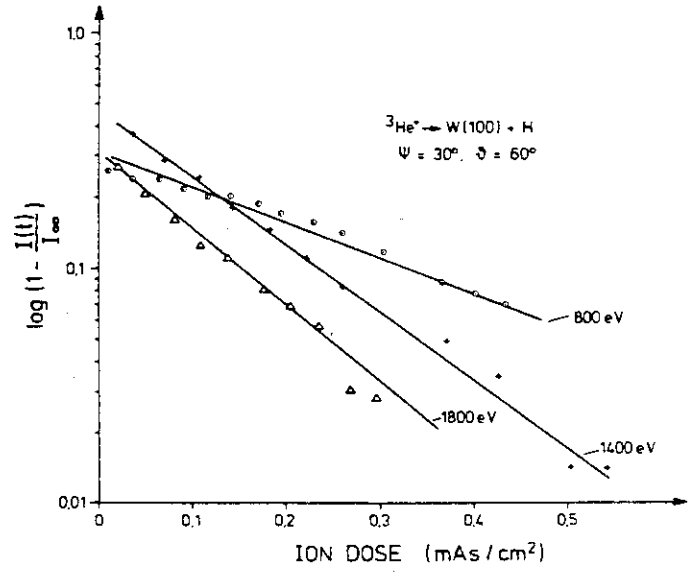

Fig. 2. Desorption of H from W (100) by $^3He^+$. The ISS data are evaluated according to eq. (1).

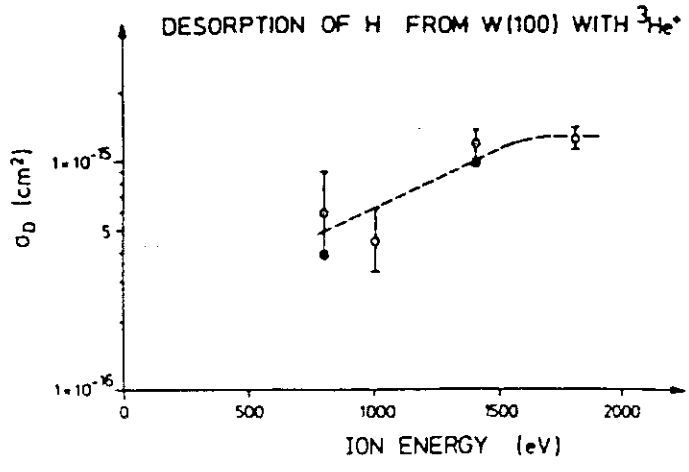

Fig. 3. Dependence of the $^3He^+$–H desorption cross section on the primary $^3He^+$ ion energy.

ID-22

Title	Investigation of Ion Impact Desorption of Atoms and Molecules by Low Energy Ion Scattering (ISS)
Reference	Nucl. Instr. Methods, 149 (1978) 605
Authors	E. Taglauer, U. Beitat, W. Heiland
Institution	Max-Plank-Institut für Plasmaphysik, Garching, F.R.G.

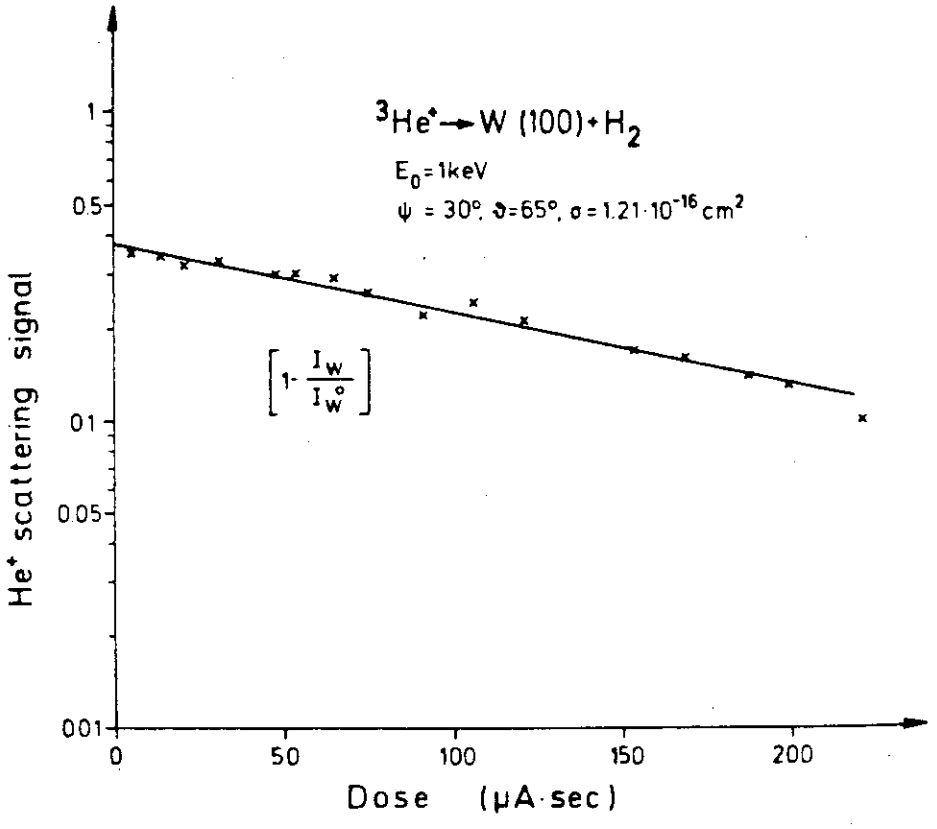

Fig. 4. Dose dependence of the He^+ backscattering signal of W during desorption of H from W(100).

ID-31

Title	ISS Observation of Ti Films on Mo Substrate
Reference	J. Nucl. Mat., 93 & 94 (1980) 847
Authors	A. Sagara, K. Akaishi, K. Kamada, A. Miyahara
Institution	Institute of Plasma Physics, Nagoya University, Japan

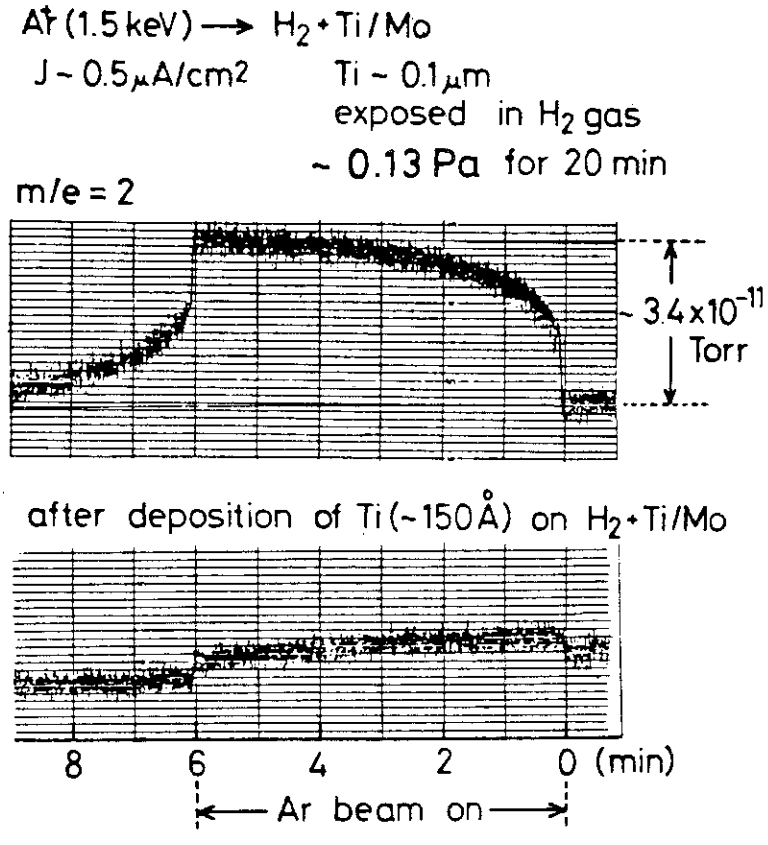

Fig. 7. Gas pressure changes caused by H_2 desorption from Ti-films due to Ar^+ ion bombardment before (upper part) and after (lower part) the deposition of subsequent evaporated Ti layers (~150 Å).

References

ID-01 R. Bastasz and L.G. Haggmark : Ion Impact Desorption and Hydrogen Release, J. Nucl. Mat., 103 & 104 (1981) 499.

ID-11 G. McCracken : Desorption of Adsorbed and Condensed Gas on Metals by Deuterons, Vacuum, 24 (1974) 463.

ID-21 E. Taglauer and W. Heiland : Ion Impact Desorption Cross Sections of Hydrogen and Oxygen from Metals by Light Ion Bombardment, J. Nucl. Mat., 76 & 77 (1978) 328.

ID-22 E. Taglauer, U. Beitat and W. Heiland : Investigation of Ion Impact Desorption of Atoms and Molecules by Low Energy Ion Scattering (ISS), Nucl. Instr. Methods, 149 (1978) 605.

ID-31 A. Sagara, K. Akaishi, K. Kamada and A. Miyahara : ISS Observation of Ti Films on Mo Substrate, J. Nucl. Mat., 93 & 94 (1980) 847.

4. Closing Remarks

In this report, data are collected on materials implanted with hydrogen isotopes and summarized from the view point of implantation effects.

Many data are concerned with stainless steel and graphite but only a few are shown on pure metals such as Ni, Mo, W. V, Ti, etc. and coating materials such as TiC. Experiments on re-emission, retention exceed in numbers and not so many on permeation are reported. As for experimental conditions, variety of items are selected such as temperature, fluence, flux, thickness and surface condition of targets that make systematic arrangement of data and direct application for design work difficult. Concerning irradiation effects, the major purpose of the report, difference in hydrogen isotopes capture mechanism caused by different ions such as hydrogen isotopes and He implanted in the target are not clarified enough and a few are reported on re-emission induced by implantation.

Systematically planned experiments and systematic arrangement of data are hereafter expected. Data should be arranged according to parameters such as temperature, fluence, etc. from the view point of arranging and utilizing those data.